RESULTS OF 2D AND 3D IP INVERSIONS WESTERN KIDD'S LOVELAND PROPERTY NORTHWEST OF TIMMINS ONTARIO

Prepared for:

Dave Meunier

Prepared by:

GeoScott Exploration Consultants Inc.
30 Monkstown Road
St. John's, NL
A1C 3T3

2.35105

30 May 2006

Table of Contents

List of Figures

1.0 INTRODUCTION

This report presents the results of inversions carried out on the IP and resistivity data, from the Loveland property. Data were received for Lines 8900N to 10600N, 11300N, 11400N, 13800N and 13900N. For interpretation the lines were grouped into the South Block (Lines 8900N to 9700N) and the North Block (Lines 9800N to 10600N). The other lines were treated individually.

1.1 Inversion Process

The data were first set up in a spreadsheet and formatted for input into the Res2DInv and Res3DInv inversion programs, designed by Geotomo Software. Two dimensional inversions were carried out for each line in Res2DInv. This program generates a two-dimensional model distribution of the resistivity and IP data collected. Measurements calculated from this distribution are compared to the observed values and the model is adjusted in successive iterations until the calculated and observed data sets agree as closely as possible. The resulting distributions of IP phase angle and resistivity are displayed as sections. These sections are presented in Appendix A.

Two-dimensional data from several parallel lines can be collated in Res2DInv and then handled as a three-dimensional data set in Res3DInv. By a process similar to that of Res2DInv, Res3DInv generates a three dimensional model distribution of the resistivity and IP phase angle values, with the resulting distributions portrayed in horizontal and vertical slices. Two sets of parallel lines were collated for three dimensional inversion: lines 8900N to 9700N (south block) and lines 9800N to 10600N (north block). Figure 1 shows the line locations.

2.0 INVERSION RESULTS

2.1 2D Inversion Results

Before the 3D inversion models were constructed, 2D inversions were carried out for each line and then interpreted. The results of the 2D inversions for each of the survey lines are given in appendix A. For each line the inverted phase angle and resistivity models are shown. The interpretations for each line are given in Tables 1, 2 and 3 in the appendix, where Table 1 gives interpretation of the lines comprising the south block, Table 2 gives interpretation of the lines comprising the north block and Table 3 gives interpretation for Lines 11300N, 11400N, 13800N and 13900N.

2.2 South Block 3D Inversion Results

The results of the 3D inversions are shown in vertical and horizontal slices. Figures 2a and 2b show eight west-east vertical slices through the model, representing sections taken between each consecutive line. Figure 2a shows the resistivity values and 2b shows the phase angle values. Figures 3a and 3b show the horizontal distribution of resistivity and phase angle respectively, for two ranges of depth: 37.6 to 60.8 m and 118 to 153.2 m.

The resistivity values reflect the presence of overburden and the nature of the bedrock topography. Overburden resistivity values range from less then 100 ohm-m to several hundred ohm-m, whereas the bedrock resistivity values are significantly higher (several thousand ohm-m). In general, the depth extent of the overburden in the area of the south block is fairly regular at around 50 m. However, from 9300N to 9550N, at about 2800E, the bedrock appears to be close to surface.

The inverted values of phase angle range from 0 to just over 5 milliradians (mrad). These values are only weakly anomalous. The models show two zones. The first zone extends from 9450N to 9650N, between 2275E and 2500E. From the horizontal sections the zone is strongest at 9650N and appears to weaken toward the south. The zone is also weaker at depth.

The second zone extends from 9250N to 9550N and is centered at 2700E. The source appears to be close to vertical and has strongest response in the near surface. This anomaly is associated with the zone of high resistivity in the near surface.

The correlation between the area of high resistivity and the weak phase angle response suggests that the source is an area of bedrock that has been altered, possibly silicified, with minor sulphide mineralization present.

2.3 North Block 3D Inversion Results

Figures 4a, 4b and 4c show the eight west-east vertical slices through the 3D model constructed for the north block. Figure 4a shows the resistivity values and Figures 4b and 4c show the phase angle values at contour intervals of 5 and 2 mrad respectively. Figures 5a, 5b and 5c show horizontal slices through the model for two ranges of depth. Figure 5a shows the resistivity values. Figures 5b and 5c show the phase angle values at 5 and 0.5 mrad contour intervals respectively.

As in the south block the overburden resistivity values range from less then 100 to several hundred ohm-m and the bedrock resistivities are much greater then 1000 ohm-m. The horizontal and vertical resistivity sections highlight a significant difference in the electrical properties in the east and in the west of the north block. East of 4850E there is a large zone of high resistivity that extends to the surface, is open at depth and trends N-S along Lines 9800N to 10600N. The area west of 4850E has much lower resistivities in the near surface. The boundary between the two zones is almost linear and may indicate the presence of a fault scarp with the area of high resistivity corresponding to an area where the bedrock is near surface. There is a second, smaller zone of high resistivity located in the near surface at 4350E between lines 9900N and 10000N which may also reflect near surface bedrock.

The intrinsic values of phase angle range from 1 to approximately 45 mrad. These are much stronger values then seen in the South Block. Figures 4b and 5b show the phase angle distribution at a higher contour interval, highlighting the stronger sources. There is a zone of high phase angle located between 4950E and 5250E, which extends from section 10450N to section 10050N. The intrinsic phase angle values in the strongest part of the source are around

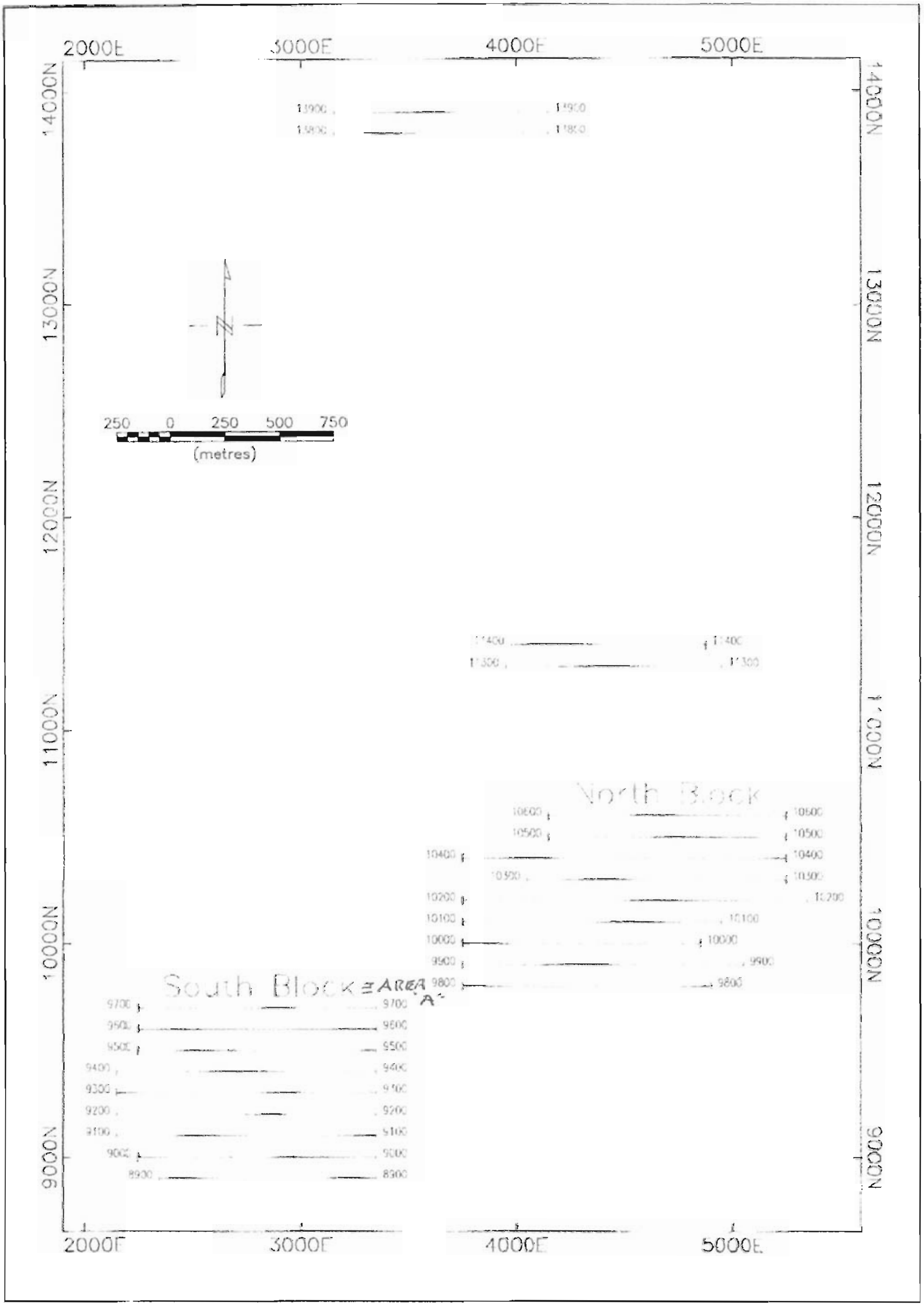

Figure 1. Line Locations

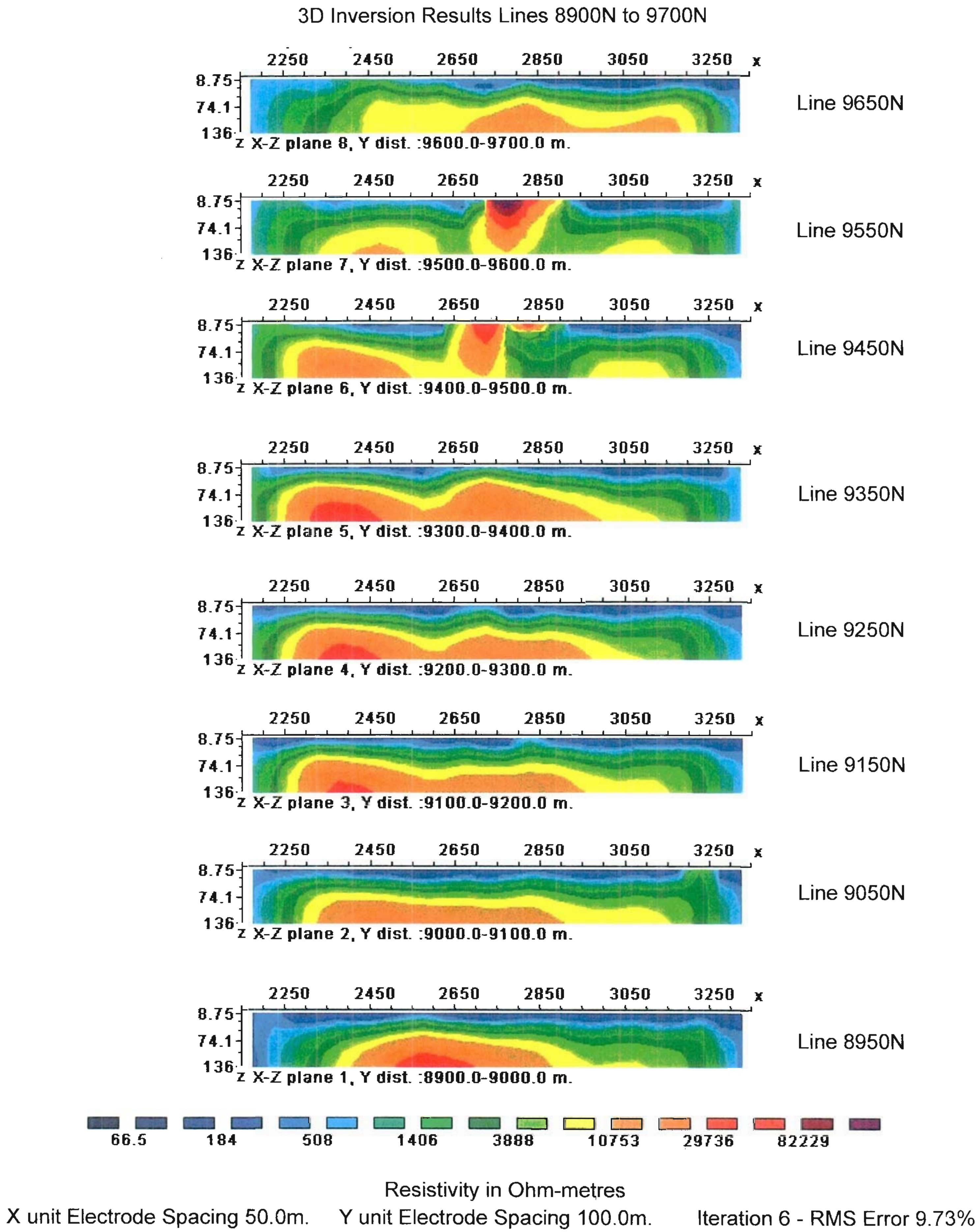

Figure 2a. Inverted Resistivity Results: vertical slices 8950N to 9650N (South block).

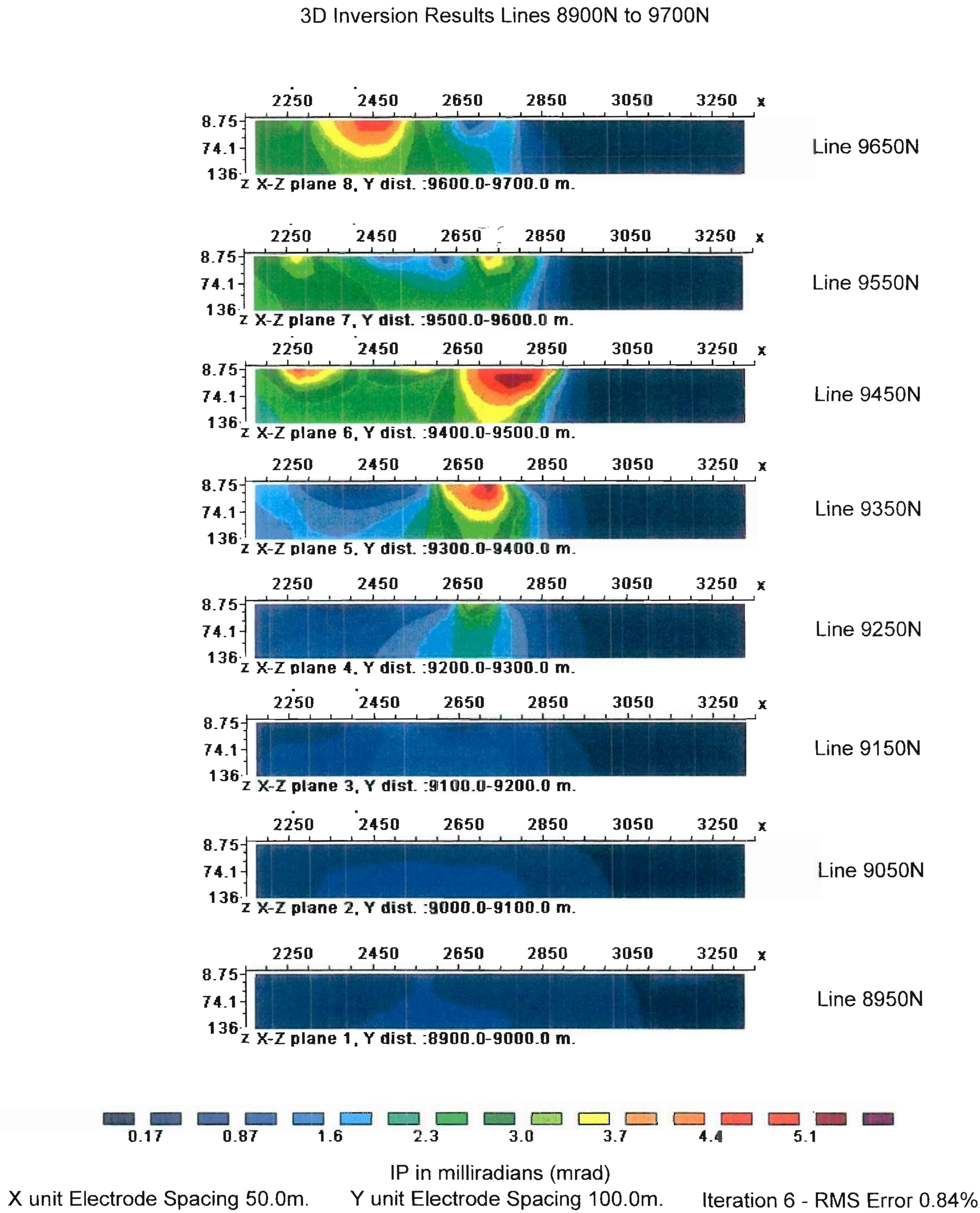

Figure 2b. Inverted Phase Angle Results: vertical slices 8950N to 9650N (South Block).

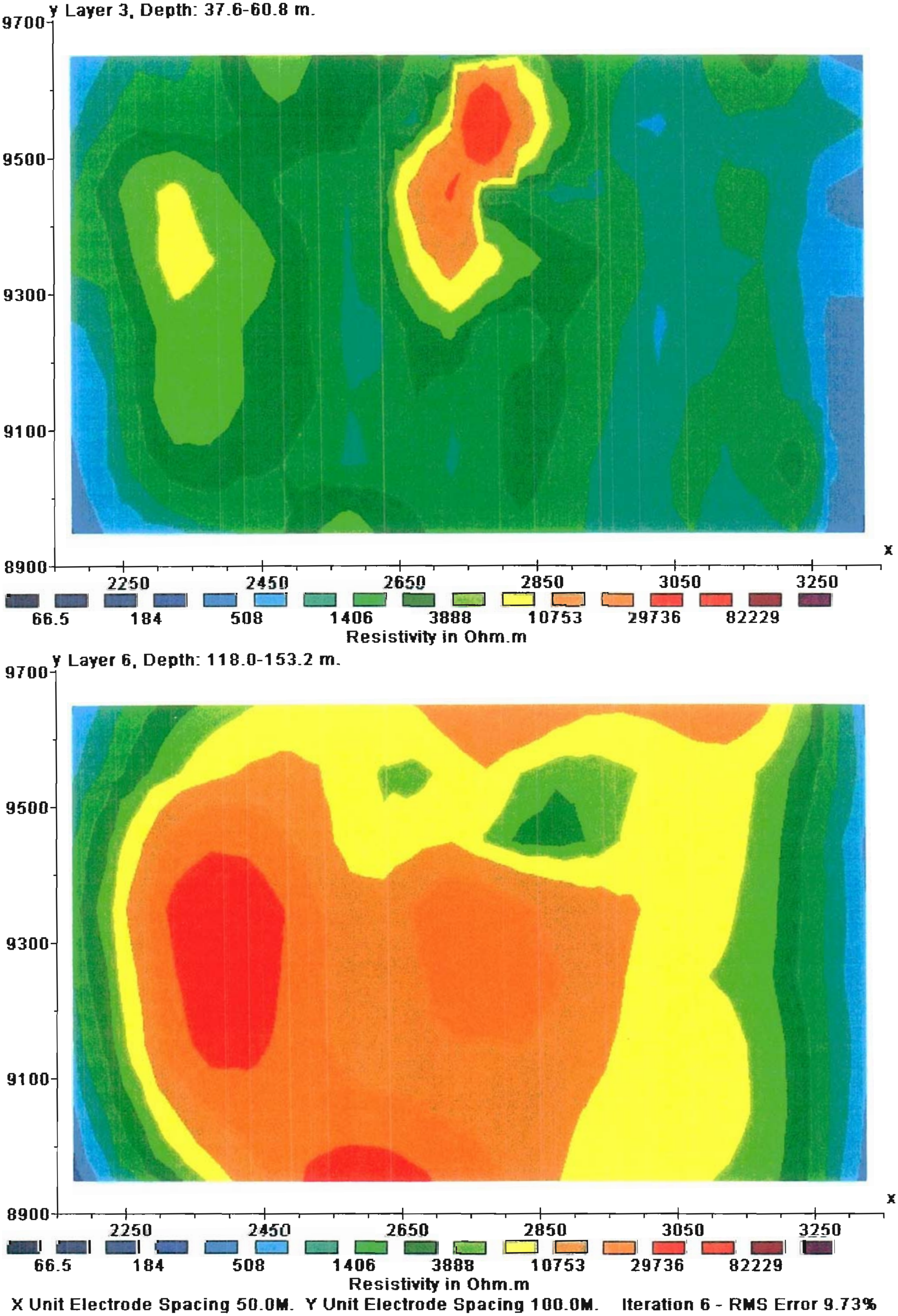

Figure 3a. Inverted Resistivity results: horizontal slices from south block. Layer 3 (top) Depth 37.6 - 60.8m and Layer 6 (bottom) Depth 118.0 - 153.2 m.

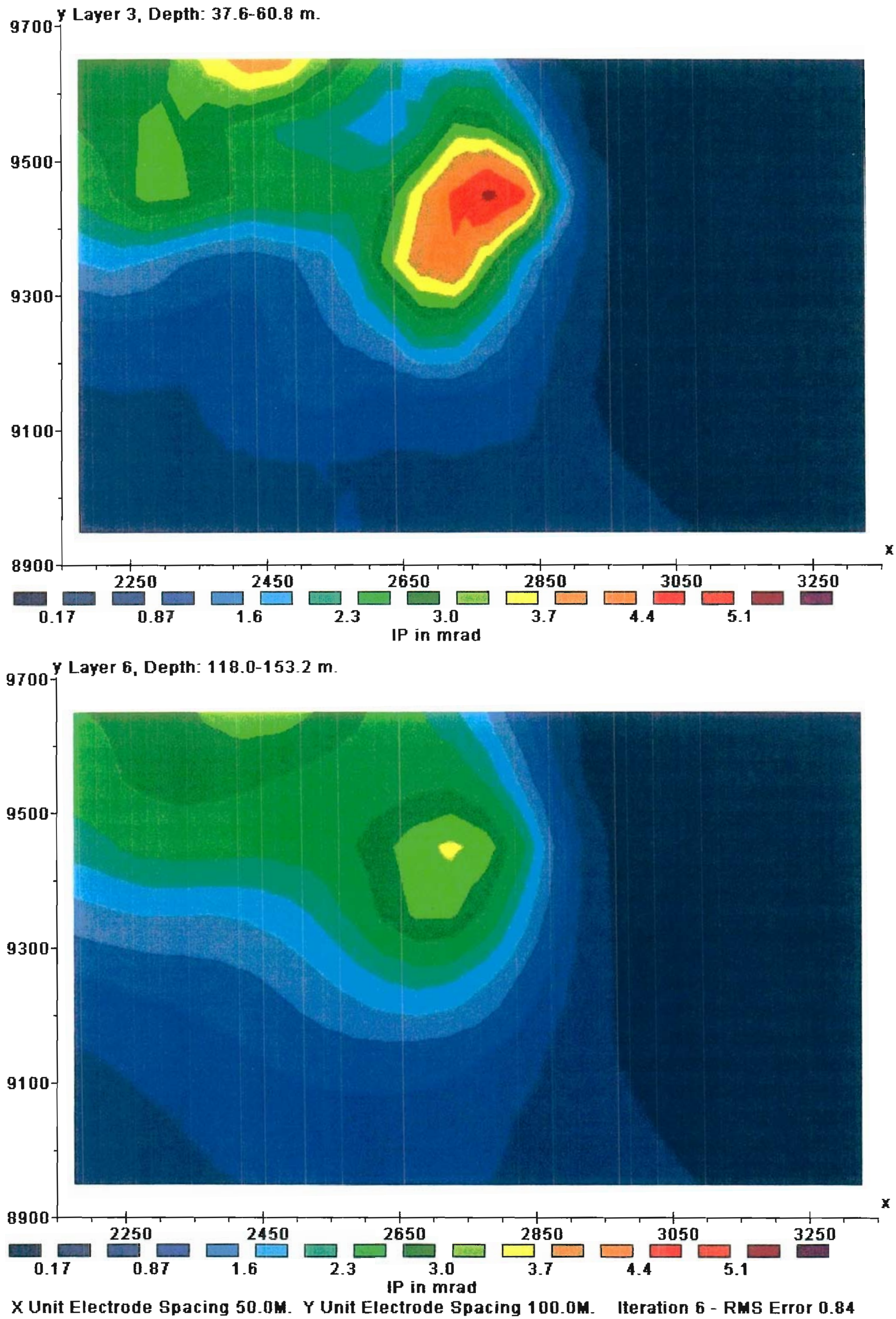

Figure 3b. Inverted Phase Angle results: horizontal slices from south block. Layer 3 (top) Depth 37.6 - 60.8m and Layer 6 (bottom) Depth 118.0 - 153.2 m.

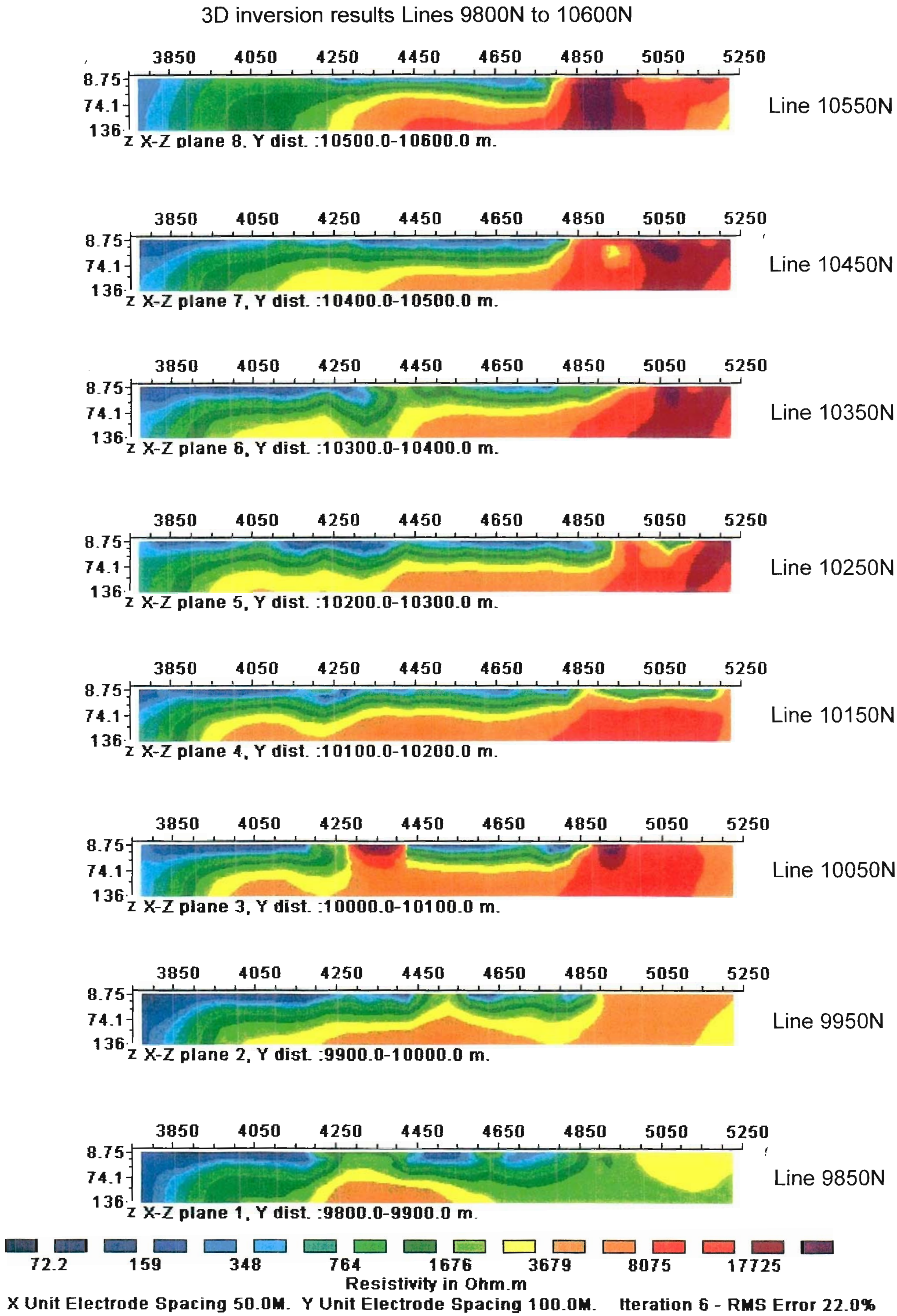

Figure 4a. Inverted Resistivity results: vertical slices 9850N to 10550N (North block).

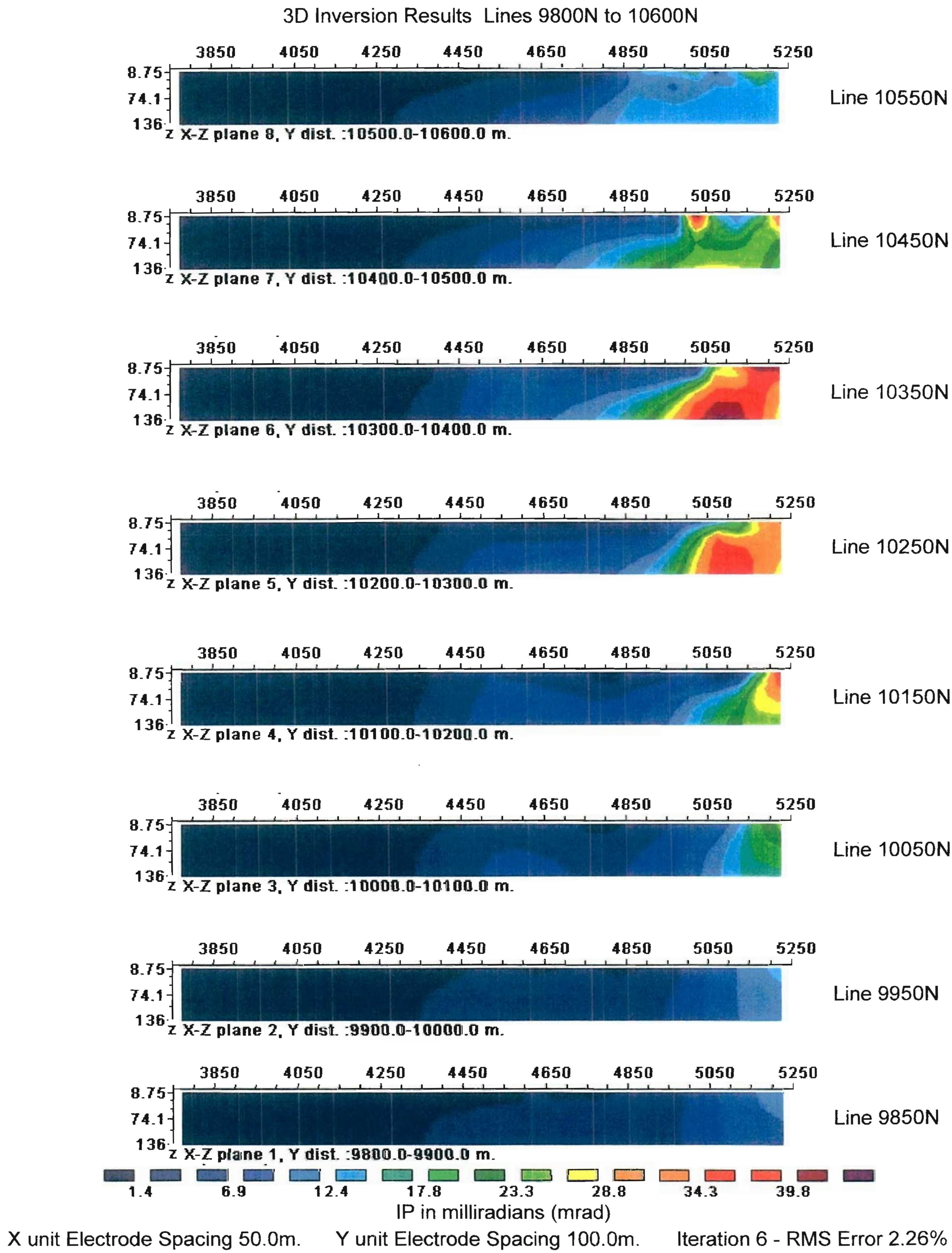

Figure 4b. Inverted Phase Angle results: vertical slices 9850N to 10550N (North Block).

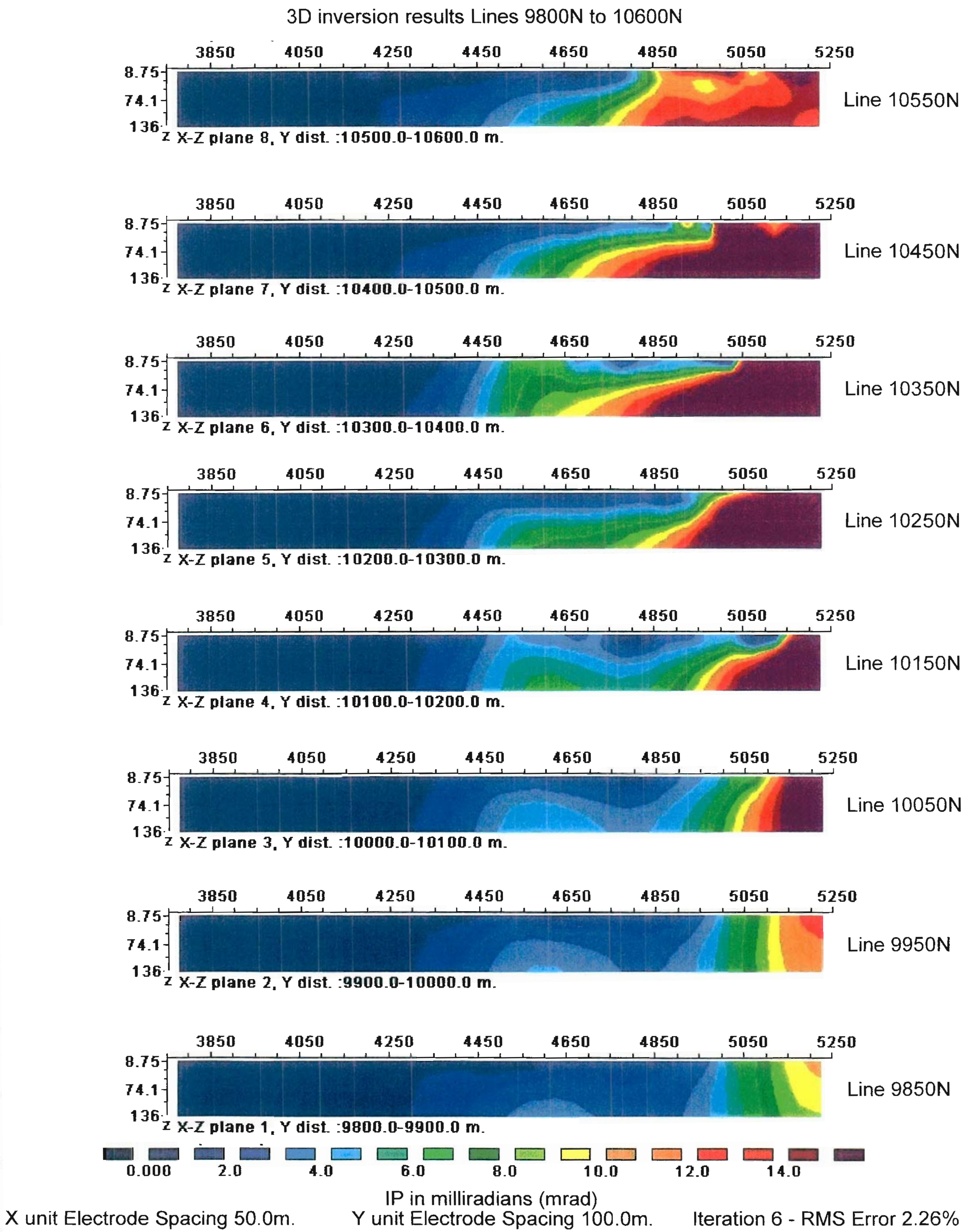

Figure 4c. Inverted Phase Angle results: vertical slices 9850N to 10550N with smaller contour interval to highlight subtle features.

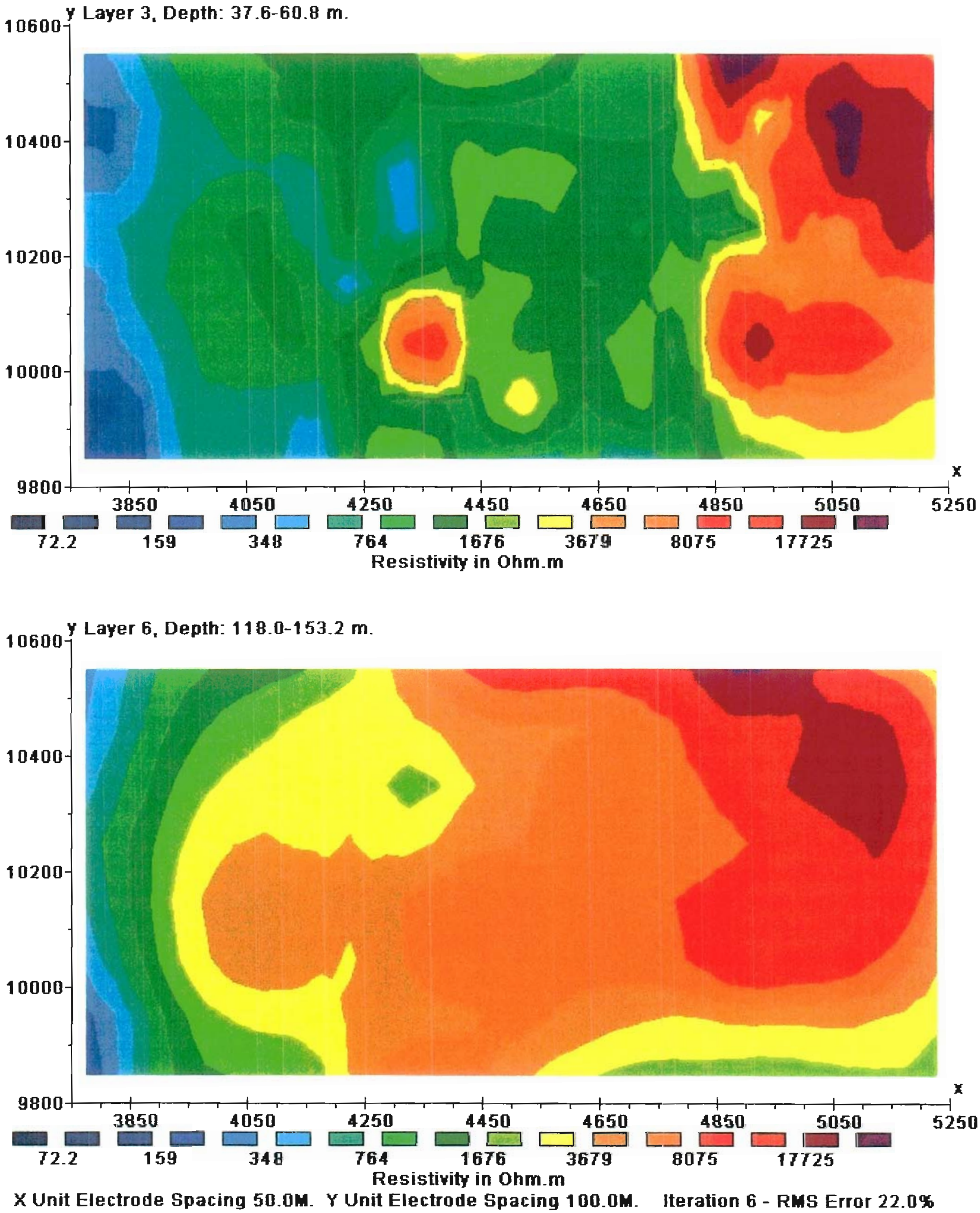

Figure 5a. Inverted Resistivity results: horizontal slices from north block. Layer 3 (top) Depth 37.6 - 60.8m and Layer 6 (bottom) Depth 118.0 - 153.2 m.

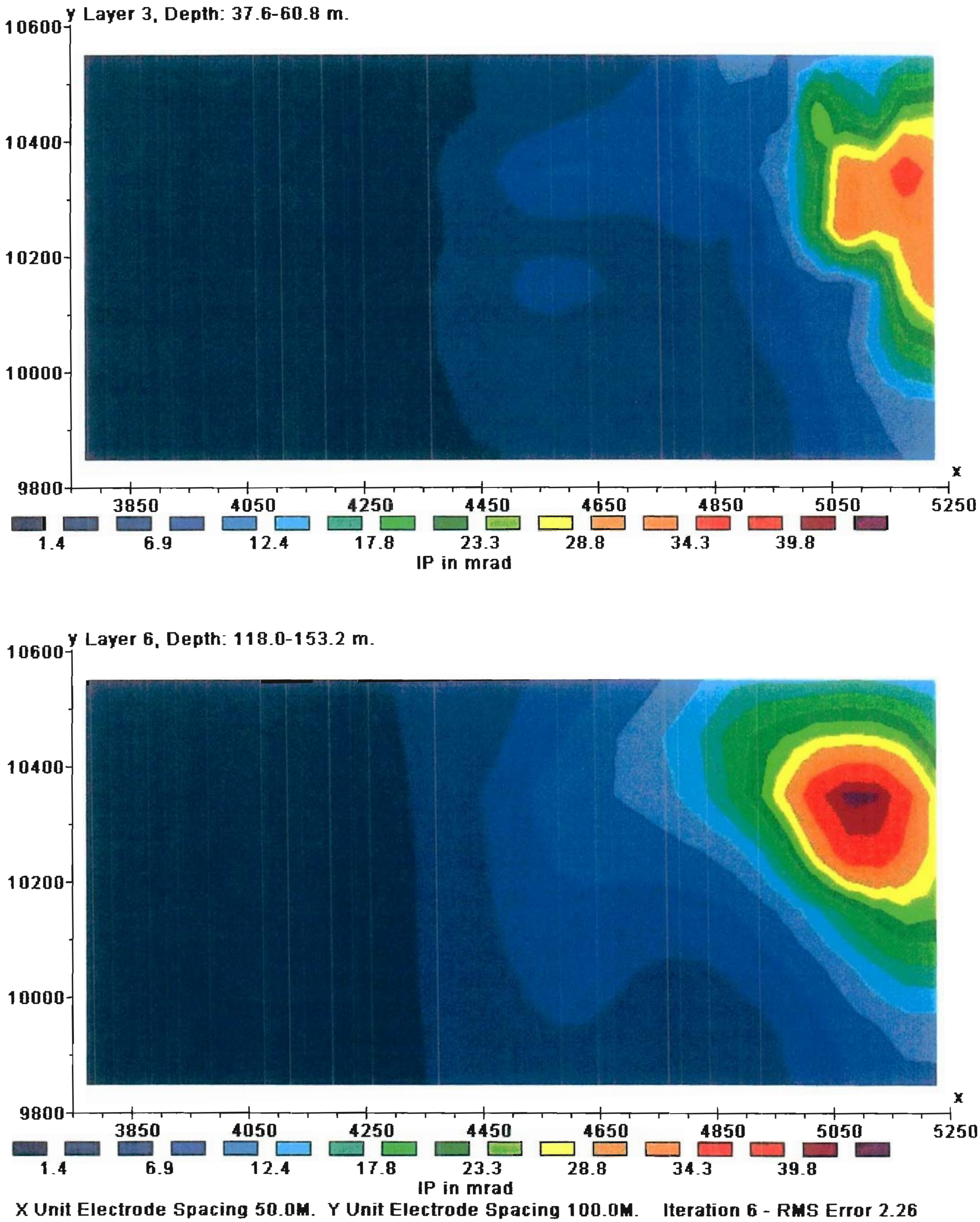

Figure 5b. Inverted Phase Angle results: horizontal slices from north block. Layer 3 (top) Depth 37.6 - 60.8m and Layer 6 (bottom) Depth 118.0 - 153.2 m.

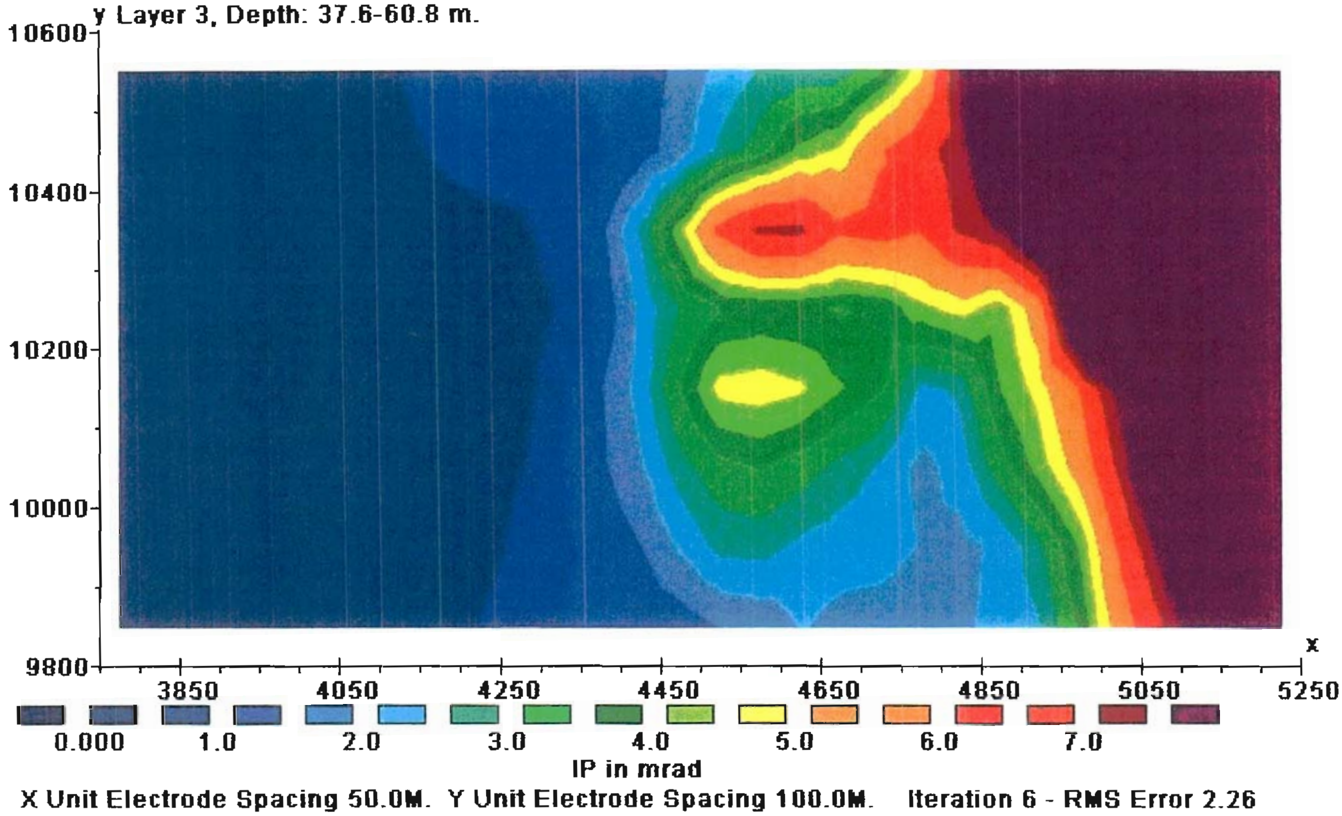

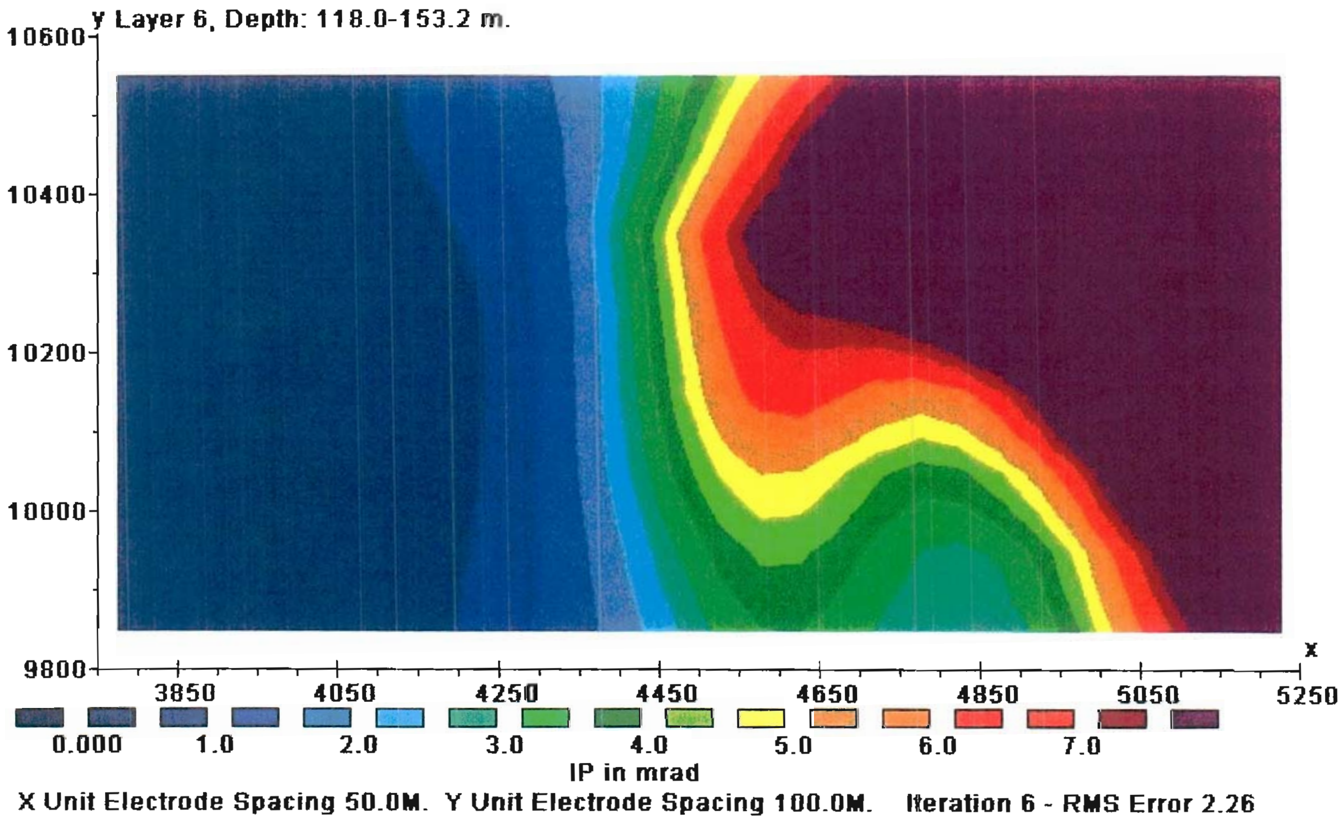

Figure 5c. Inverted Phase Angle results: horizontal slices from north block, plotted with 0.5 mrad contour interval. Layer 3 (top) Depth 37.6 0-60.8 m, Layer 6 (bottom) Depth 118.0-153.2 m.

40 to 45 mrad which is ten times stronger then the zones defined in the south block. The zone is strongest on section 10350N located at a depth of approximately 100m. The source is possibly near vertical, is open at depth and has an extension to the surface at about 5200E. The zone strikes NE-SW and correlates with the area in the east where the bedrock is near surface.

There is a weak zone that extends from 9850N to 10150N, between 4450E and 4700E. In figures 4c and 5c the phase angle values are contoured at smaller intervals so that the weaker zones are better defined. The top of the strongest part of the source is at a depth of 50 to 80 m. This corresponds with the zone drilled on Line 10000N. The response becomes weaker toward the south, which may suggest that the source is plunging in that direction.

From the horizontal sections there is a third zone located between 4450E and 4750E, extending from 10300N to 10500N. In figures 4c and 5c, the zone has strongest values of around 12 mrad and appears to be an extension of the larger IP anomaly in the east, which has been separated by faulting. It is difficult to define the two weaker zones at depth because of the stronger response in the east.

3.0 DISSCUSSION

The inverted resistivity values for both the north and south blocks reflect the overburden and bedrock topography. Overburden resistivity values range from less then 100 to several hundred ohm-m, whereas bedrock resistivity values range from 1000 to several thousand ohm-m.

In the South block the depth to bedrock is fairly consistent at around 50 m, with one area at 2800E, between sections 9500N and 9300N where the bedrock appears to be near surface. The values of phase associated with the south block are only weakly anomalous (0 to 5 mrad). Two weak IP anomalies were defined. The first zone extends from 9450N to 9650N and is located between 2275E and 2550E. The response of this zone weakens to the south and is limited at depth. The second zone was located in the near surface centered at 2700E, extending from 9250N to 9550N. This correlates with the area of near surface bedrock. The correlation between the high resistivity and high phase angle responses suggests that the source is minor sulphide mineralization within silicified bedrock.

Within the north block there is a distinct change in the resistivity at 4850E. East of 4850E there is a shallow high resistivity zone trending N-S across each of the survey lines. The area west of 4850E has lower resistivity in the near surface and higher resistivity at depth. The boundary between the two zones is almost linear and possibly reflects the presence of a fault scarp within the bedrock. The zone of high resistivity in the east is a section of bedrock which is located in the near surface.

Phase angle values in the north block are up to ten times higher then in the south block. The inversion results show a strong IP response (40 to 45 mrad) in the east that extends from 10050N to10450N and correlates with the area of near surface bedrock. The source appears to be near vertical, is open at depth and has an extension to the surface at about 5200E on sections 10250N to 10350N.

Within the lower resistivity zone in the west there are two weaker IP anomalies present. The first zone correlates with the anomaly drilled on Line 10000N. The response is strongest on section 10150N between 4450E and 4700E, at a depth of approximately 80m. The response weakens toward the south which may be an indication that the source is plunging to the south. The second zone defined by the horizontal section extends from 10300N to 10500N and is located between 4450E and 4750E. From the horizontal sections the zone appears to be an extension of the stronger source in the east, that has been separated by faulting.

From the inversions on Lines 13800N and 13900N, it appears that the presence of the power line does not effect the IP response. Power line effects appear as surface anomalies with little or no depth extent, while the anomaly on Line 13900N is at considerable depth, and is too deep to arise from a power line response.

A number of the sources identified in the inversions appear to be at the limit of depth detection for the survey, particularly on lines 11300, 11400 and 13900N. Before drilling, consideration should be given to running more IP on the same lines but with 100 m dipoles. The data so obtained could be used in conjunction with the current data to extend the inverted depth to more than 150 metres, and thus give better definition to the sources. Also the stronger anomaly discussed in the 3D inversion of the northern block occurs at the end of the lines. If possible consideration should also be given to extending these lines toward the east.

In general, inversion routines have the most difficulty depicting narrow vertical sources at depth. The inverted source generally appears somewhat wider then the true one. It is possible that this characteristic is in effect for a number of the sources discussed. It is possible that the hole on Line 10000N has just missed the source, if it is narrower than shown on the inversion. On Line 102N, however, the first hole should still have intersected the source. On Line 105N hole W-04#7 could have stopped short of the western part of the strong source, but the other hole should have intersected it at depth.

4.0 RECOMMENDATIONS

1. Consideration should be given to carrying out more IP on each of the survey lines with 100 m dipoles to extend the depth of inversion.

2. The 100 m dipole data should be combined with the original 50 m dipole data and then re-inverted.

Respectfully Submitted:

REGISTERED PROFESSIONAL GEOSCIENTIST
WILLIAM J. SCOTT
SIGNATURE
2 Jun 06
DATE
NEWFOUNDLAND & LABRADOR

Krystal O'Neill

Krystal O'Neill, B.Sc., GIT
Geophysicist

W.J. Scott, Ph.D., P.Eng., P.Geo., FGAC
President

PROVINCE OF NEWFOUNDLAND
PERMIT HOLDER
CLASS "A"
This Permit Allows
GEO[illegible] EXPLORATION CONSULT INC.
To practice [illegible] in Newfoundland and Labrador.
Permit No. as issued by APEGN G0102
which is valid for the year 2006.

APPENDIX A

2D INVERSION RESULTS

Table 1: South Block

Line/Figure	Interpretation
8900N	Resistivity increasing with depth. Low resistivity layer in near surface representing fairly thick layer of overburden. Inverted phase angle values range from -0.5 to 4 mrad. No sources present within the range of the measurements.
9000N	Fairly thick layer of low resistivity overburden. Inverted phase angle values range from -0.5 to 4 mrad. No sources present
9100N	Resistivity increasing with depth. About 40 m of overburden (low resistivity) Inverted phase angle values range from -0.5 to 11.5 mrad. Source from 2550E to 2625E, with top of strongest response at about 80m below surface. The strongest part of the source is at 11.5 mrad which is not a very strong response. The source appears to be just at the detection depth limit of the survey.
9200N	Phase angle values range from -0.5 to 11.5 mrad. Source located from 2425E to 2550E, at 80m depth from the surface. Strongest part of source is at 11.5 mrad, which is moderate. The source appears to be at the detection depth limit of the survey, and may be a northwest extension of the source seen on Line 9100N.
9300N	Phase angle values range from -0.5 to 7.5 mrad. There is an increase in phase with depth between 2350E and 2800E. The strongest part of the zone is at 2725E at 80m depth. The structure appears to come close to surface near 2750E and is open at depth.
9400N	Bedrock is shallower (around 20m) west of 2750E, and deeper (around 50m) east of 2750E. Source located at 2750E, has width of 250m, is present in the near surface and is open at depth. The strongest part of the source is 9.5 mrad located at around 80m depth. Possible correlation with the source detected on Line 9300N.
9500N	Bedrock is irregular, shallow to the west coming close to the surface from 2700E to 2900E, and then is deeper to the east. Zone located at around 2800E. Extends from the surface to about 50m depth, but not deeper. Strongest part of the source is in the near surface at 9.5 mrad. Some indication that it is near vertical and may correlate with the sources indicated on Lines 9300N and 9400N.
9600N	Steeply east dipping source located at around 2725E, where bedrock rises to near surface. Strongest part of the source is around 7.5 mrad which is only moderate in strength. The source extends from the surface, is open at depth, and is not associated with low resistivity in bedrock. Possible correlation with source discussed on the previous three lines.
9700N	Bedrock shallow at the west end, deepening to more than 50m at the east end. Weak phase angle source (values around 5.5 mrad) centred at 2450E, even weaker at depth.

Table 2: North Block

Line/Figure	Interpretation
9800N	Bedrock is very irregular, near surface between 4225E and 4425E, then to the west of this area is at depths of around 50m and similarly on the east end of the line deepening to around 80m at 4725E. Intrinsic phase angle values range from less then -0.5 to 2.5 mrad with no significant zones present.
9900N	Source extending from 4500E to 4725E, with the top of the strongest response at about 80m below surface. The intrinsic phase angle in the strongest part of the source is around 14 to 16 mrad. Weaker sources located at 4100, from 4275E to 4350E. All sources are open at depth and are near the detection limit of the survey. The bedrock depth is variable, but from 4725E to 4775E, there appears to be a zone of lower resistivity that cuts off the strong phase anomaly.
10000N	Source extending from 4500E to 4640E, with the top of the strongest response at about 80m below surface. The intrinsic phase angle in the strongest part of the source is around 12 to 14 mrad, which is not a strong response in comparison to the other lines. Hole W-06#10 passed through the anomalous source about 15m west of the centre of the anomaly at 80m depth. The resistivity section highlights a very irregular bedrock surface, close to outcropping in the centre of the line. There is some evidence of a low resistivity zone at 4750E.
10100N	Intrinsic phase angle values range from -0.5 to 1.5 mrad. No significant source present. Bedrock possibly outcropping near 4350E and possibly near 4750E.
10200N	On this line the bedrock is shallower and less irregular then on line 10100N. The inversion shows a source extending from about 4500E to 4580E, with the top of the strongest response (intrinsic phase angles of about 20 mrad) at about 80m depth. Because only the top of the source is visible in the model, it is difficult to say about attitude, but it appears that the source dips fairly steeply to the east. Hole W-06#12 intersects the centre of the source at about 80m vertical depth, and the hole to the east of #12 (number not visible on section) should intersect the source at about 150m vertical depth.
10300N	There are three zones detected on this line. The first source has a lower response of about 20 mrad. It is located at about 80m depth, and extends from about 4550E to about 4675E. This source appears to correlate with the source previously discussed on Line 10200N. A second zone is located at about 80m depth, extending from 4750E to about 4925E. The intrinsic phase angle of the zone is about 45 to 50 mrad which is strong in comparison to those detected on the previously discussed lines. The third zone which is even stronger, has an intrinsic phase angle response of about 70 mrad. The zone extends from 5025E to 5600E, with the top of the strongest response located at about 40 to 50m depth. The bedrock is quite deep to the west of 4600E, shallower to the east of 4600E coming close to the surface from 4925E to 5050.

10400N	On this line the inversion shows a zone extending from 4425E to about 4600E, with the top of the strongest part at about 82 m depth. The inverted phase angle values in the strongest part of the zone are around 38 mrad. The zone correlates with a rise in the bedrock surface. There is a second zone located between 4725E and 5050E at a depth of about 80m. The intrinsic values in the strongest part of the zone are around 60 to 65 mrad. Only the top of the zone is defined but it is possible that the response is from two parties; one located at 4725E to 4925E, and the other from 4950E to 5050E. There are two near surface zones; one extending from 5050E to 5125E with intrinsic phase angle values of about 48 mrad, and the other at the very east end of the line with values greater then 150mrad. The two near surface zones correlate with an area of very high resistivity, in shallow bedrock.
10500N	The Bedrock depth is about 70 m west of 4800E, then irregular but close to surface in the east. This line shows a source with top at 80m depth, extending from about 4500E to about 4725E which appears to be exposed on bedrock surface. Again only the top of the source is defined, but it is possible that there are two parts, one from 4500E to 4600E and the other from 4625E to 4725E. The intrinsic phase angle of the combined zone is about 60 to 70 mrad. A second weaker zone extends from about 4800E to 4960E, at the same depth, with an intrinsic phase angle of about 38 mrad. Hole W-04#7 appears to have passed through between the two parts of the largest zone but should have intersected the western one by the end of the hole. The more easterly hole should have intersected the easterly part of the large zone at a vertical depth of about 200m, close to the end of the hole. The eastern source at 4935E was not intersected.
10600N	West of 4825E, bedrock is around 50 m deep and smooth. To the east of 4825E bedrock is close to the surface. The section shows a zone with top at about 70m depth, extending from 4375E to 4475E. The intrinsic phase angle of the zone is about 40 mrad. As on Line 10500N there is a zone extending from about 4525E to 4775E located at about 80m depth which may possibly have two parts. The overall intrinsic phase angle of the combined two is lower then the source on Line 10500N, at about 21 to 25 mrad. There is another anomalous zone which extends from 4900E to 5175E. Within this zone there are two areas with strong intrinsic phase angle values. The first has strongest value of about 27 mrad and is located at a depth of about 80m; the second is about 24 mrad and is located nearer surface at about 30m. The response may represent two separate sources or one source with variation in IP response due to variation in minerals present.

Table 3: Lines 11300N, 11400N, 13800N and 13900N

11300N	The inversion shows one source which extends from 4250E to 4475E, with the top of the strongest part of the source located at a depth of about 75m. The inverted phase angle values for the strongest part of the source are about 25 mrad. This zone does correspond to a zone of very high resistivity within bedrock. There is another source that extends from 4575E to 4635E, located in the near surface to a depth of approximately 50m. The source has strongest value of about 20 mrad. Beneath this near surface anomaly there is another zone with increased phase values located at a depth of about 80 m. The zone has strongest value of about 19 to 20 mrad, extending from 4625E to 4700E and may be either an extension of the source above or a separate zone. The inverted resistivity values corresponding to this area are also very high and highlight a subvertical structure possibly a dyke.
11400N	The resistivity section highlights irregular bedrock, having depth greater then 80m west of 4325E, rising to very shallow depths from 4500E to 4650E and then deepening again in the east. The inversion shows more or less, continuous high phase angles on the entire line with maximum values near 4375E and 4725E at a depth of about 75m. High values located at 4500E and 4575E in the near surface may reflect the sub-vertical structure highlighted by the resistivity data. This also correlates with those zones previously discussed on Line 10300N.
13800N	Inverted phase angle values range from less than -0.5 to 3.5 mrad. No high phase angle zones detected. The very weak response may possibly reflect the powerline located at 3705E.
13900N	The inversion shows a single source extending from 3675E to 3400E, with the strongest part of the source (inverted phase angle values of 56 mrad) located at a depth of about 75m.

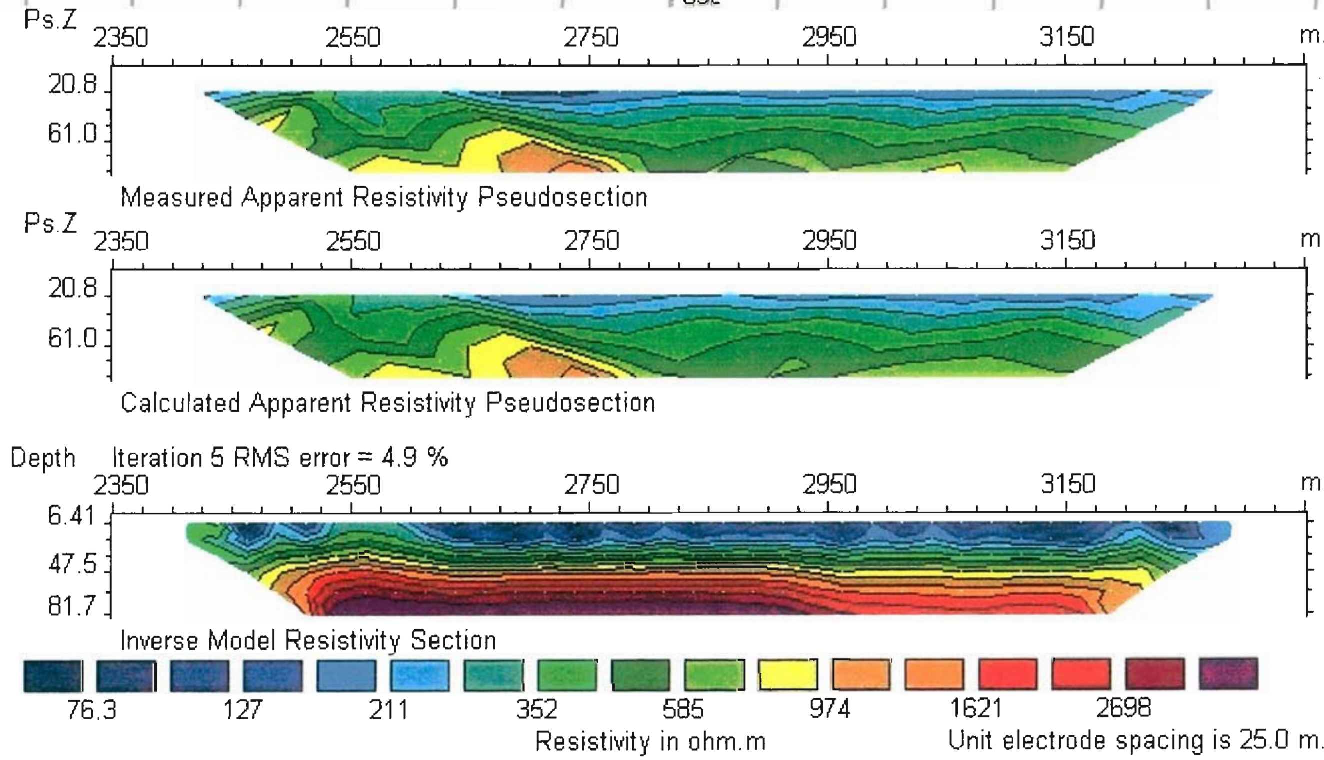
Ps.Z
2350 2550 2750 2950 3150 m.
20.8
61.0
Measured Apparent Resistivity Pseudosection
Ps.Z
2350 2550 2750 2950 3150 m.
20.8
61.0
Calculated Apparent Resistivity Pseudosection
Depth
Iteration 5 RMS error = 4.9 %
2350 2550 2750 2950 3150 m.
6.41
47.5
81.7
Inverse Model Resistivity Section
76.3 127 211 352 585 974 1621 2698
Resistivity in ohm.m
Unit electrode spacing is 25.0 m.

Line 8900N

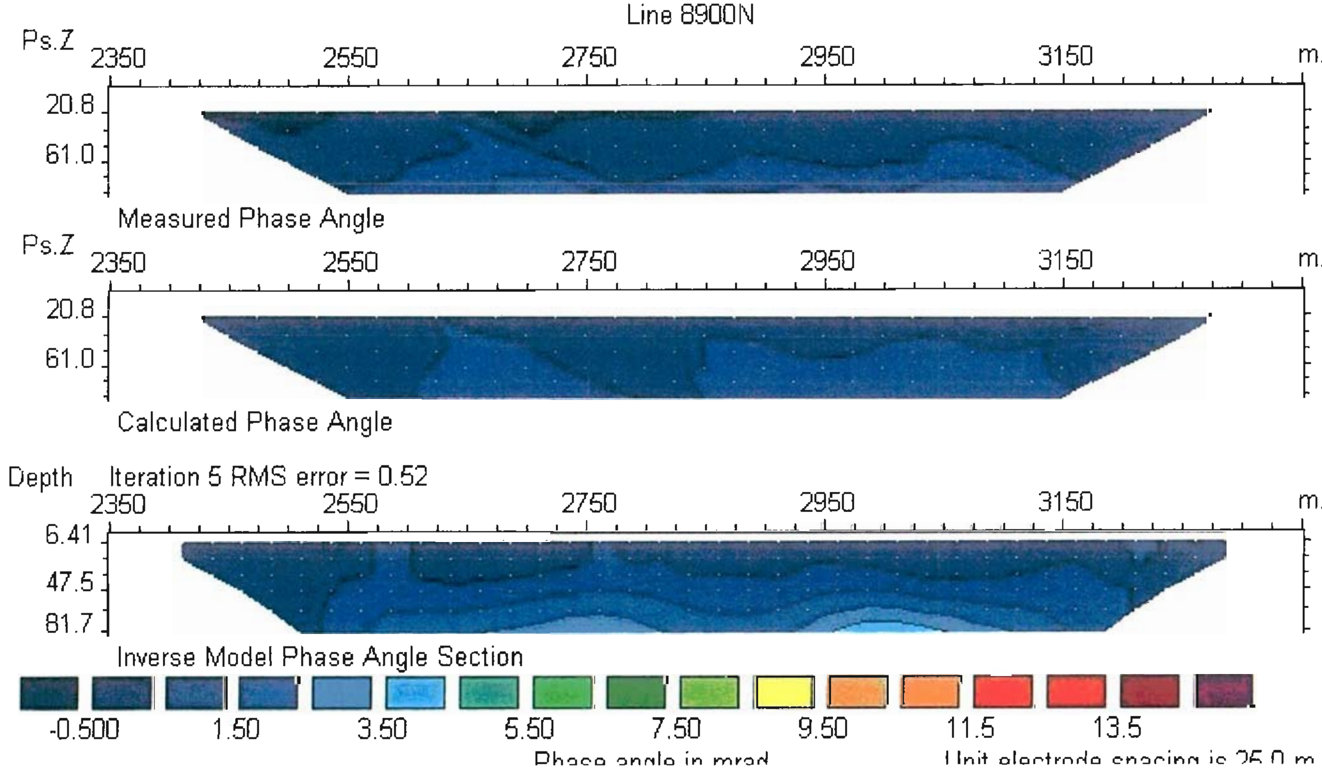
Ps.Z
2350 2550 2750 2950 3150 m.
20.8
61.0
Measured Phase Angle
Ps.Z
2350 2550 2750 2950 3150 m.
20.8
61.0
Calculated Phase Angle
Depth
Iteration 5 RMS error = 0.52
2350 2550 2750 2950 3150 m.
6.41
47.5
81.7
Inverse Model Phase Angle Section
-0.500 1.50 3.50 5.50 7.50 9.50 11.5 13.5

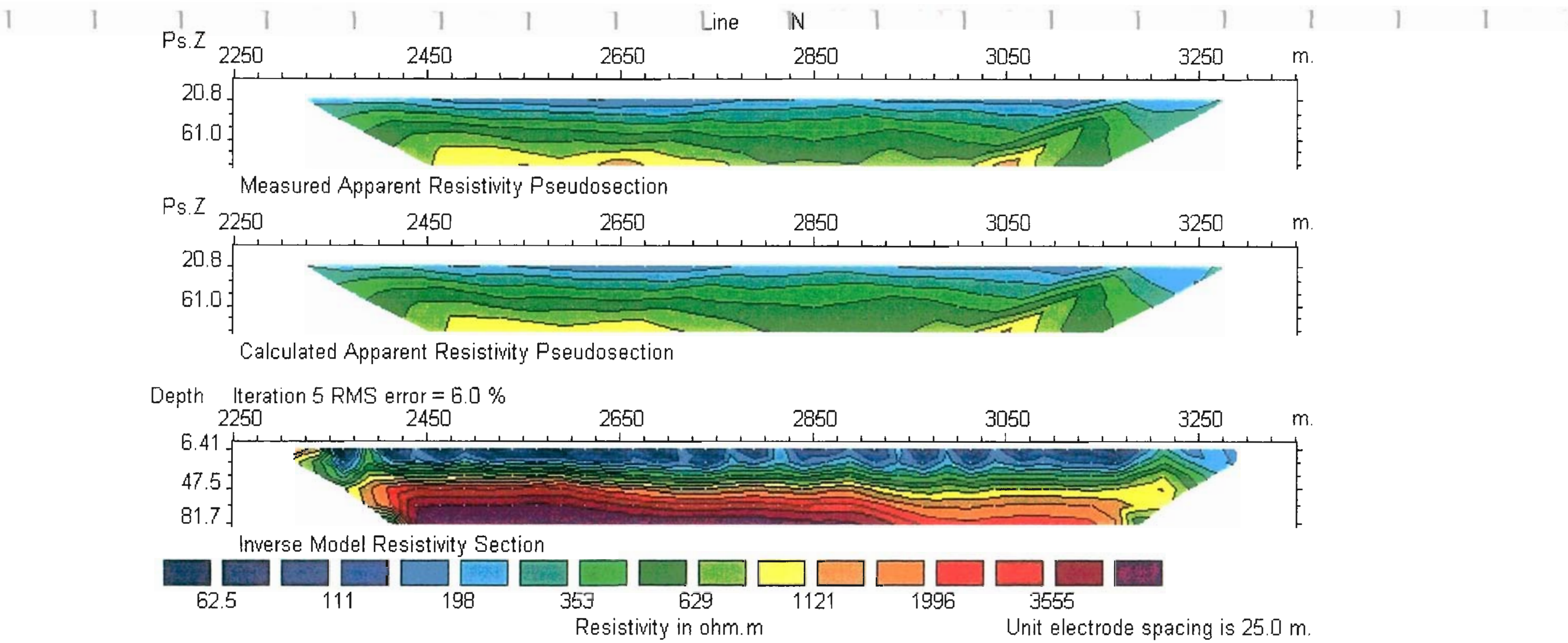
Line N
Ps.Z
2250 2450 2650 2850 3050 3250 m.
20.8
61.0
Measured Apparent Resistivity Pseudosection
Ps.Z
2250 2450 2650 2850 3050 3250 m.
20.8
61.0
Calculated Apparent Resistivity Pseudosection
Depth Iteration 5 RMS error = 6.0 %
2250 2450 2650 2850 3050 3250 m.
6.41
47.5
81.7
Inverse Model Resistivity Section
62.5 111 198 353 629 1121 1996 3555
Resistivity in ohm.m
Unit electrode spacing is 25.0 m.

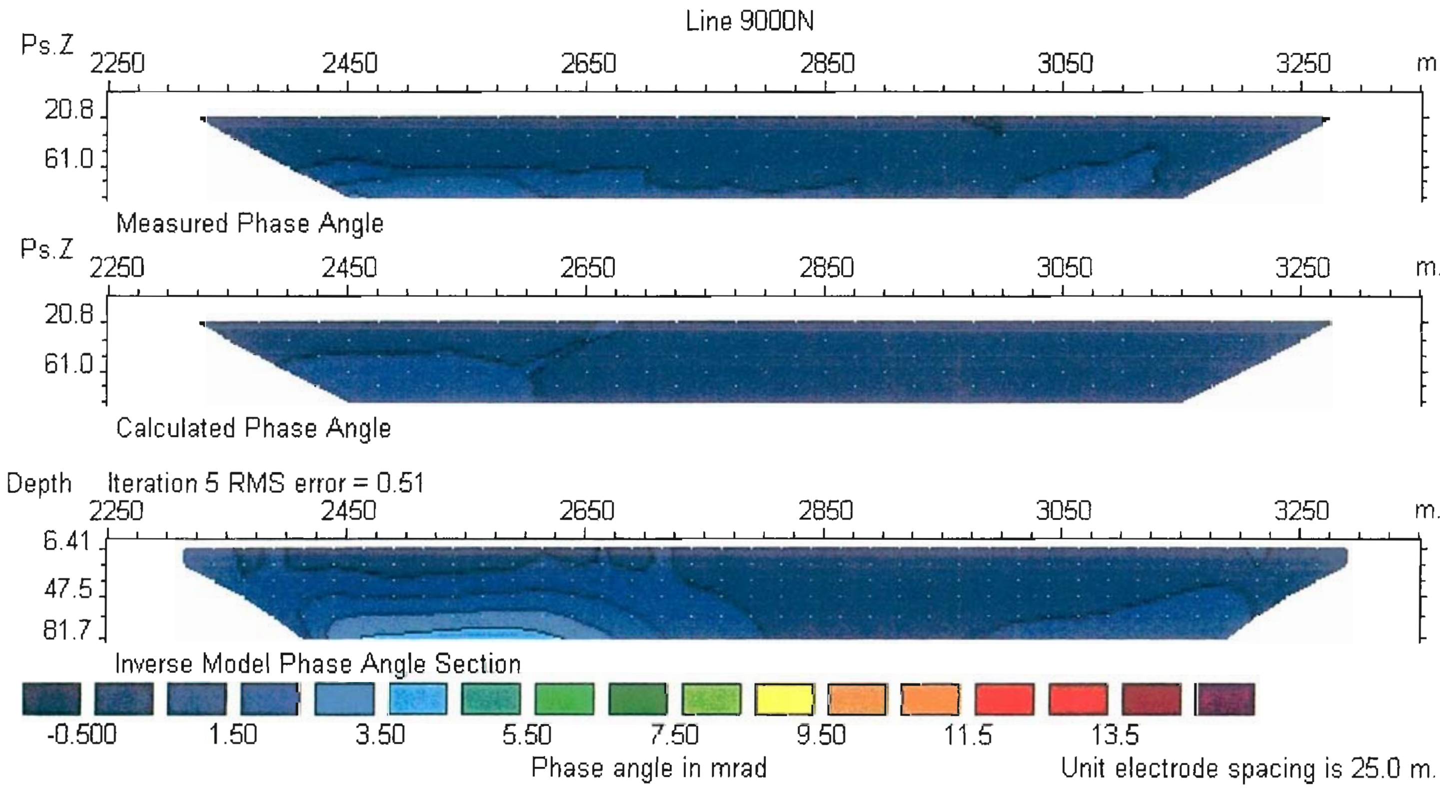
Line 9000N
Ps.Z
2250 2450 2650 2850 3050 3250 m.
20.8
61.0
Measured Phase Angle
Ps.Z
2250 2450 2650 2850 3050 3250 m.
20.8
61.0
Calculated Phase Angle
Depth Iteration 5 RMS error = 0.51
2250 2450 2650 2850 3050 3250 m.
6.41
47.5
81.7
Inverse Model Phase Angle Section
-0.500 1.50 3.50 5.50 7.50 9.50 11.5 13.5
Phase angle in mrad
Unit electrode spacing is 25.0 m.

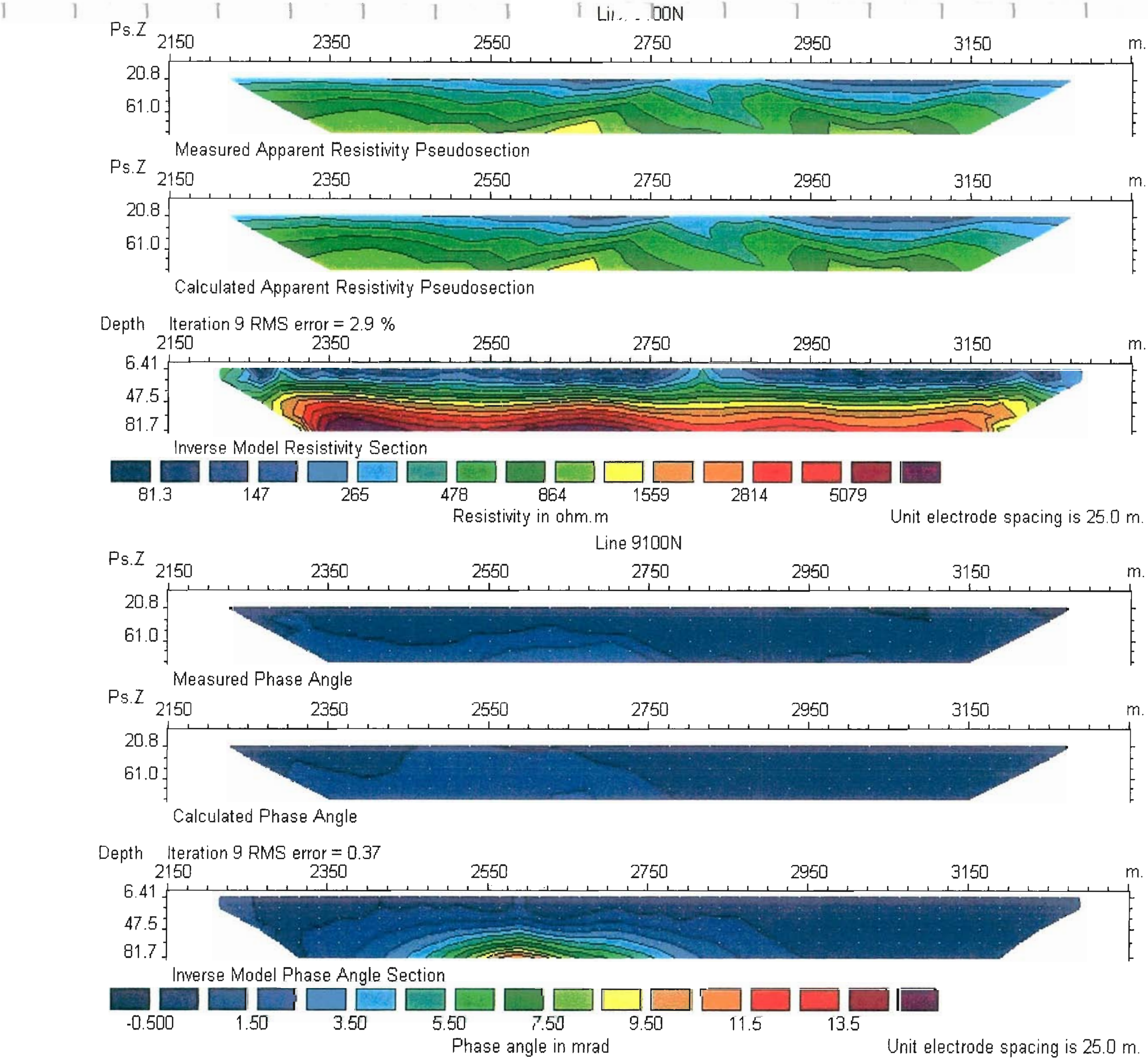

Ps.Z
2150
2350
2550
2750
2950
3150
m.
20.8
61.0
Measured Apparent Resistivity Pseudosection
Calculated Apparent Resistivity Pseudosection
Depth
Iteration 9 RMS error = 2.9 %
6.41
47.5
81.7
Inverse Model Resistivity Section
81.3
147
265
478
864
1559
2814
5079
Resistivity in ohm.m
Unit electrode spacing is 25.0 m.
Line 9100N
Measured Phase Angle
Calculated Phase Angle
Iteration 9 RMS error = 0.37
Inverse Model Phase Angle Section
-0.500
1.50
3.50
5.50
7.50
9.50
11.5
13.5
Phase angle in mrad
Unit electrode spacing is 25.0 m.

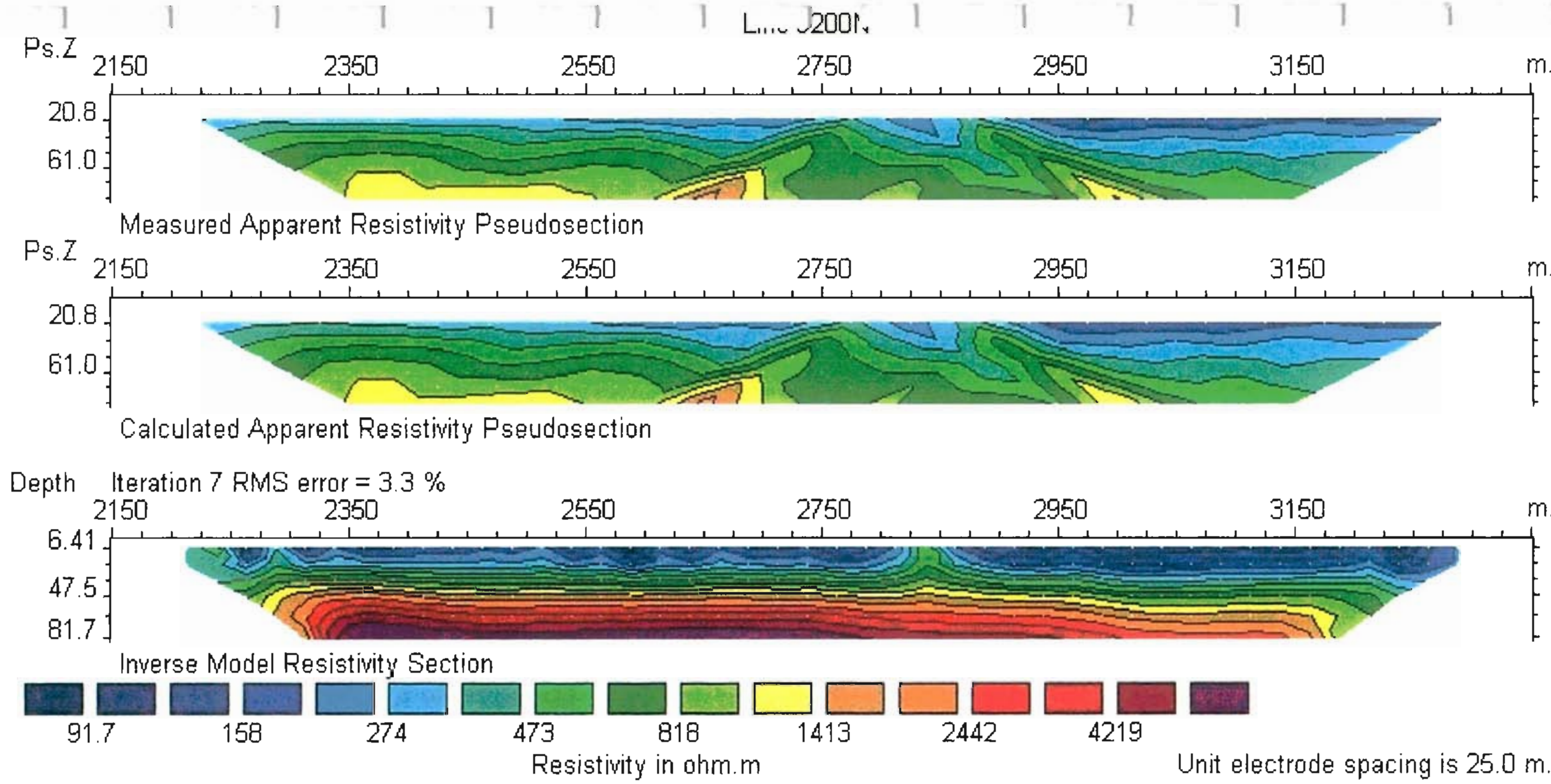
Line 9200N
Ps.Z
2150
2350
2550
2750
2950
3150
m.
20.8
61.0
Measured Apparent Resistivity Pseudosection
Ps.Z
2150
2350
2550
2750
2950
3150
m.
20.8
61.0
Calculated Apparent Resistivity Pseudosection
Depth
Iteration 7 RMS error = 3.3 %
2150
2350
2550
2750
2950
3150
m.
6.41
47.5
81.7
Inverse Model Resistivity Section
91.7
158
274
473
818
1413
2442
4219
Resistivity in ohm.m
Unit electrode spacing is 25.0 m.

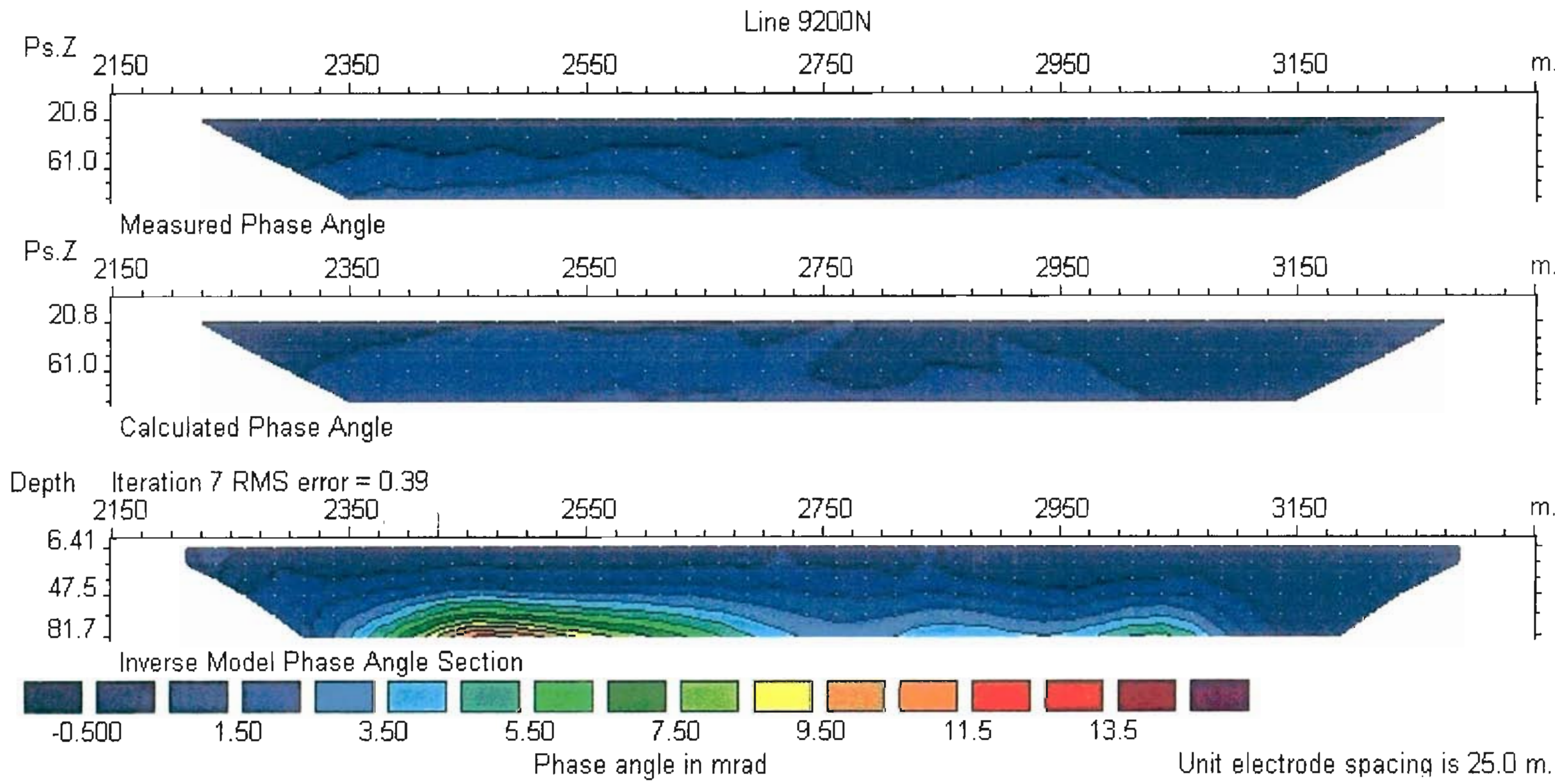
Line 9200N
Ps.Z
2150
2350
2550
2750
2950
3150
m.
20.8
61.0
Measured Phase Angle
Ps.Z
2150
2350
2550
2750
2950
3150
m.
20.8
61.0
Calculated Phase Angle
Depth
Iteration 7 RMS error = 0.39
2150
2350
2550
2750
2950
3150
m.
6.41
47.5
81.7
Inverse Model Phase Angle Section
-0.500
1.50
3.50
5.50
7.50
9.50
11.5
13.5
Phase angle in mrad
Unit electrode spacing is 25.0 m.

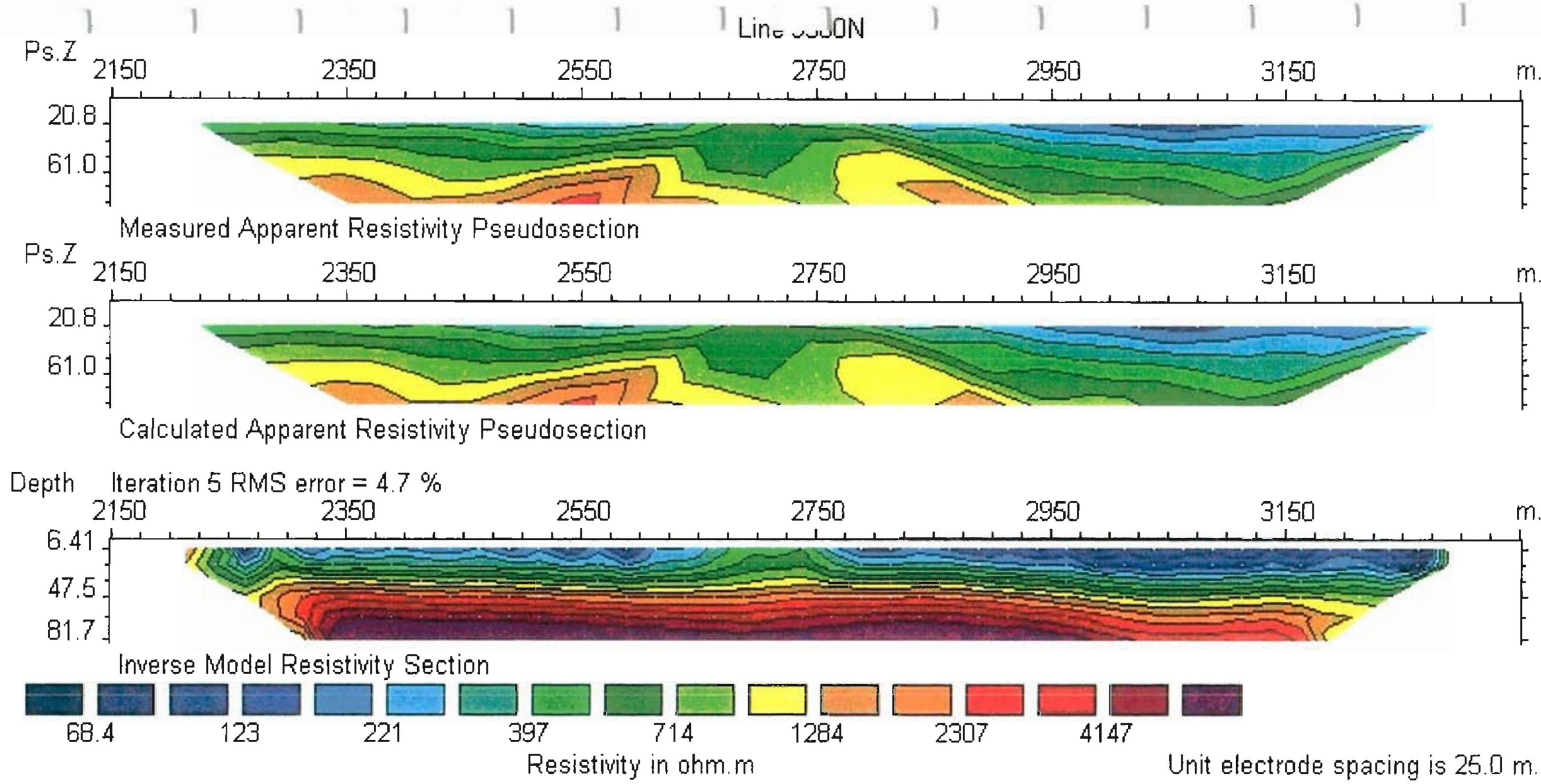
Ps.Z
2150
2350
2550
2750
2950
3150
m.
20.8
61.0
Measured Apparent Resistivity Pseudosection
Calculated Apparent Resistivity Pseudosection
Depth
Iteration 5 RMS error = 4.7 %
6.41
47.5
81.7
Inverse Model Resistivity Section
68.4
123
221
397
714
1284
2307
4147
Resistivity in ohm.m
Unit electrode spacing is 25.0 m.

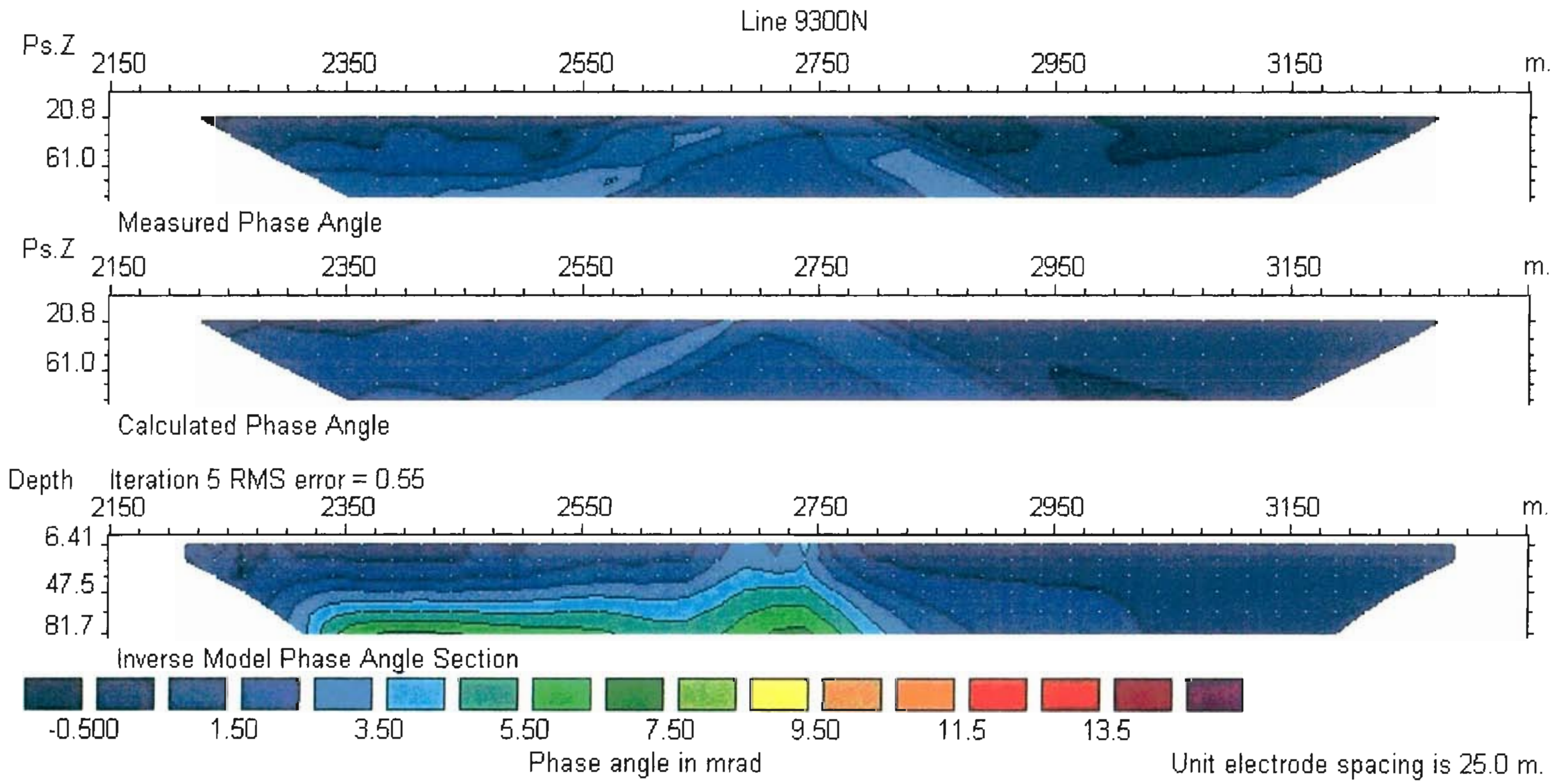
Line 9300N
Ps.Z
2150
2350
2550
2750
2950
3150
m.
20.8
61.0
Measured Phase Angle
Calculated Phase Angle
Depth
Iteration 5 RMS error = 0.55
6.41
47.5
81.7
Inverse Model Phase Angle Section
-0.500
1.50
3.50
5.50
7.50
9.50
11.5
13.5
Phase angle in mrad
Unit electrode spacing is 25.0 m.

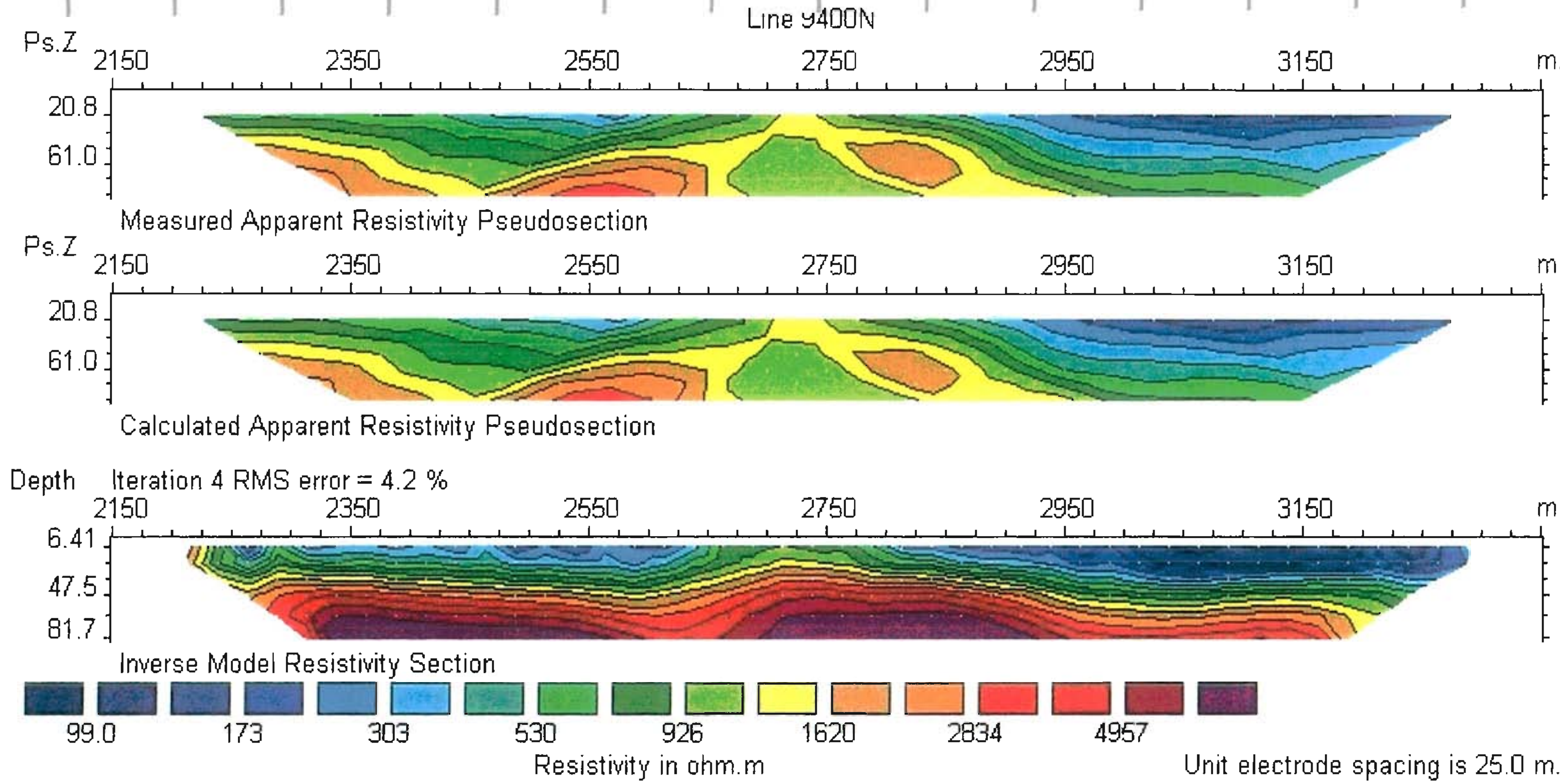
Line 9400N
Ps.Z
2150
2350
2550
2750
2950
3150
m.
20.8
61.0
Measured Apparent Resistivity Pseudosection
Ps.Z
2150
2350
2550
2750
2950
3150
m.
20.8
61.0
Calculated Apparent Resistivity Pseudosection
Depth
Iteration 4 RMS error = 4.2 %
2150
2350
2550
2750
2950
3150
m.
6.41
47.5
81.7
Inverse Model Resistivity Section
99.0
173
303
530
926
1620
2834
4957
Resistivity in ohm.m
Unit electrode spacing is 25.0 m.

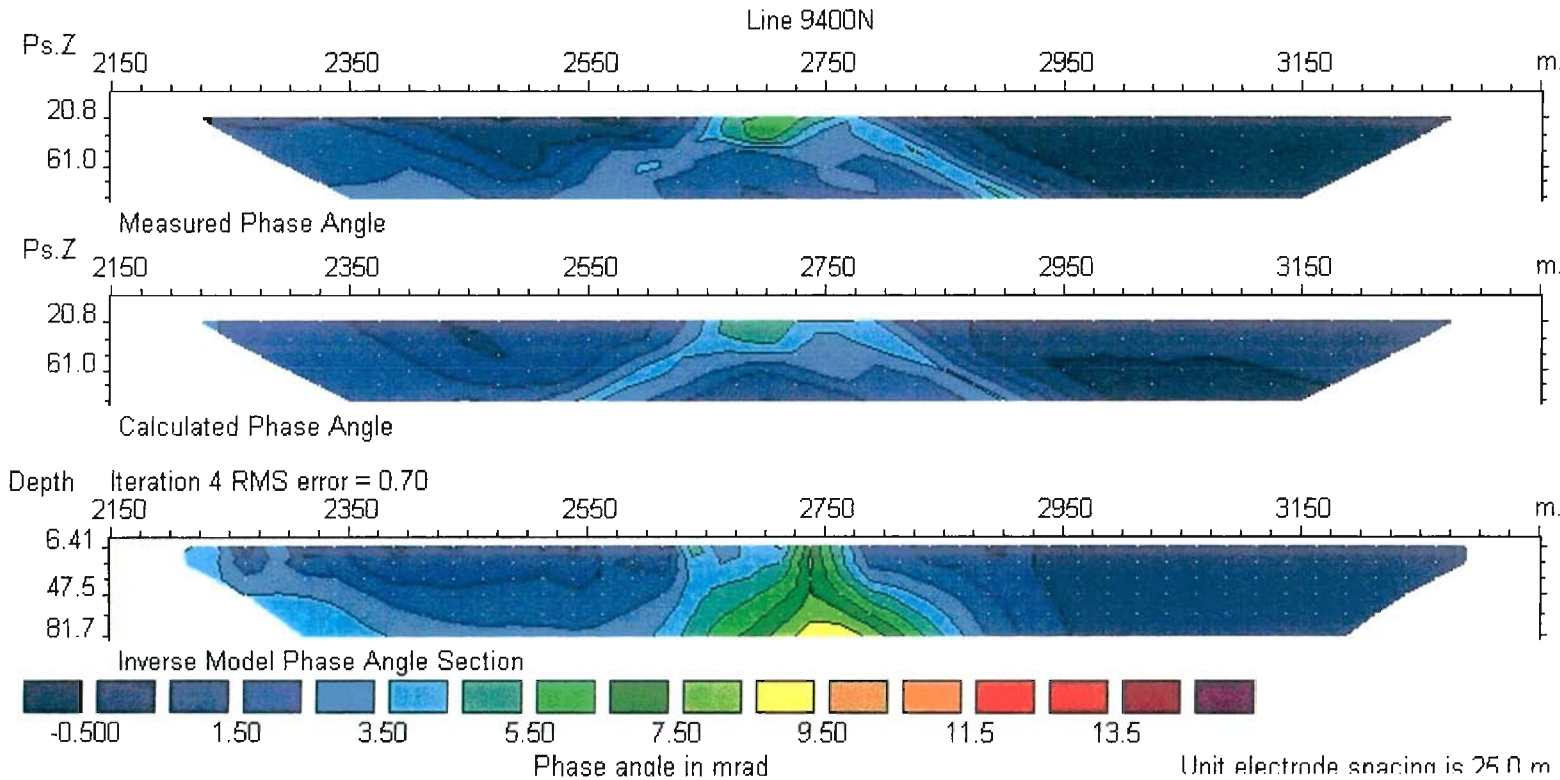
Line 9400N
Ps.Z
2150
2350
2550
2750
2950
3150
m.
20.8
61.0
Measured Phase Angle
Ps.Z
2150
2350
2550
2750
2950
3150
m.
20.8
61.0
Calculated Phase Angle
Depth
Iteration 4 RMS error = 0.70
2150
2350
2550
2750
2950
3150
m.
6.41
47.5
81.7
Inverse Model Phase Angle Section
-0.500
1.50
3.50
5.50
7.50
9.50
11.5
13.5
Phase angle in mrad
Unit electrode spacing is 25.0 m.

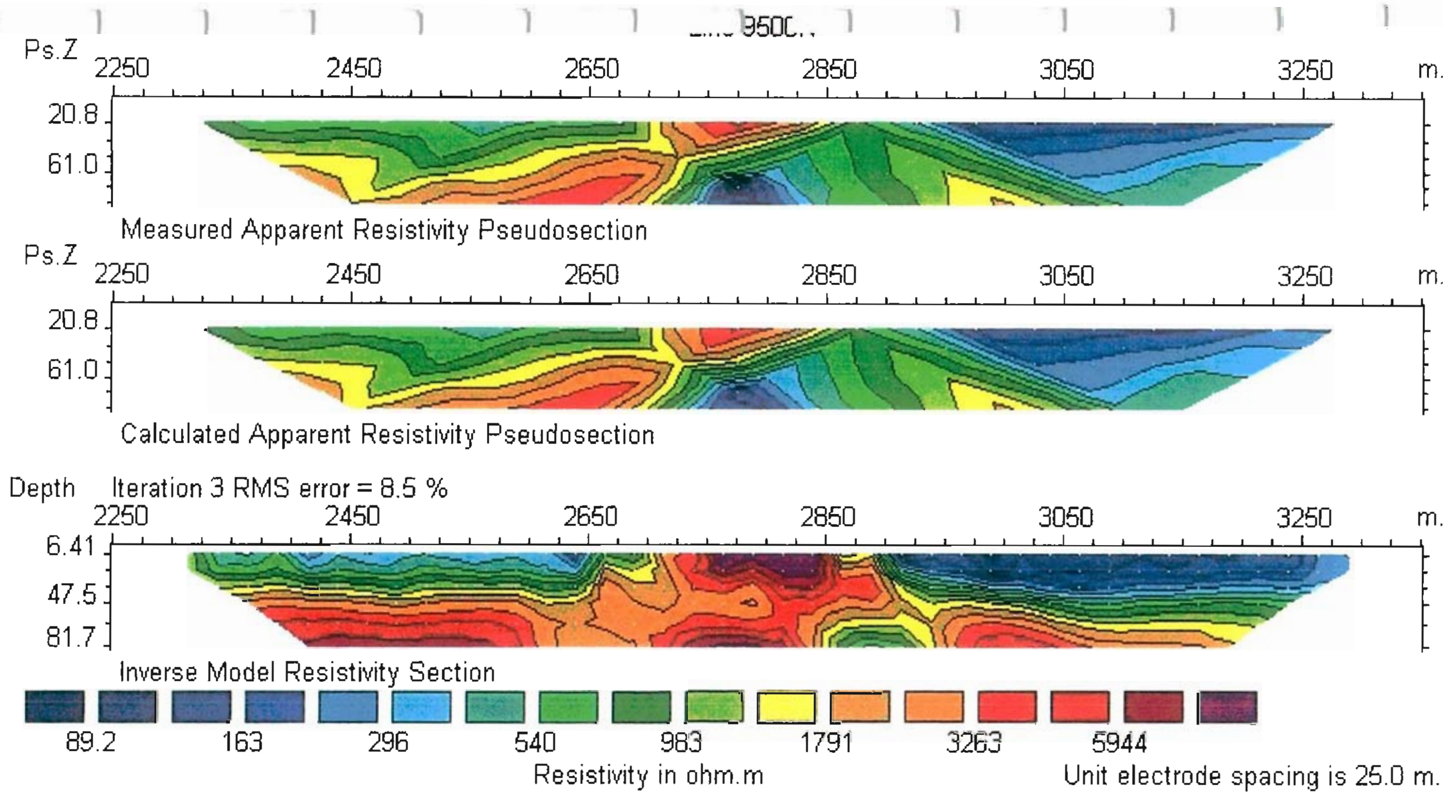

Ps.Z
2250 2450 2650 2850 3050 3250 m.
20.8
61.0
Measured Apparent Resistivity Pseudosection
Ps.Z
2250 2450 2650 2850 3050 3250 m.
20.8
61.0
Calculated Apparent Resistivity Pseudosection
Depth Iteration 3 RMS error = 8.5 %
2250 2450 2650 2850 3050 3250 m.
6.41
47.5
81.7
Inverse Model Resistivity Section
89.2 163 296 540 983 1791 3263 5944
Resistivity in ohm.m
Unit electrode spacing is 25.0 m.

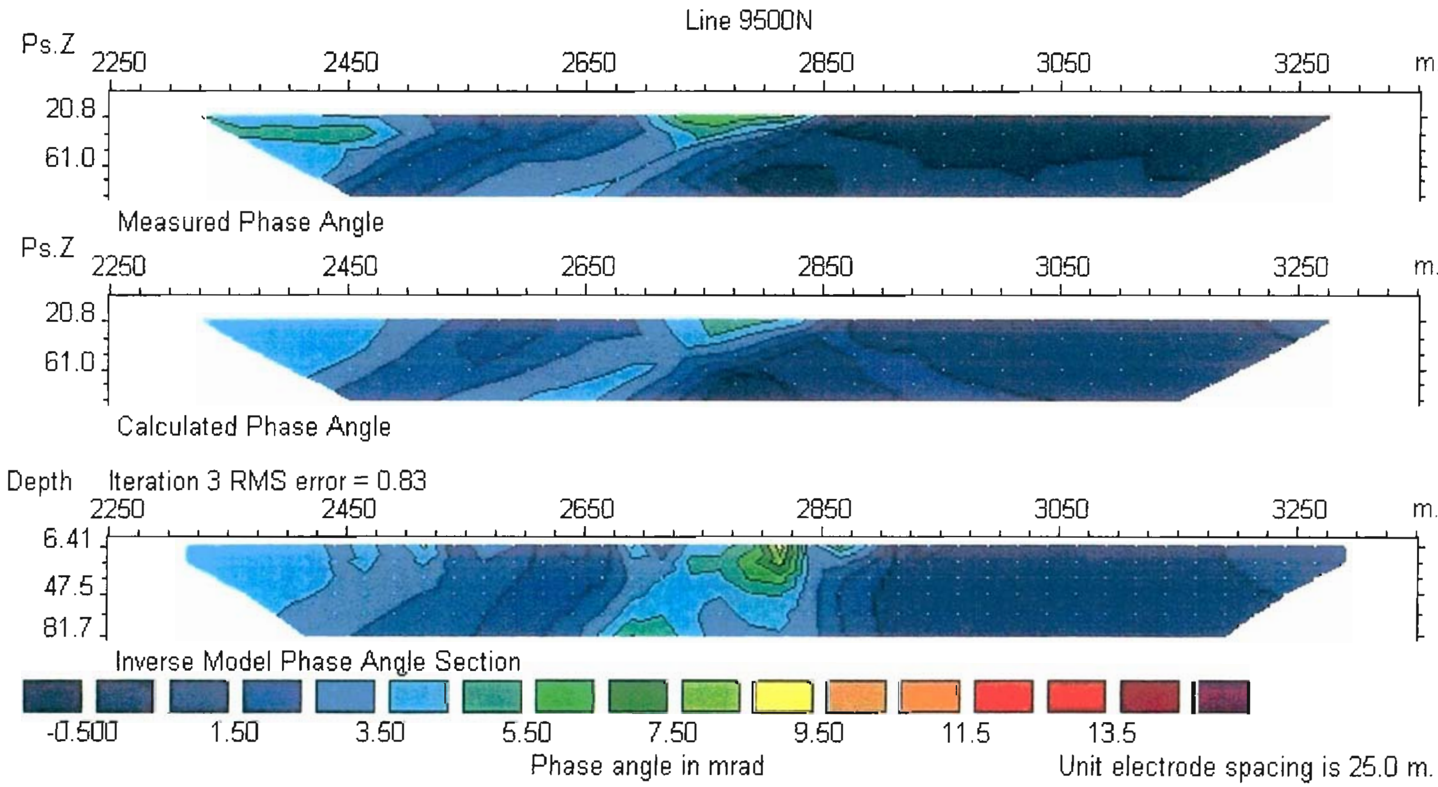

Line 9500N
Ps.Z
2250 2450 2650 2850 3050 3250 m.
20.8
61.0
Measured Phase Angle
Ps.Z
2250 2450 2650 2850 3050 3250 m.
20.8
61.0
Calculated Phase Angle
Depth Iteration 3 RMS error = 0.83
2250 2450 2650 2850 3050 3250 m.
6.41
47.5
81.7
Inverse Model Phase Angle Section
-0.500 1.50 3.50 5.50 7.50 9.50 11.5 13.5
Phase angle in mrad
Unit electrode spacing is 25.0 m.

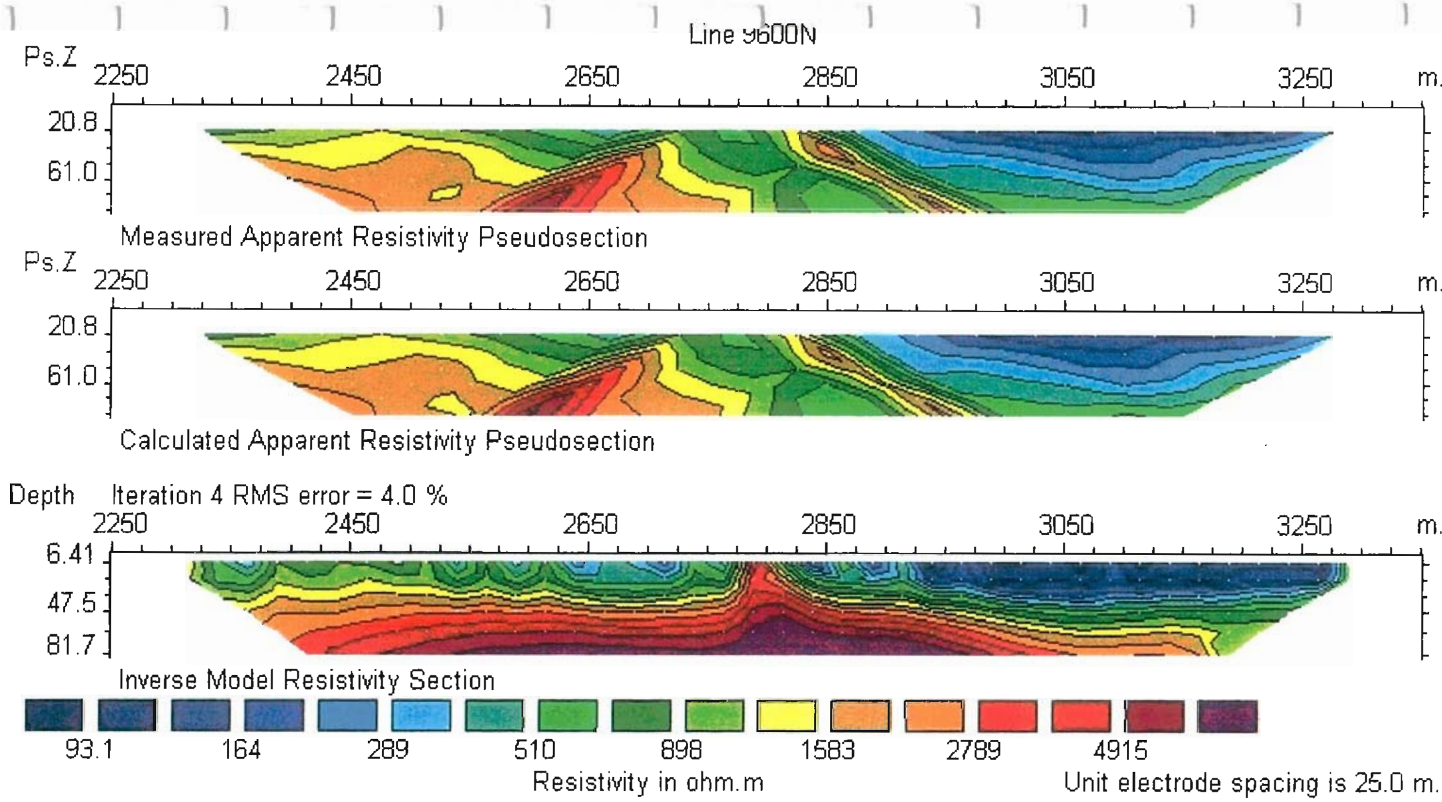
Line 9600N
Ps.Z
2250 2450 2650 2850 3050 3250 m.
20.8
61.0
Measured Apparent Resistivity Pseudosection
Ps.Z
2250 2450 2650 2850 3050 3250 m.
20.8
61.0
Calculated Apparent Resistivity Pseudosection
Depth
Iteration 4 RMS error = 4.0 %
2250 2450 2650 2850 3050 3250 m.
6.41
47.5
81.7
Inverse Model Resistivity Section
93.1 164 289 510 898 1583 2789 4915
Resistivity in ohm.m
Unit electrode spacing is 25.0 m.

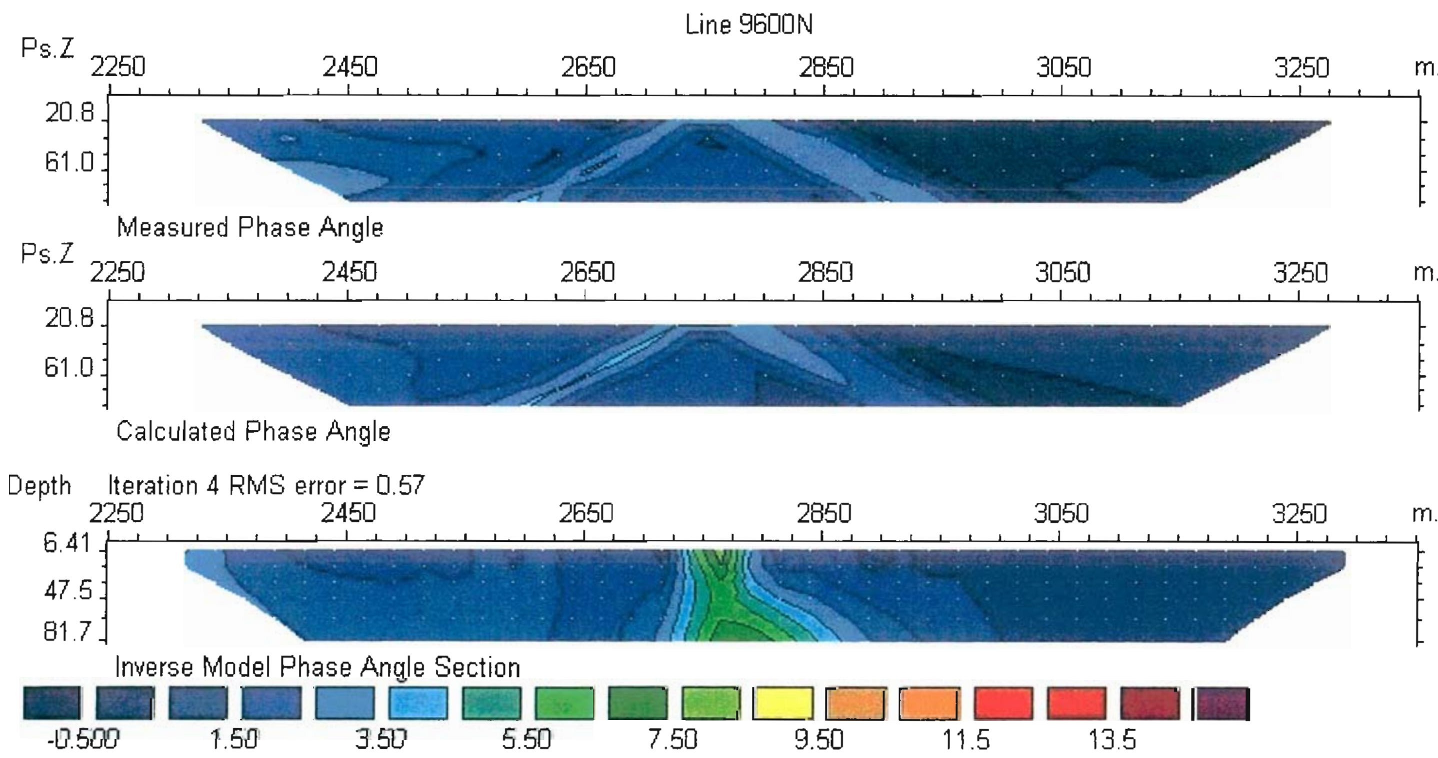
Line 9600N
Ps.Z
2250 2450 2650 2850 3050 3250 m.
20.8
61.0
Measured Phase Angle
Ps.Z
2250 2450 2650 2850 3050 3250 m.
20.8
61.0
Calculated Phase Angle
Depth
Iteration 4 RMS error = 0.57
2250 2450 2650 2850 3050 3250 m.
6.41
47.5
81.7
Inverse Model Phase Angle Section
-0.500 1.50 3.50 5.50 7.50 9.50 11.5 13.5

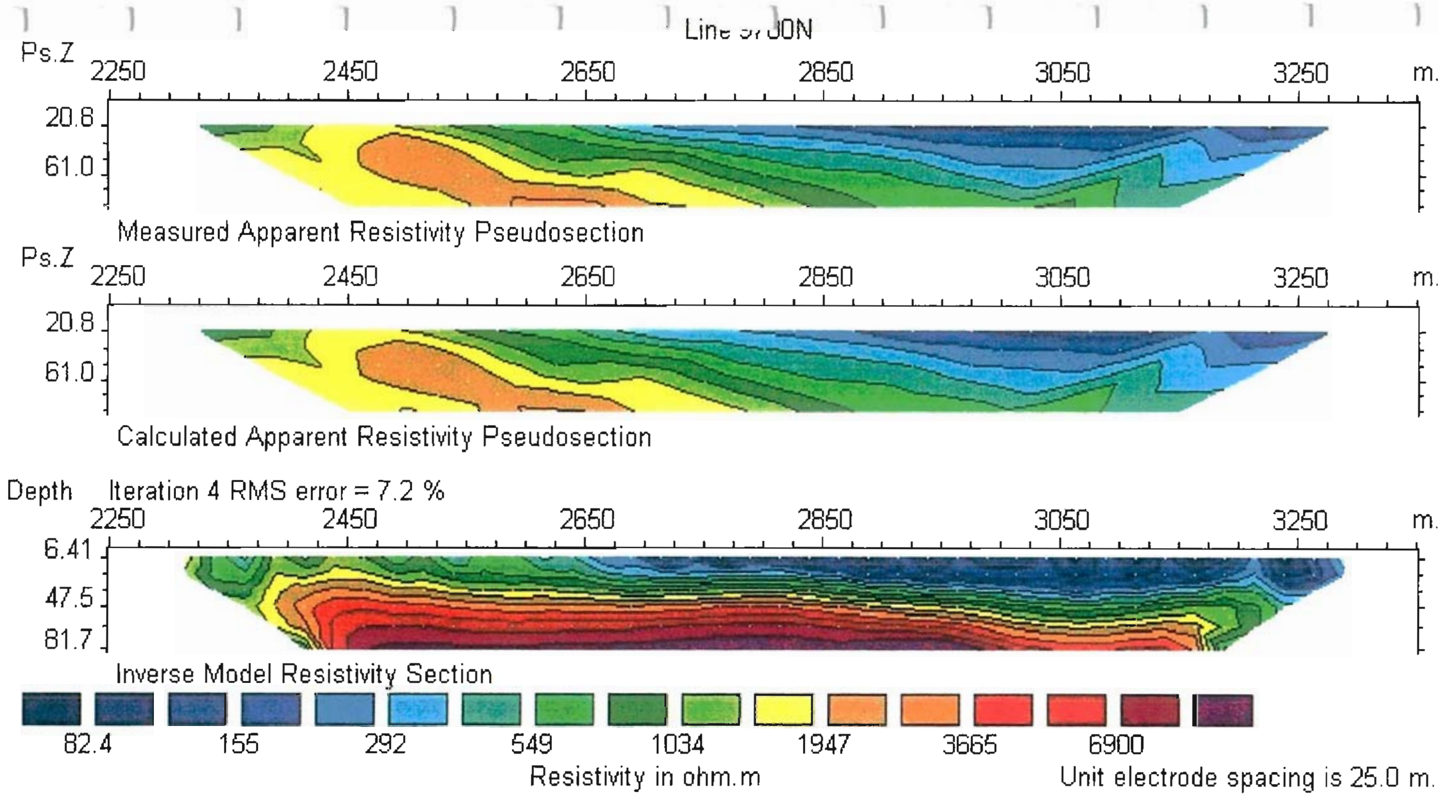
Ps.Z
2250 2450 2650 2850 3050 3250 m.
20.8
61.0
Measured Apparent Resistivity Pseudosection
Ps.Z
2250 2450 2650 2850 3050 3250 m.
20.8
61.0
Calculated Apparent Resistivity Pseudosection
Depth
Iteration 4 RMS error = 7.2 %
2250 2450 2650 2850 3050 3250 m.
6.41
47.5
81.7
Inverse Model Resistivity Section
82.4 155 292 549 1034 1947 3665 6900
Resistivity in ohm.m
Unit electrode spacing is 25.0 m.

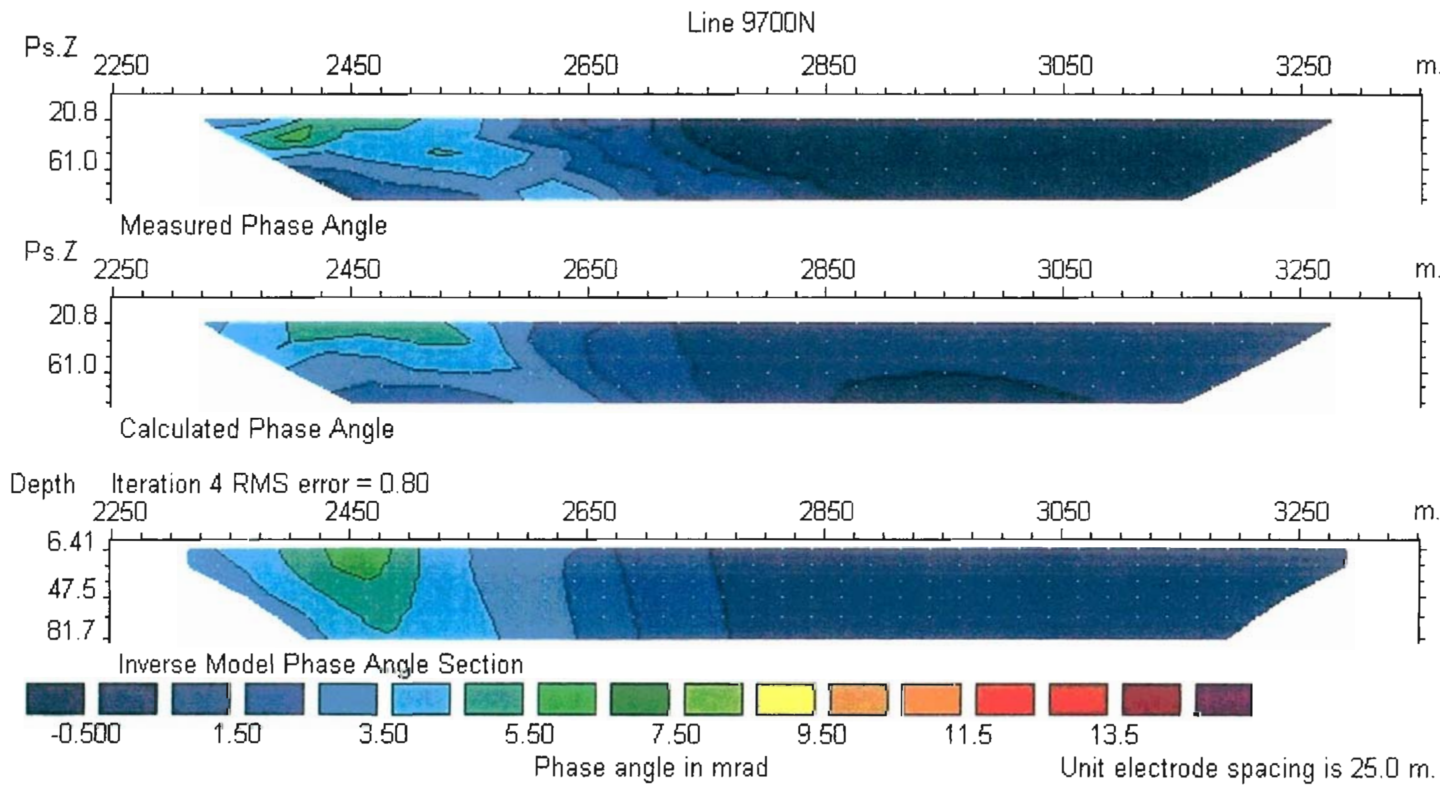
Line 9700N
Ps.Z
2250 2450 2650 2850 3050 3250 m.
20.8
61.0
Measured Phase Angle
Ps.Z
2250 2450 2650 2850 3050 3250 m.
20.8
61.0
Calculated Phase Angle
Depth
Iteration 4 RMS error = 0.80
2250 2450 2650 2850 3050 3250 m.
6.41
47.5
81.7
Inverse Model Phase Angle Section
-0.500 1.50 3.50 5.50 7.50 9.50 11.5 13.5
Phase angle in mrad
Unit electrode spacing is 25.0 m.

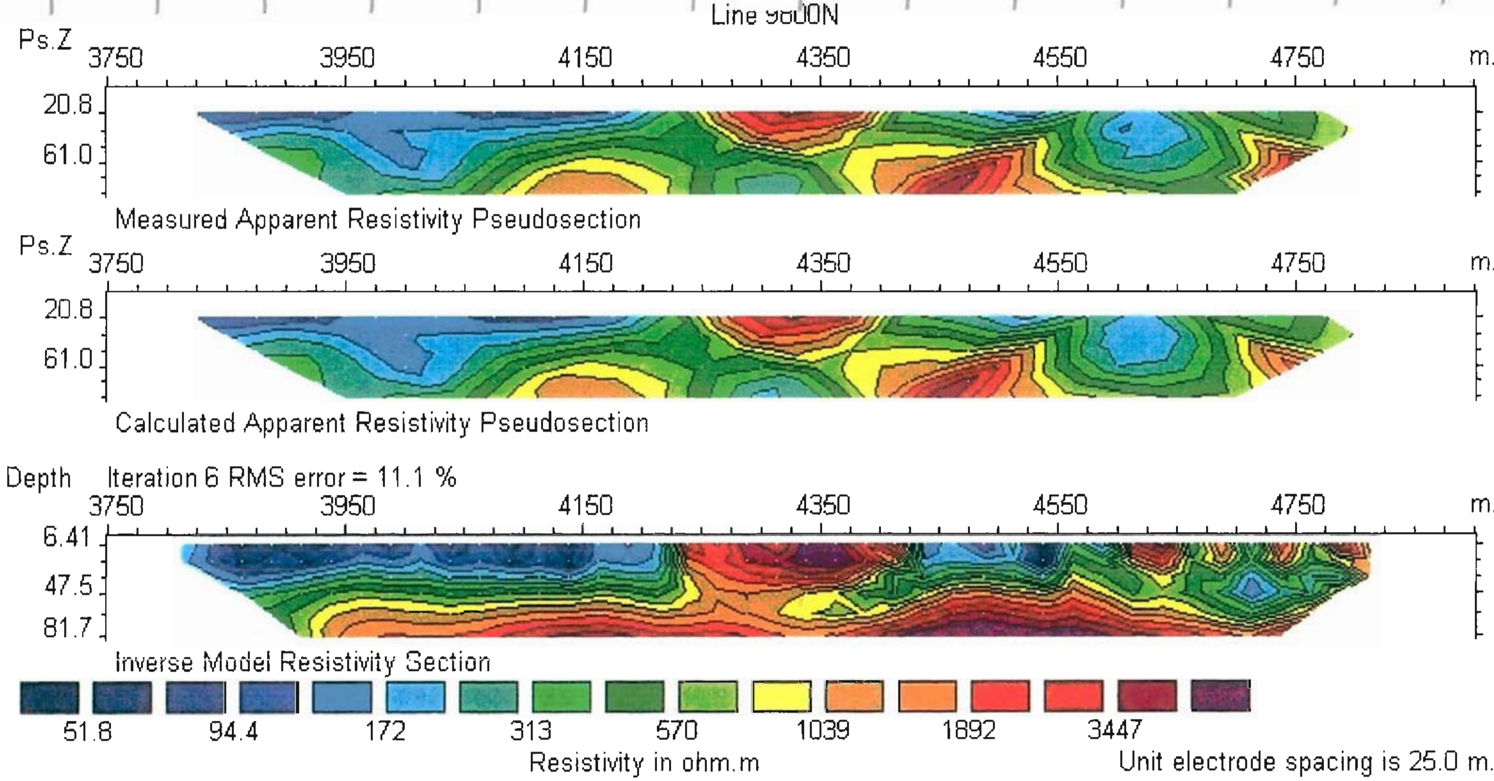
Line 9800N
Ps.Z
3750 3950 4150 4350 4550 4750 m.
20.8
61.0
Measured Apparent Resistivity Pseudosection
Ps.Z
3750 3950 4150 4350 4550 4750 m.
20.8
61.0
Calculated Apparent Resistivity Pseudosection
Depth
Iteration 6 RMS error = 11.1 %
3750 3950 4150 4350 4550 4750 m.
6.41
47.5
81.7
Inverse Model Resistivity Section
51.8 94.4 172 313 570 1039 1892 3447
Resistivity in ohm.m
Unit electrode spacing is 25.0 m.

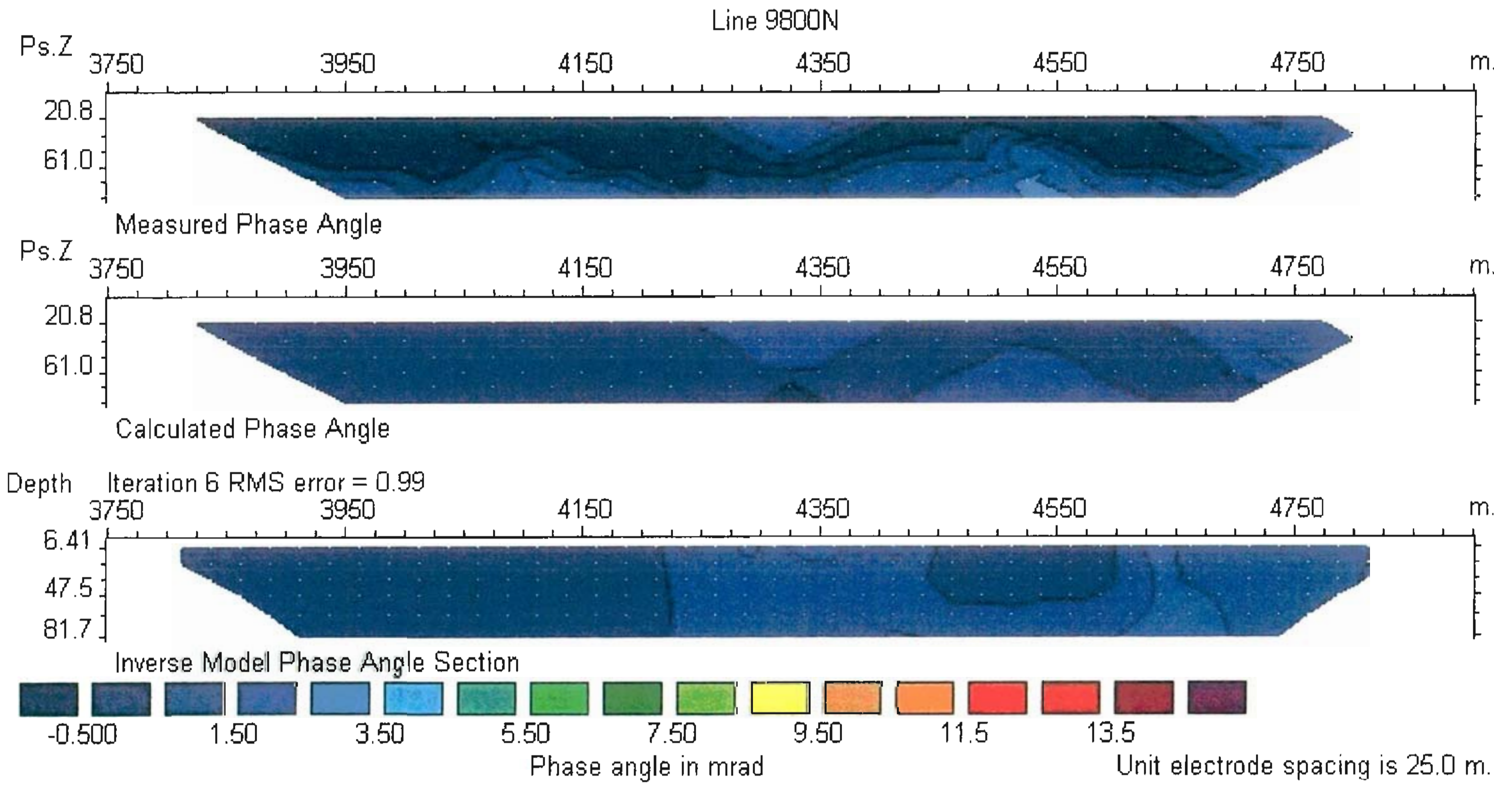
Line 9800N
Ps.Z
3750 3950 4150 4350 4550 4750 m.
20.8
61.0
Measured Phase Angle
Ps.Z
3750 3950 4150 4350 4550 4750 m.
20.8
61.0
Calculated Phase Angle
Depth
Iteration 6 RMS error = 0.99
3750 3950 4150 4350 4550 4750 m.
6.41
47.5
81.7
Inverse Model Phase Angle Section
-0.500 1.50 3.50 5.50 7.50 9.50 11.5 13.5
Phase angle in mrad
Unit electrode spacing is 25.0 m.

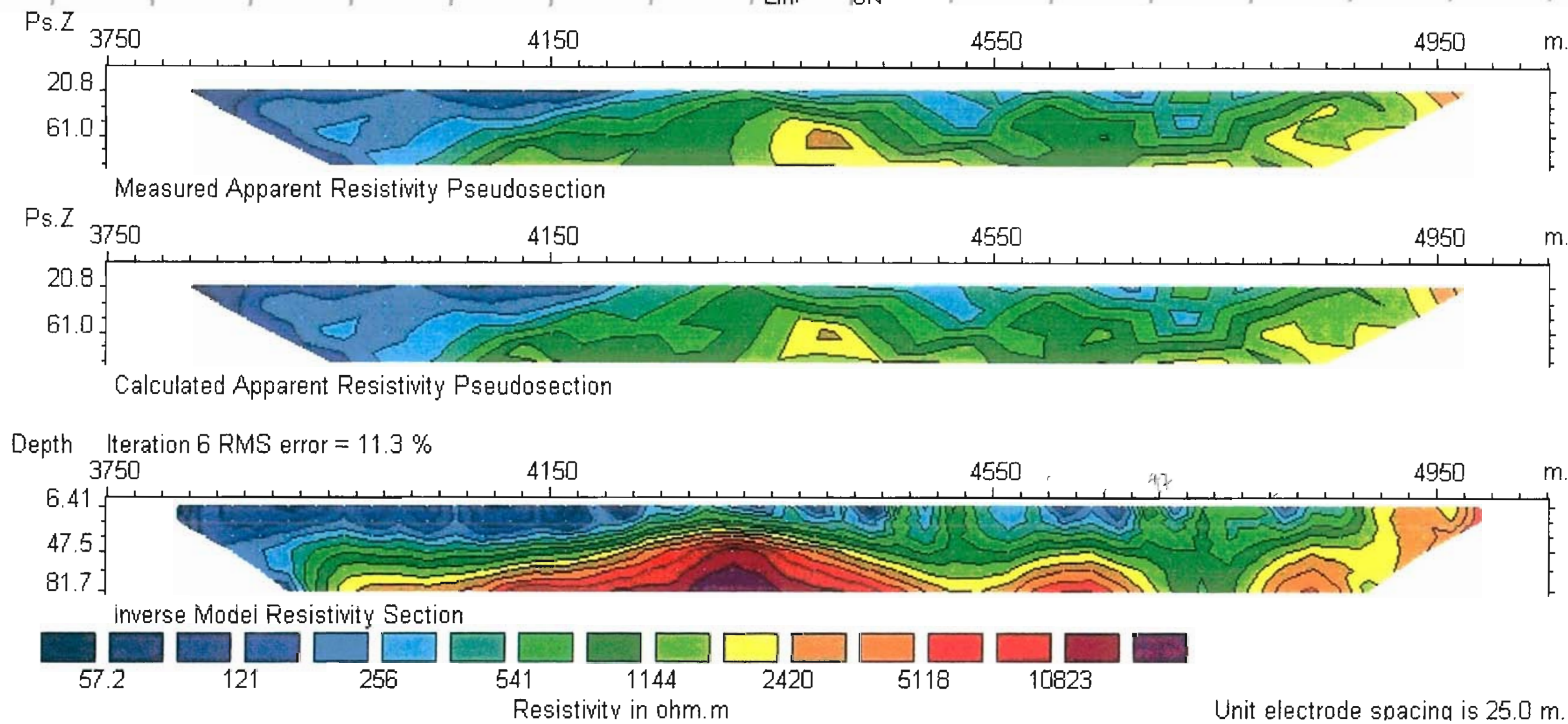
Ps.Z
3750
4150
4550
4950
m.
20.8
61.0
Measured Apparent Resistivity Pseudosection
Ps.Z
3750
4150
4550
4950
m.
20.8
61.0
Calculated Apparent Resistivity Pseudosection
Depth
Iteration 6 RMS error = 11.3 %
3750
4150
4550
4950
m.
6.41
47.5
81.7
Inverse Model Resistivity Section
57.2
121
256
541
1144
2420
5118
10823
Resistivity in ohm.m
Unit electrode spacing is 25.0 m.

Line 9900N

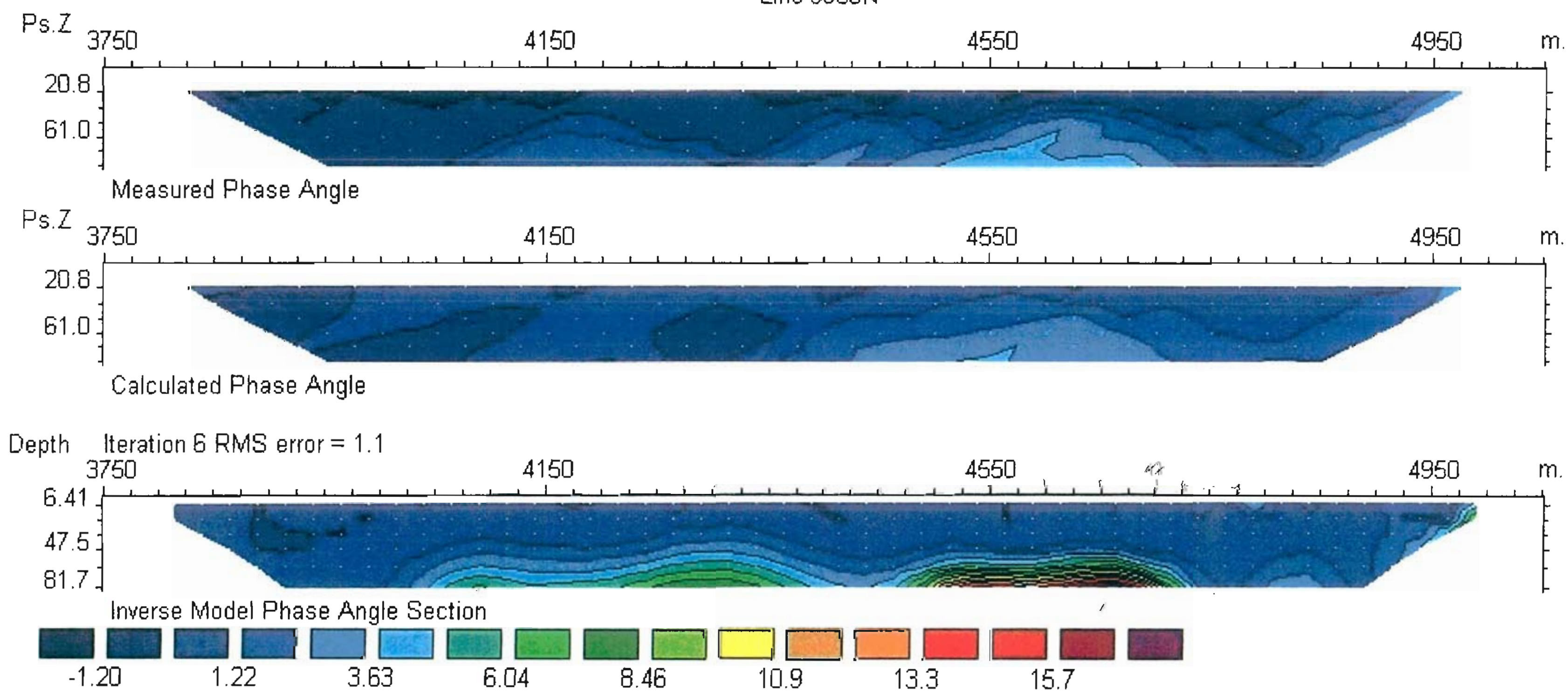
Ps.Z
3750
4150
4550
4950
m.
20.8
61.0
Measured Phase Angle
Ps.Z
3750
4150
4550
4950
m.
20.8
61.0
Calculated Phase Angle
Depth
Iteration 6 RMS error = 1.1
3750
4150
4550
4950
m.
6.41
47.5
81.7
Inverse Model Phase Angle Section
-1.20
1.22
3.63
6.04
8.46
10.9
13.3
15.7

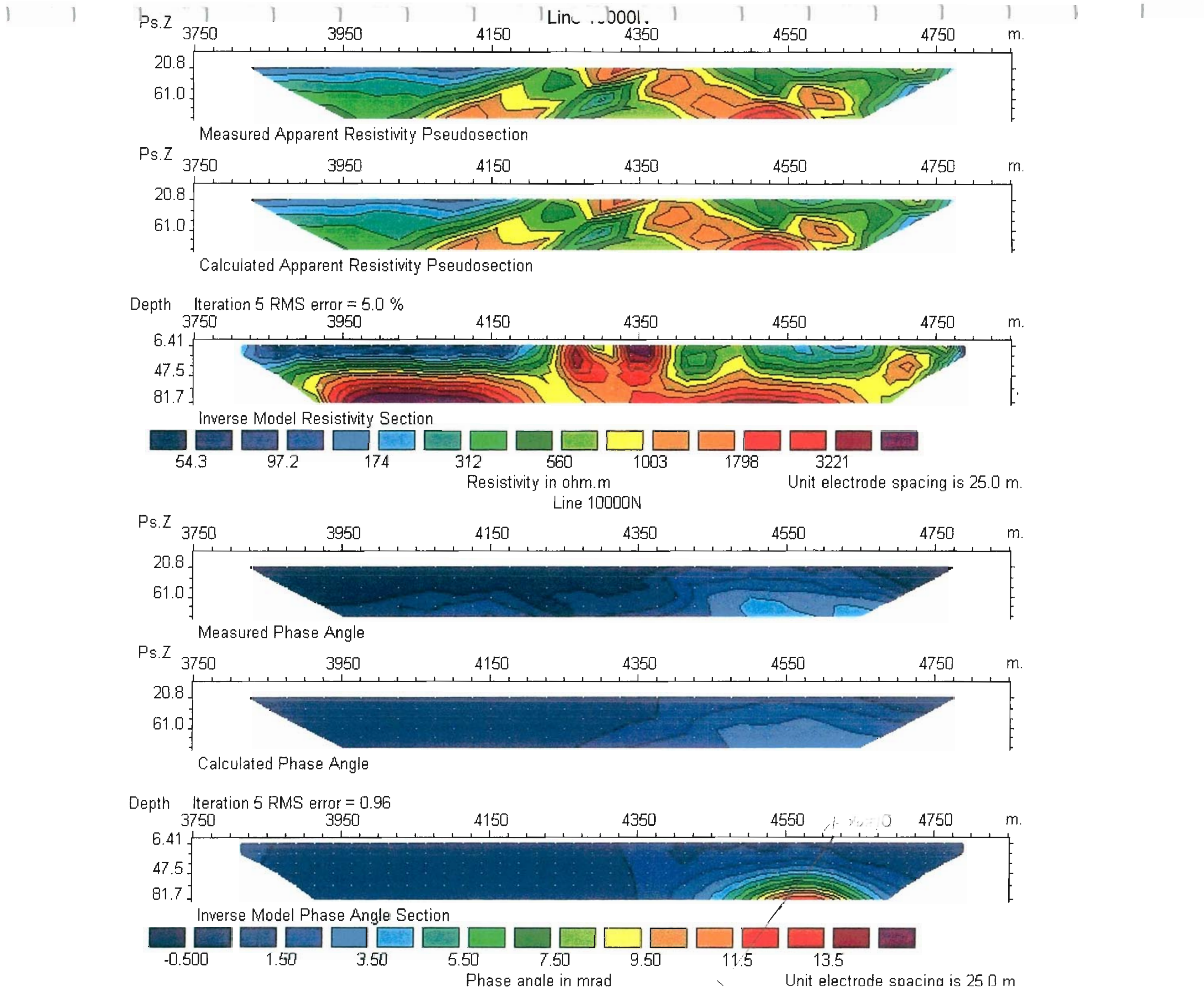
Ps.Z
3750
3950
4150
4350
4550
4750
m.
20.8
61.0
Measured Apparent Resistivity Pseudosection
Ps.Z
3750
3950
4150
4350
4550
4750
m.
20.8
61.0
Calculated Apparent Resistivity Pseudosection
Depth
Iteration 5 RMS error = 5.0 %
3750
3950
4150
4350
4550
4750
m.
6.41
47.5
81.7
Inverse Model Resistivity Section
54.3
97.2
174
312
560
1003
1798
3221
Resistivity in ohm.m
Unit electrode spacing is 25.0 m.
Line 10000N
Ps.Z
3750
3950
4150
4350
4550
4750
m.
20.8
61.0
Measured Phase Angle
Ps.Z
3750
3950
4150
4350
4550
4750
m.
20.8
61.0
Calculated Phase Angle
Depth
Iteration 5 RMS error = 0.96
3750
3950
4150
4350
4550
4750
m.
6.41
47.5
81.7
Inverse Model Phase Angle Section
-0.500
1.50
3.50
5.50
7.50
9.50
11.5
13.5
Phase angle in mrad
Unit electrode spacing is 25.0 m

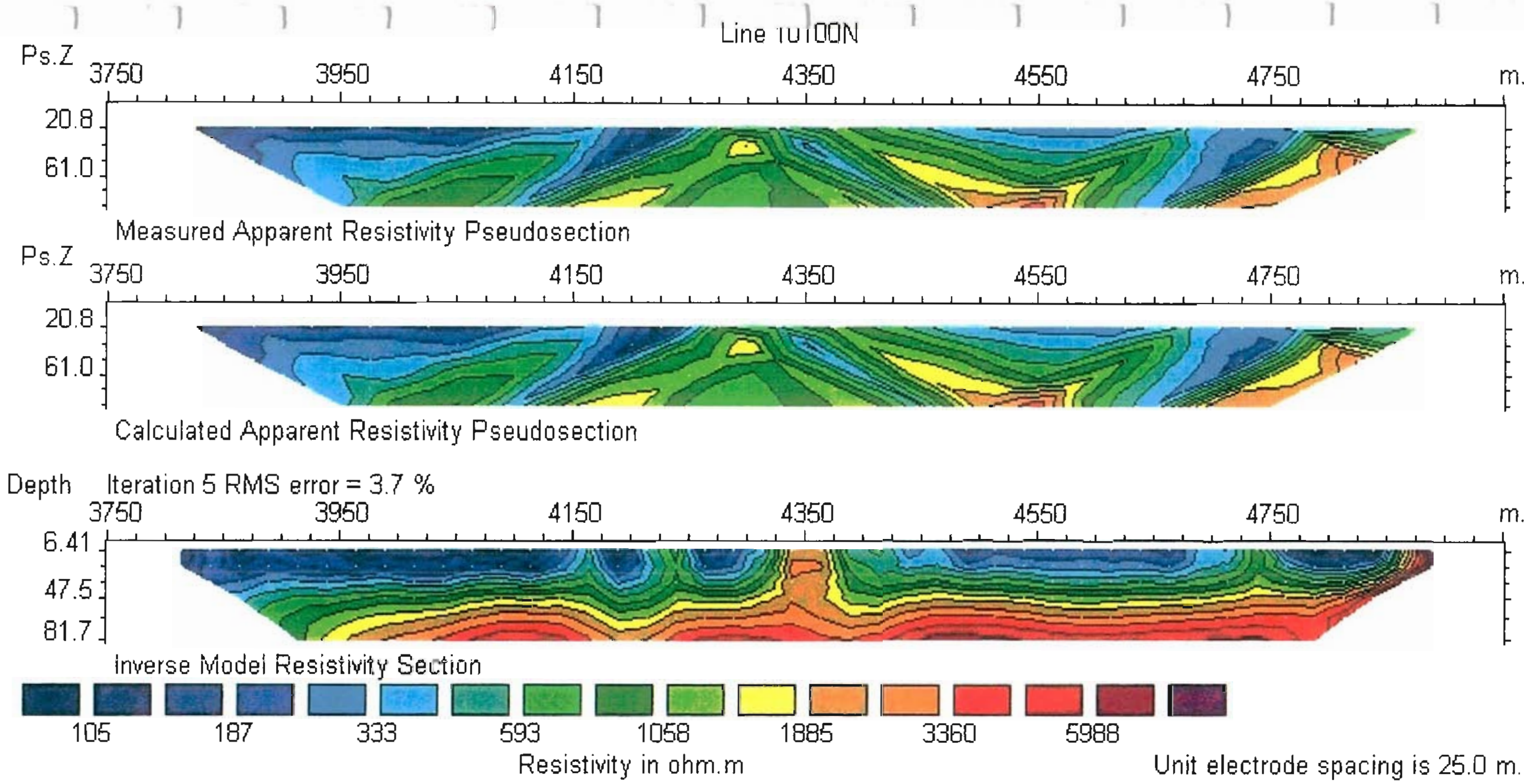

Line 10100N
Ps.Z
3750 3950 4150 4350 4550 4750 m.
20.8
61.0
Measured Apparent Resistivity Pseudosection
Ps.Z
3750 3950 4150 4350 4550 4750 m.
20.8
61.0
Calculated Apparent Resistivity Pseudosection
Depth
Iteration 5 RMS error = 3.7 %
3750 3950 4150 4350 4550 4750 m.
6.41
47.5
81.7
Inverse Model Resistivity Section
105 187 333 593 1058 1885 3360 5988
Resistivity in ohm.m
Unit electrode spacing is 25.0 m.

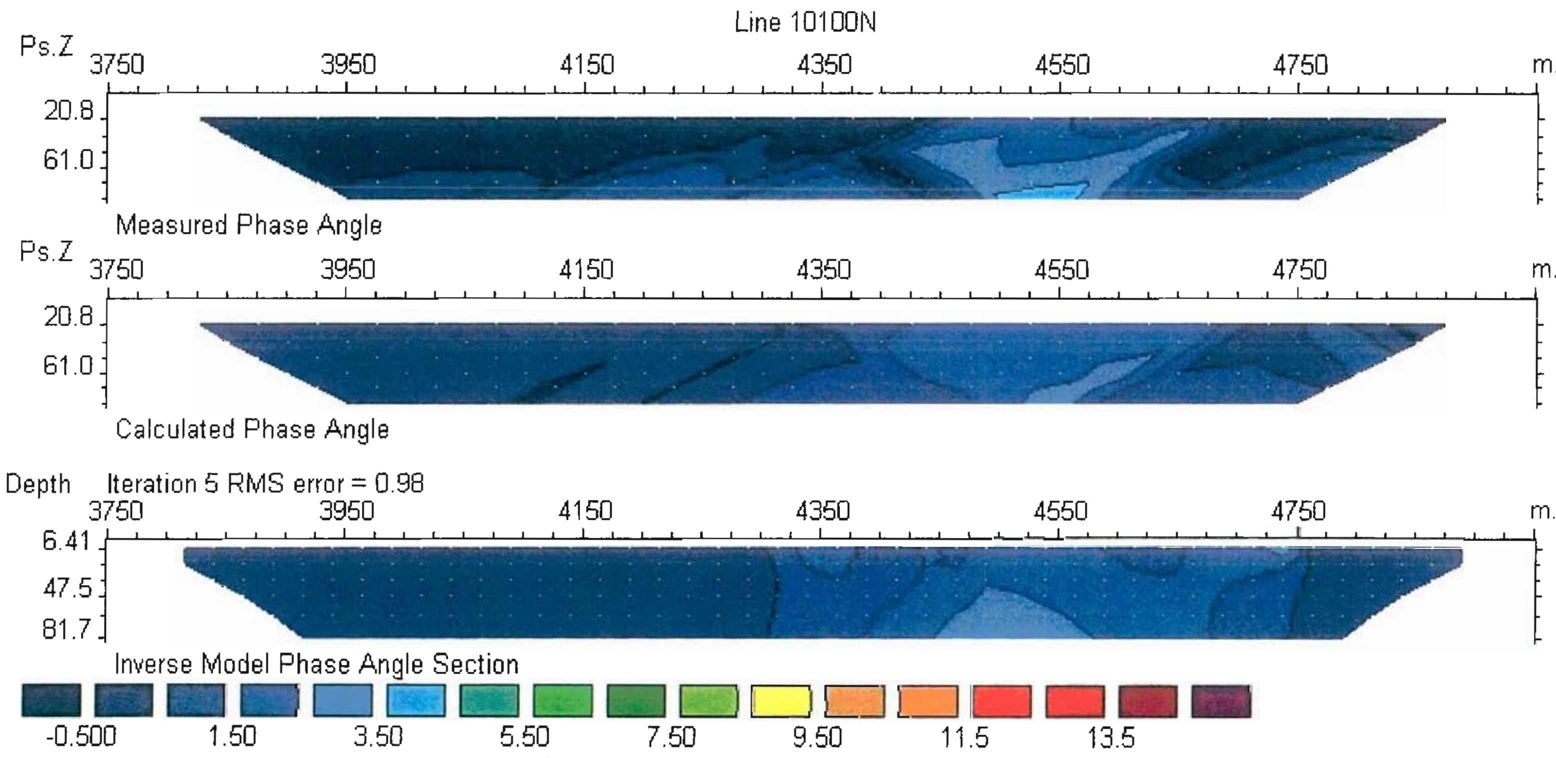

Line 10100N
Ps.Z
3750 3950 4150 4350 4550 4750 m.
20.8
61.0
Measured Phase Angle
Ps.Z
3750 3950 4150 4350 4550 4750 m.
20.8
61.0
Calculated Phase Angle
Depth
Iteration 5 RMS error = 0.98
3750 3950 4150 4350 4550 4750 m.
6.41
47.5
81.7
Inverse Model Phase Angle Section
-0.500 1.50 3.50 5.50 7.50 9.50 11.5 13.5

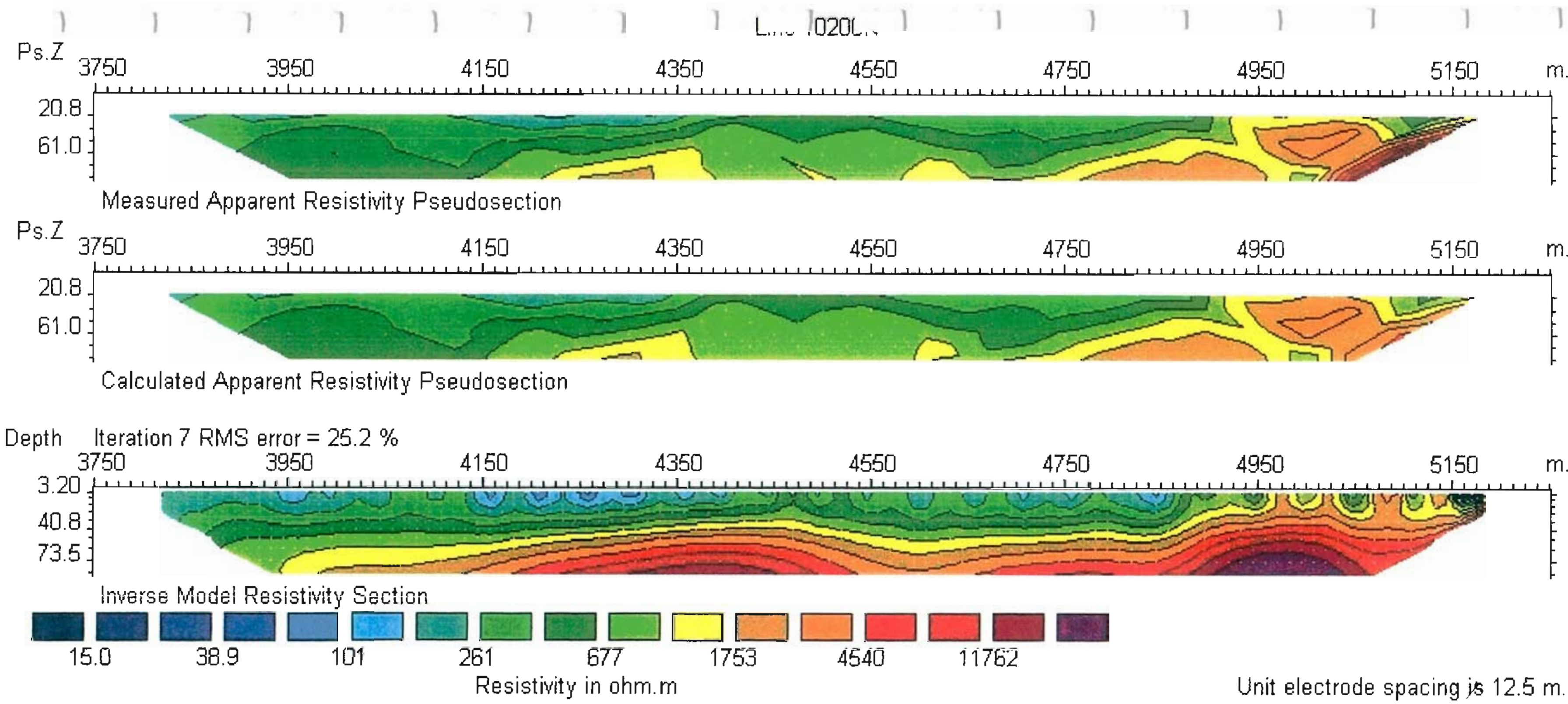
Ps.Z
3750 3950 4150 4350 4550 4750 4950 5150 m.
20.8
61.0
Measured Apparent Resistivity Pseudosection
Ps.Z
3750 3950 4150 4350 4550 4750 4950 5150 m.
20.8
61.0
Calculated Apparent Resistivity Pseudosection
Depth
Iteration 7 RMS error = 25.2 %
3750 3950 4150 4350 4550 4750 4950 5150 m.
3.20
40.8
73.5
Inverse Model Resistivity Section
15.0 38.9 101 261 677 1753 4540 11762
Resistivity in ohm.m
Unit electrode spacing is 12.5 m.

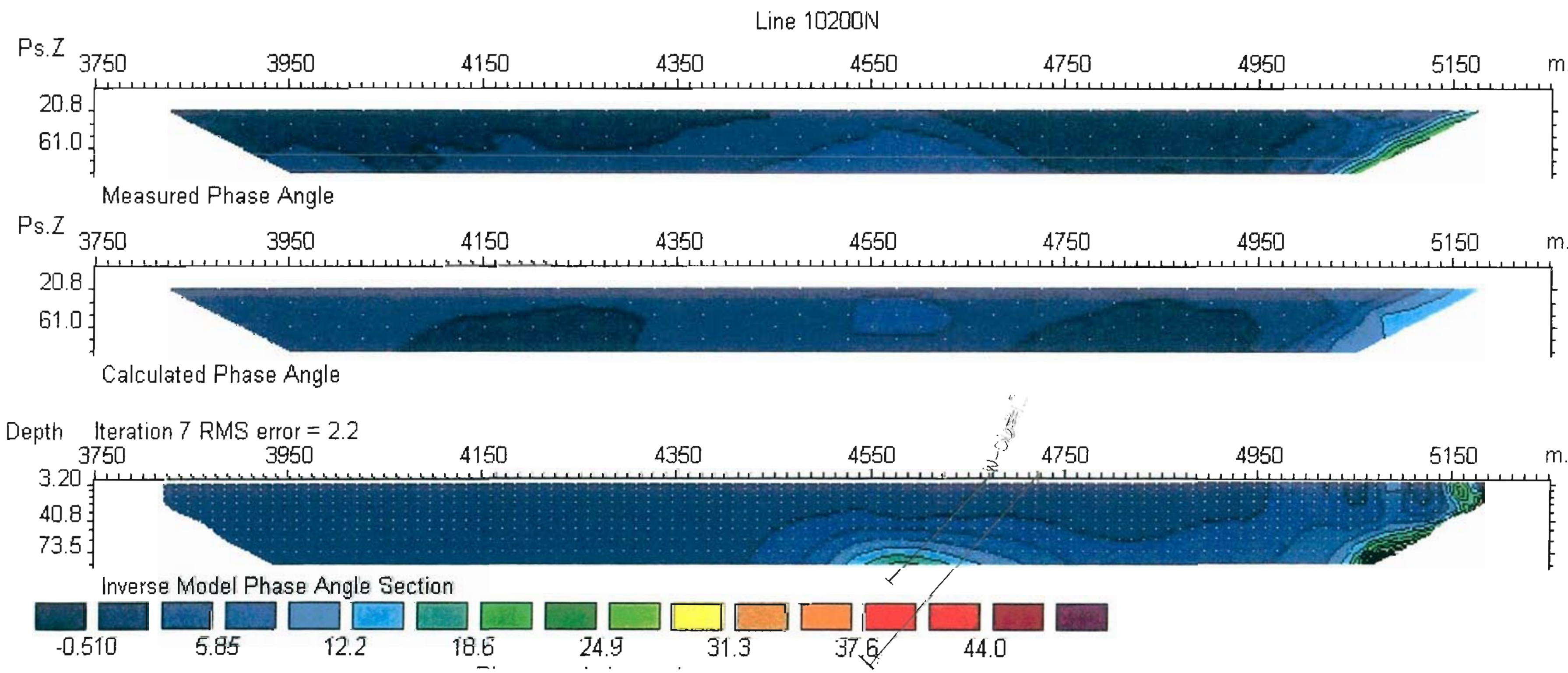
Line 10200N
Ps.Z
3750 3950 4150 4350 4550 4750 4950 5150 m.
20.8
61.0
Measured Phase Angle
Ps.Z
3750 3950 4150 4350 4550 4750 4950 5150 m.
20.8
61.0
Calculated Phase Angle
Depth
Iteration 7 RMS error = 2.2
3750 3950 4150 4350 4550 4750 4950 5150 m.
3.20
40.8
73.5
Inverse Model Phase Angle Section
-0.510 5.85 12.2 18.6 24.9 31.3 37.6 44.0

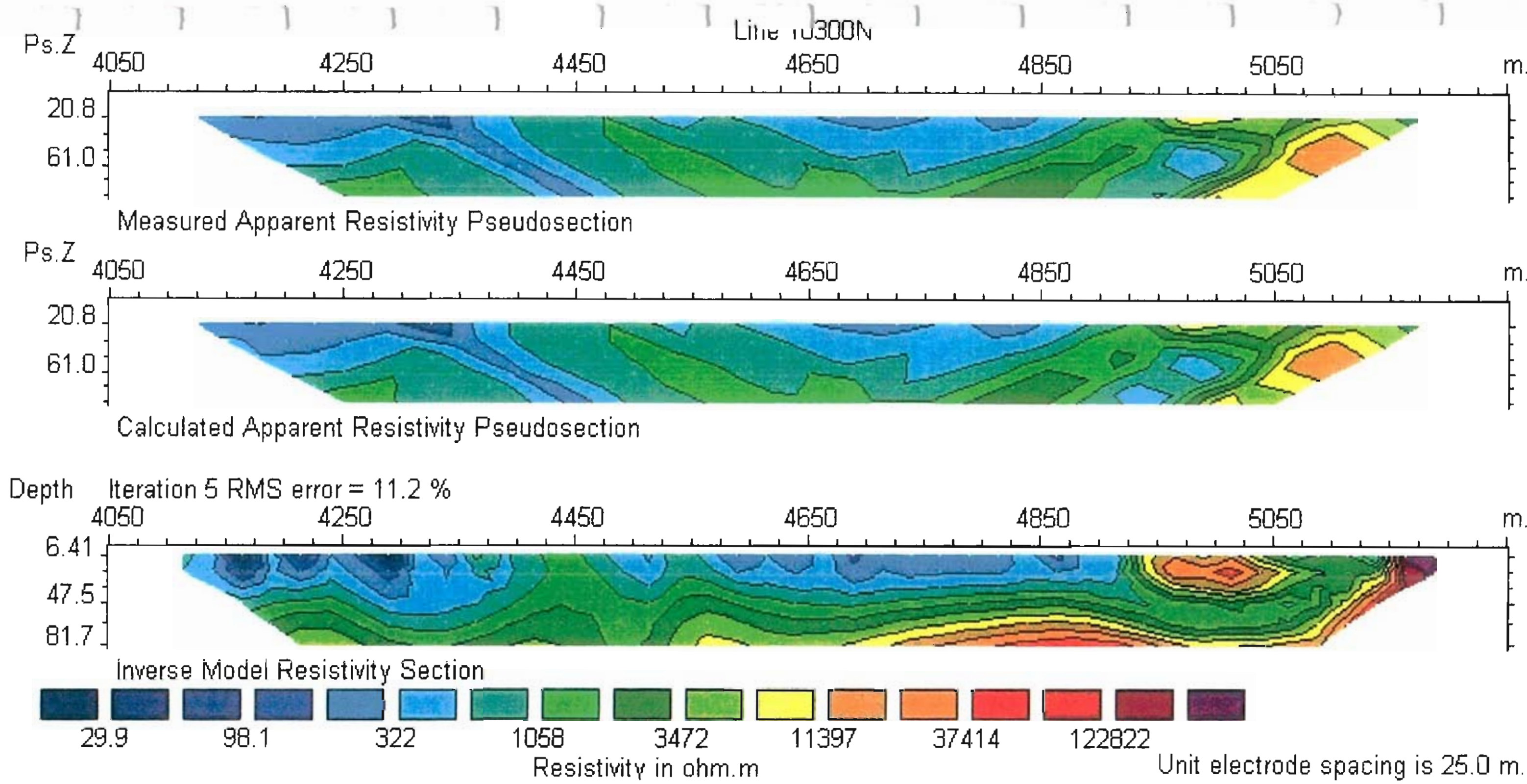
Line 10300N
Ps.Z
4050 4250 4450 4650 4850 5050 m.
20.8
61.0
Measured Apparent Resistivity Pseudosection
Ps.Z
4050 4250 4450 4650 4850 5050 m.
20.8
61.0
Calculated Apparent Resistivity Pseudosection
Depth
Iteration 5 RMS error = 11.2 %
4050 4250 4450 4650 4850 5050 m.
6.41
47.5
81.7
Inverse Model Resistivity Section
29.9 98.1 322 1058 3472 11397 37414 122822
Resistivity in ohm.m
Unit electrode spacing is 25.0 m.

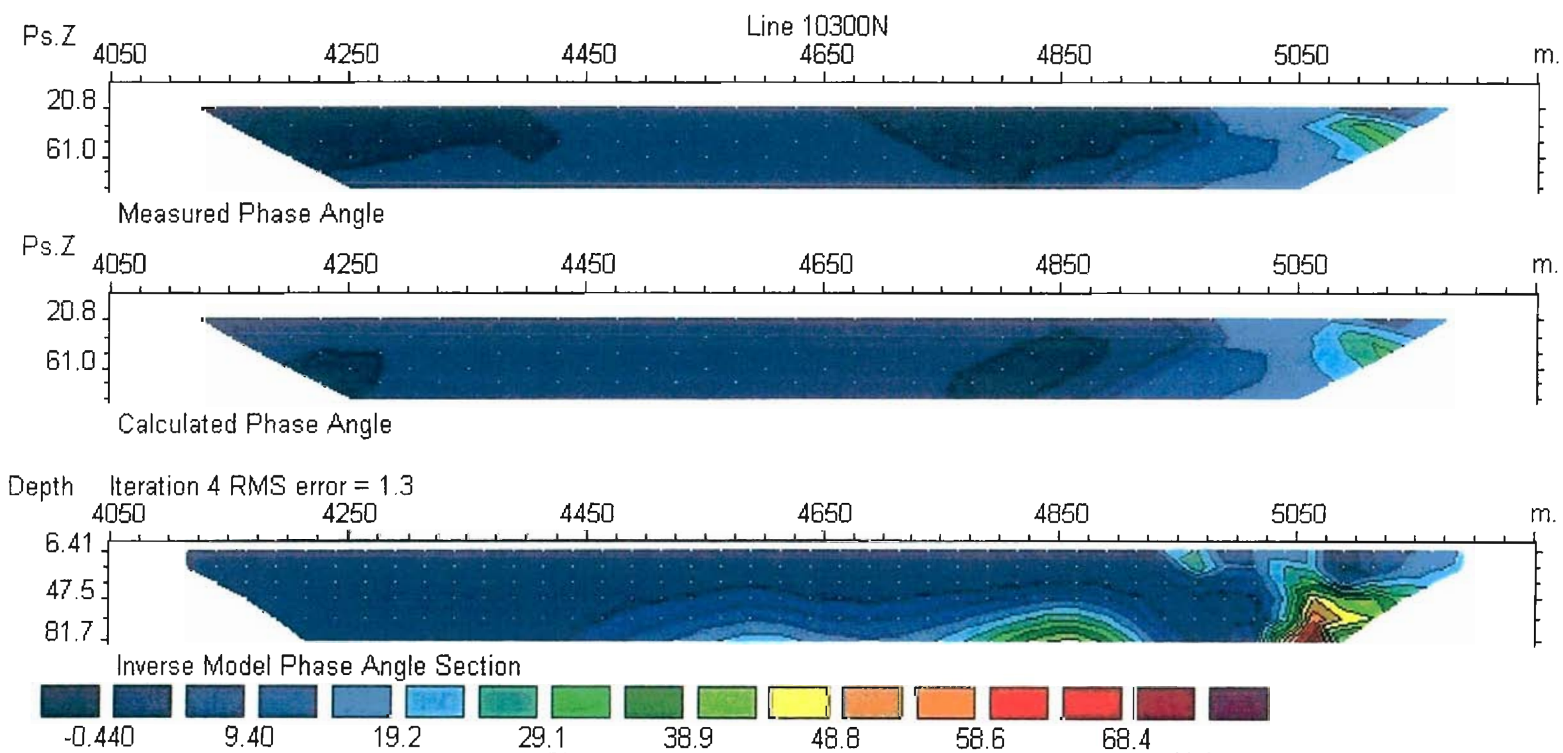
Line 10300N
Ps.Z
4050 4250 4450 4650 4850 5050 m.
20.8
61.0
Measured Phase Angle
Ps.Z
4050 4250 4450 4650 4850 5050 m.
20.8
61.0
Calculated Phase Angle
Depth
Iteration 4 RMS error = 1.3
4050 4250 4450 4650 4850 5050 m.
6.41
47.5
81.7
Inverse Model Phase Angle Section
-0.440 9.40 19.2 29.1 38.9 48.8 58.6 68.4

Line 10400N

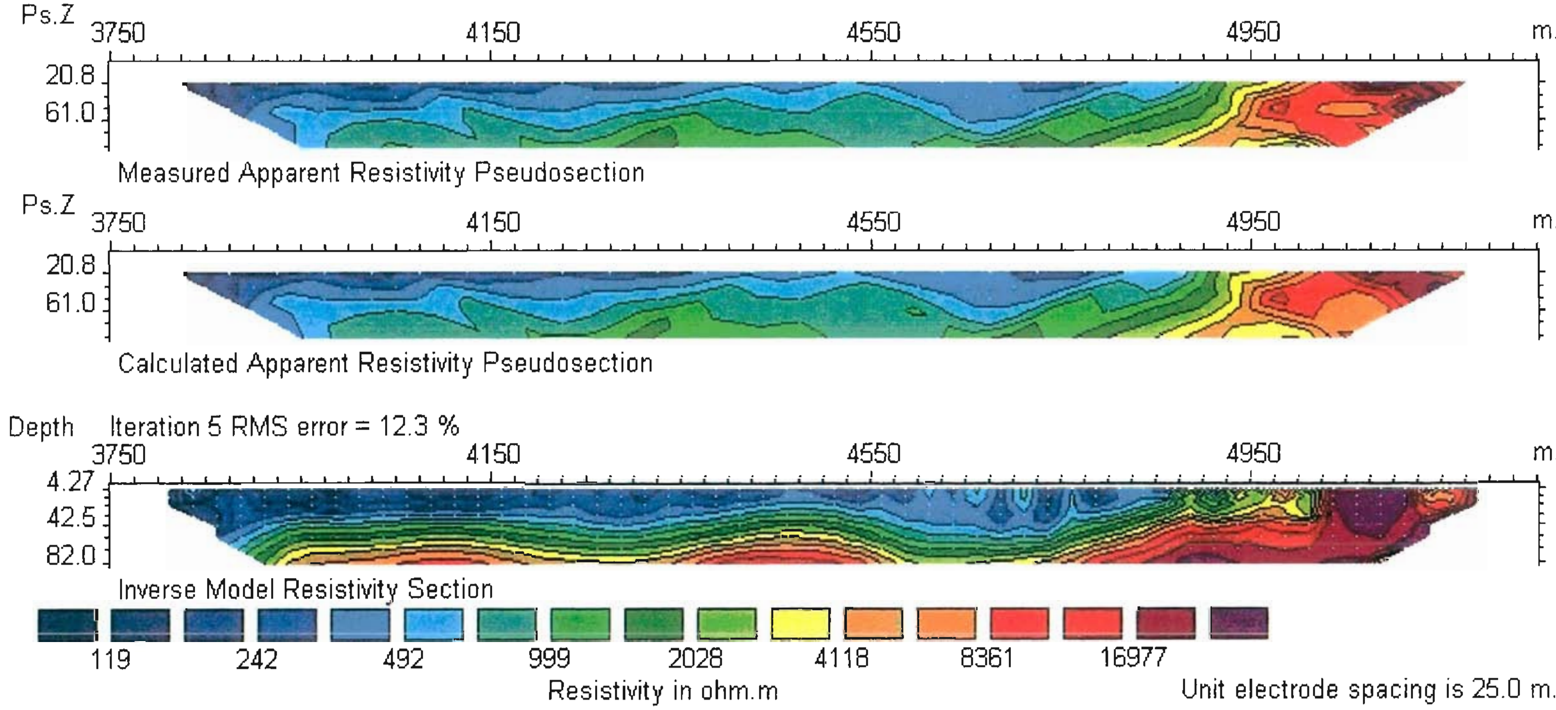

Line 10400N

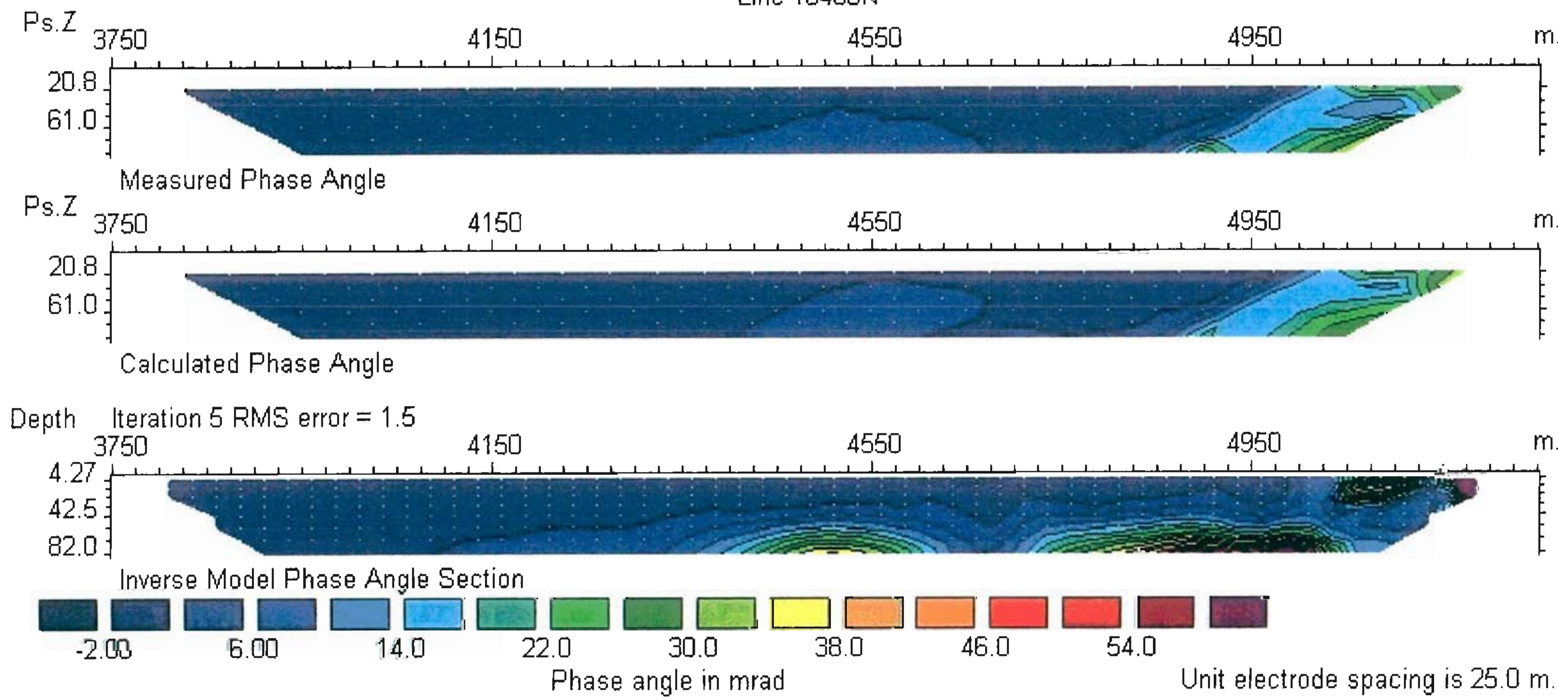

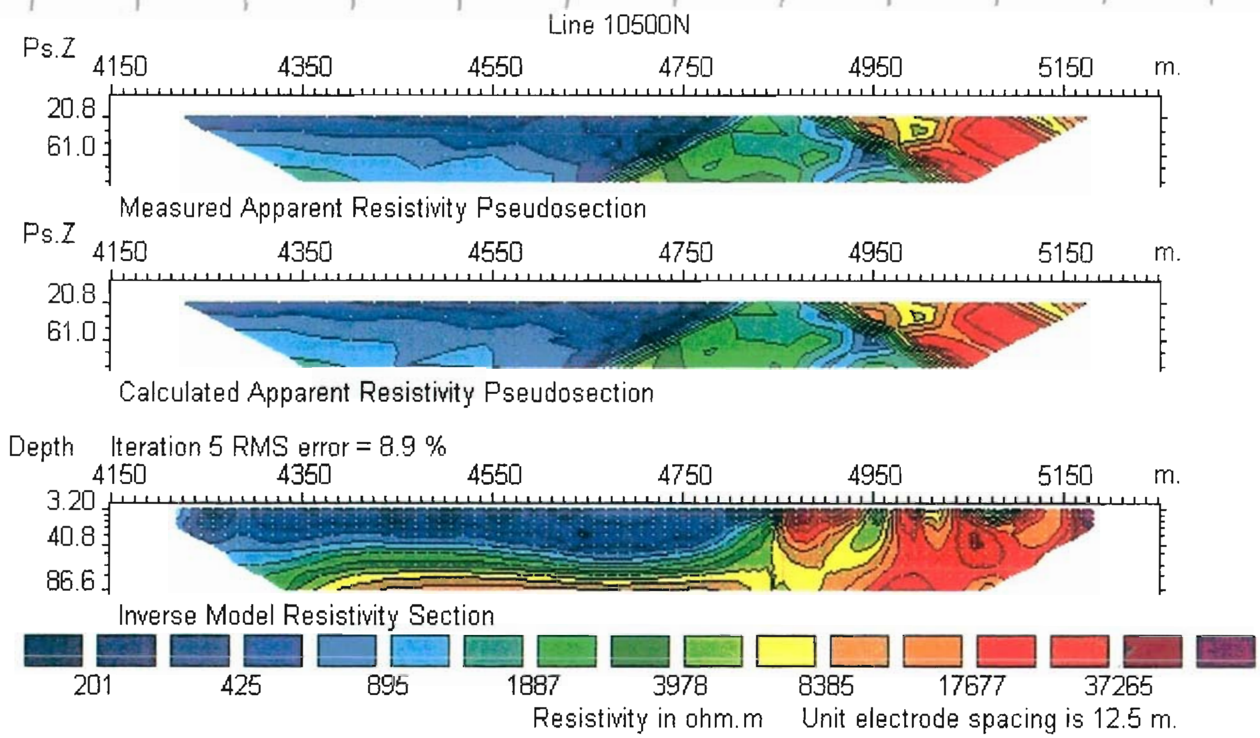
Line 10500N
Ps.Z
4150 4350 4550 4750 4950 5150 m.
20.8
61.0
Measured Apparent Resistivity Pseudosection
Ps.Z
4150 4350 4550 4750 4950 5150 m.
20.8
61.0
Calculated Apparent Resistivity Pseudosection
Depth
Iteration 5 RMS error = 8.9 %
4150 4350 4550 4750 4950 5150 m.
3.20
40.8
86.6
Inverse Model Resistivity Section
201 425 895 1887 3978 8385 17677 37265
Resistivity in ohm.m
Unit electrode spacing is 12.5 m.

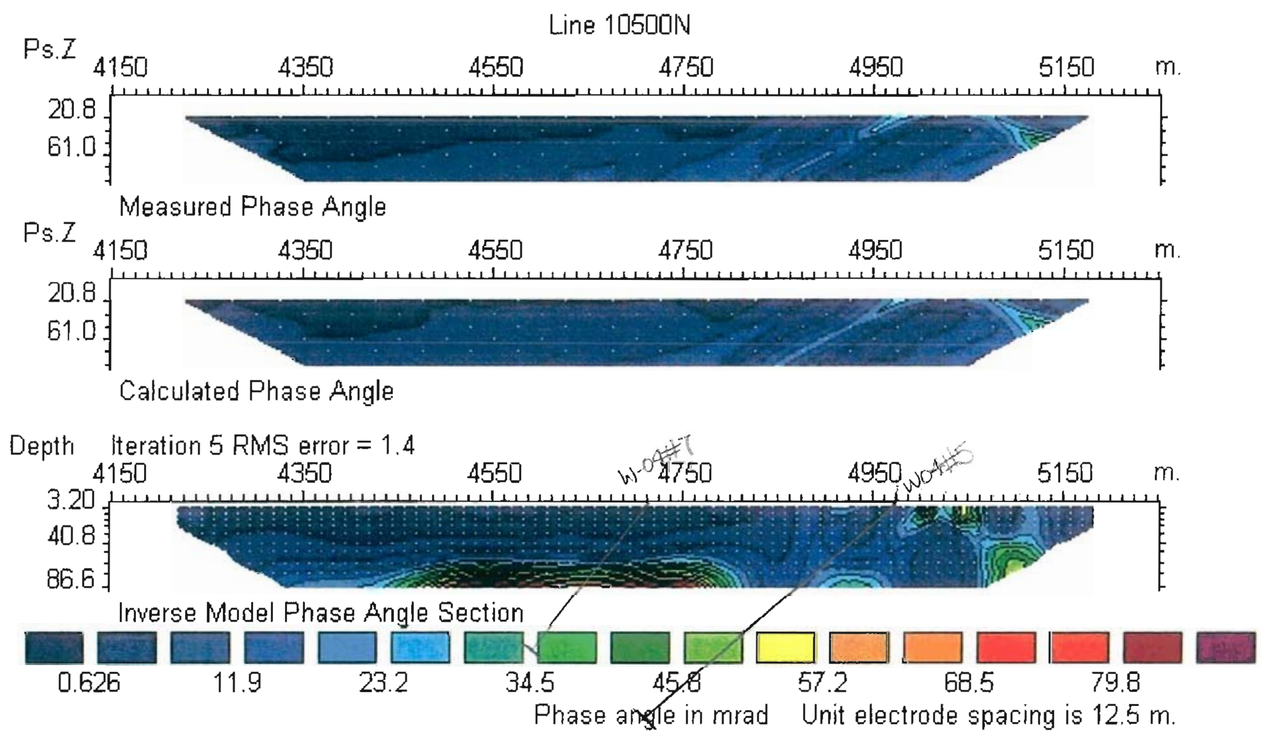
Line 10500N
Ps.Z
4150 4350 4550 4750 4950 5150 m.
20.8
61.0
Measured Phase Angle
Ps.Z
4150 4350 4550 4750 4950 5150 m.
20.8
61.0
Calculated Phase Angle
Depth
Iteration 5 RMS error = 1.4
4150 4350 4550 4750 4950 5150 m.
3.20
40.8
86.6
Inverse Model Phase Angle Section
0.626 11.9 23.2 34.5 45.8 57.2 68.5 79.8
Phase angle in mrad
Unit electrode spacing is 12.5 m.

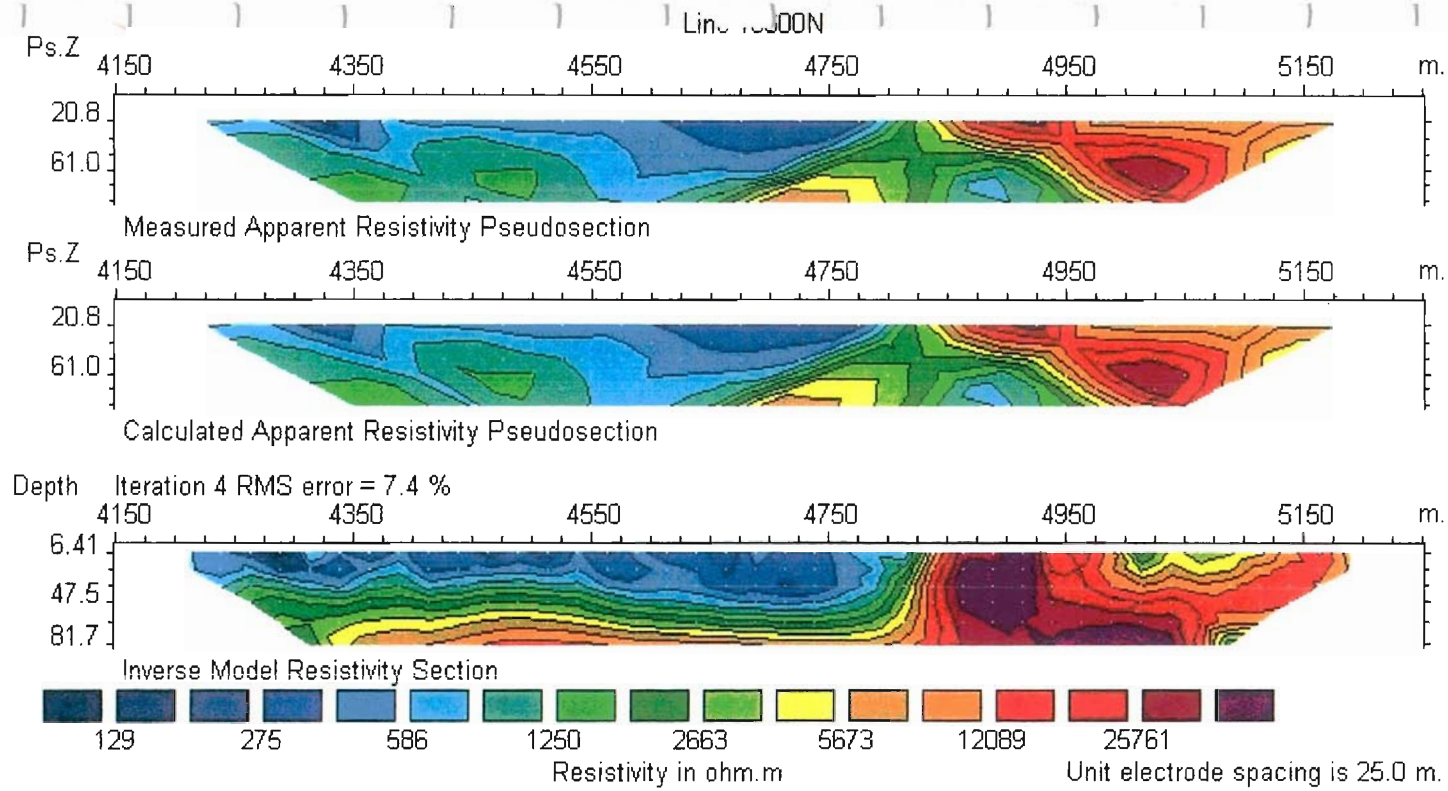
Ps.Z
4150
4350
4550
4750
4950
5150
m.
20.8
61.0
Measured Apparent Resistivity Pseudosection
Ps.Z
4150
4350
4550
4750
4950
5150
m.
20.8
61.0
Calculated Apparent Resistivity Pseudosection
Depth
Iteration 4 RMS error = 7.4 %
4150
4350
4550
4750
4950
5150
m.
6.41
47.5
81.7
Inverse Model Resistivity Section
129
275
586
1250
2663
5673
12089
25761
Resistivity in ohm.m
Unit electrode spacing is 25.0 m.

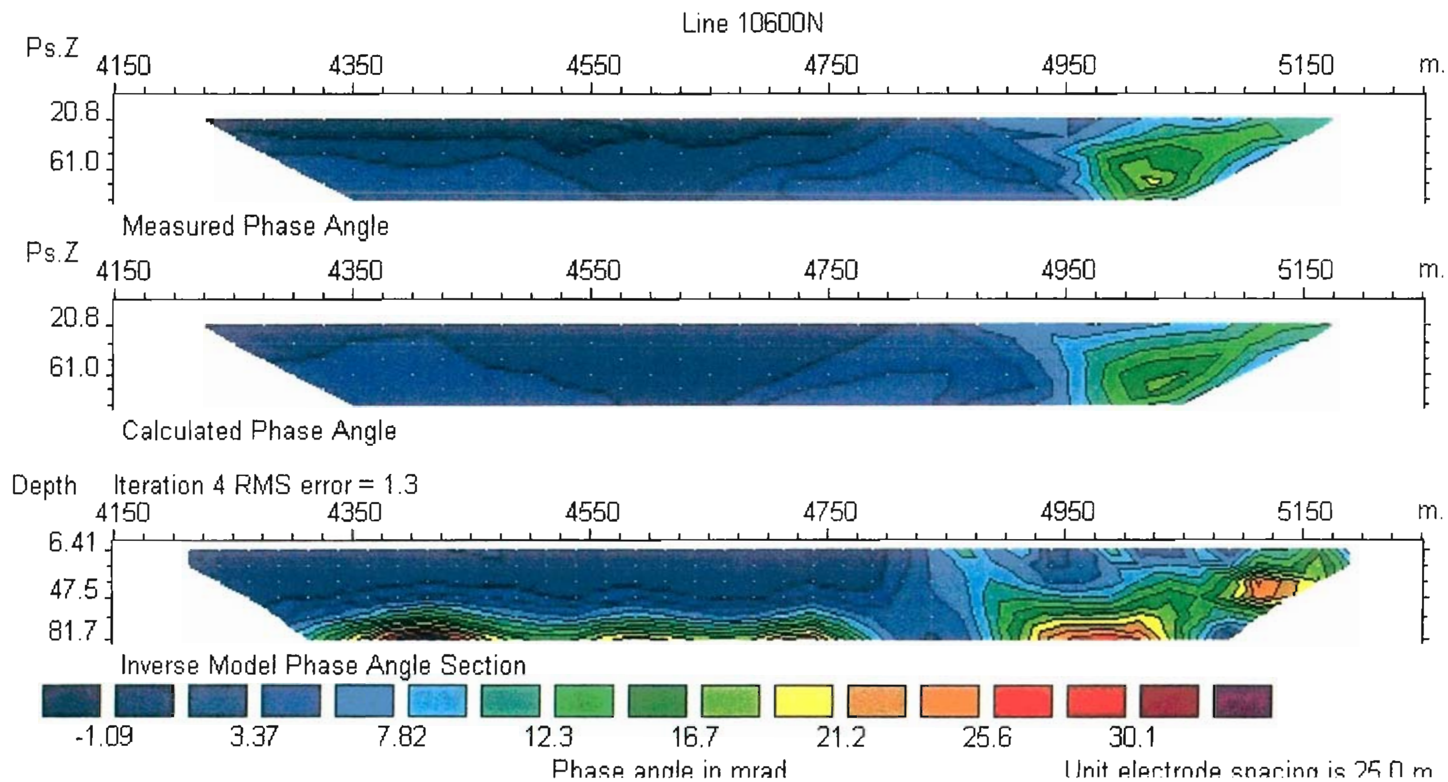
Line 10600N
Ps.Z
4150
4350
4550
4750
4950
5150
m.
20.8
61.0
Measured Phase Angle
Ps.Z
4150
4350
4550
4750
4950
5150
m.
20.8
61.0
Calculated Phase Angle
Depth
Iteration 4 RMS error = 1.3
4150
4350
4550
4750
4950
5150
m.
6.41
47.5
81.7
Inverse Model Phase Angle Section
-1.09
3.37
7.82
12.3
16.7
21.2
25.6
30.1

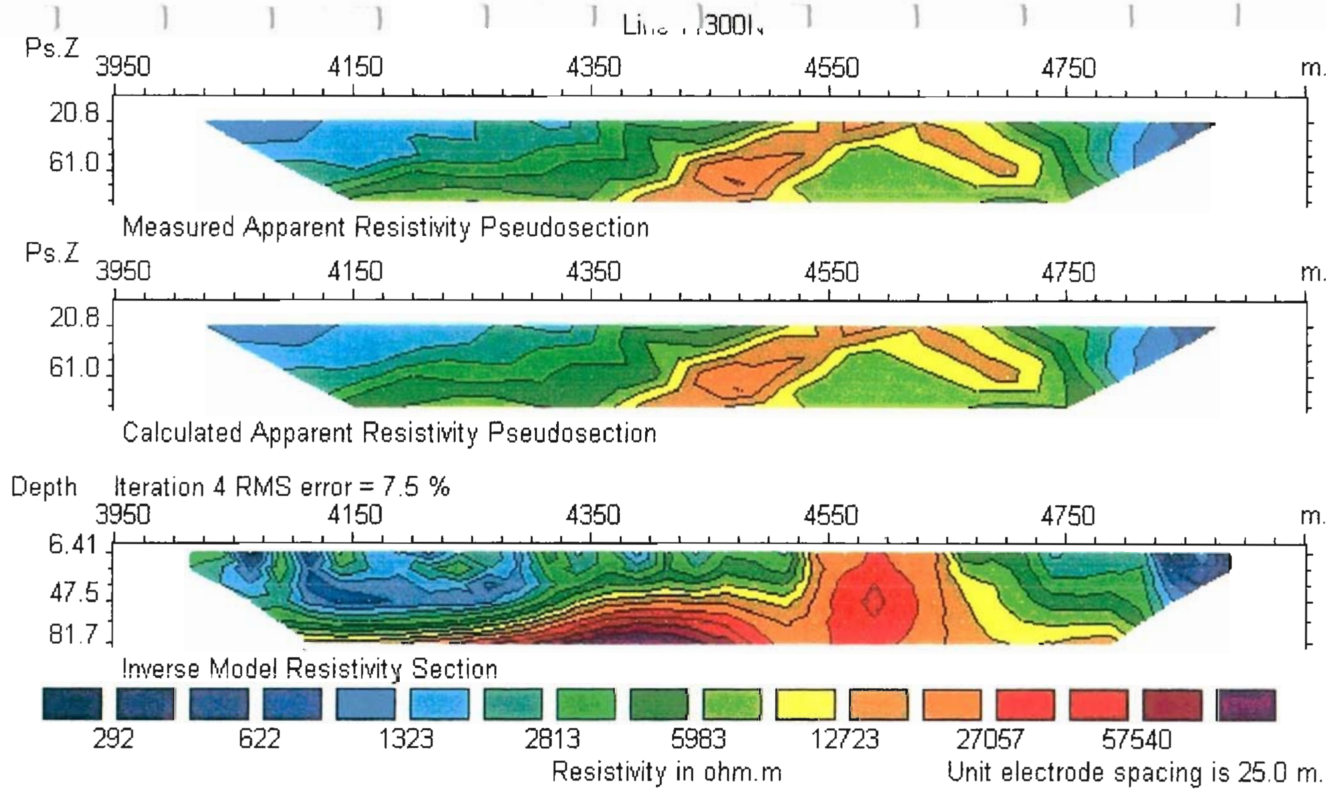

Line 11300N
Ps.Z
3950 4150 4350 4550 4750 m.
20.8
61.0
Measured Apparent Resistivity Pseudosection
Ps.Z
3950 4150 4350 4550 4750 m.
20.8
61.0
Calculated Apparent Resistivity Pseudosection
Depth
Iteration 4 RMS error = 7.5 %
3950 4150 4350 4550 4750 m.
6.41
47.5
81.7
Inverse Model Resistivity Section
292 622 1323 2813 5983 12723 27057 57540
Resistivity in ohm.m
Unit electrode spacing is 25.0 m.

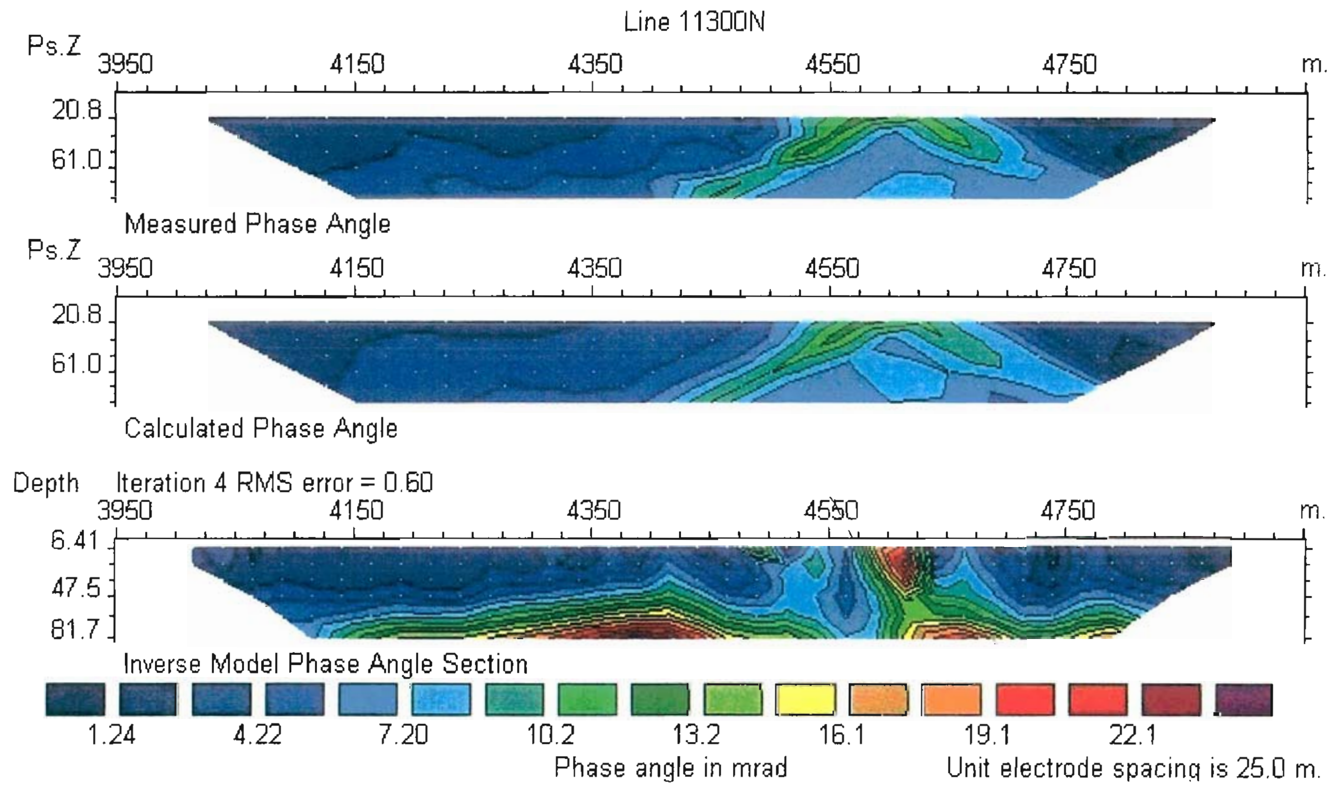

Line 11300N
Ps.Z
3950 4150 4350 4550 4750 m.
20.8
61.0
Measured Phase Angle
Ps.Z
3950 4150 4350 4550 4750 m.
20.8
61.0
Calculated Phase Angle
Depth
Iteration 4 RMS error = 0.60
3950 4150 4350 4550 4750 m.
6.41
47.5
81.7
Inverse Model Phase Angle Section
1.24 4.22 7.20 10.2 13.2 16.1 19.1 22.1
Phase angle in mrad
Unit electrode spacing is 25.0 m.

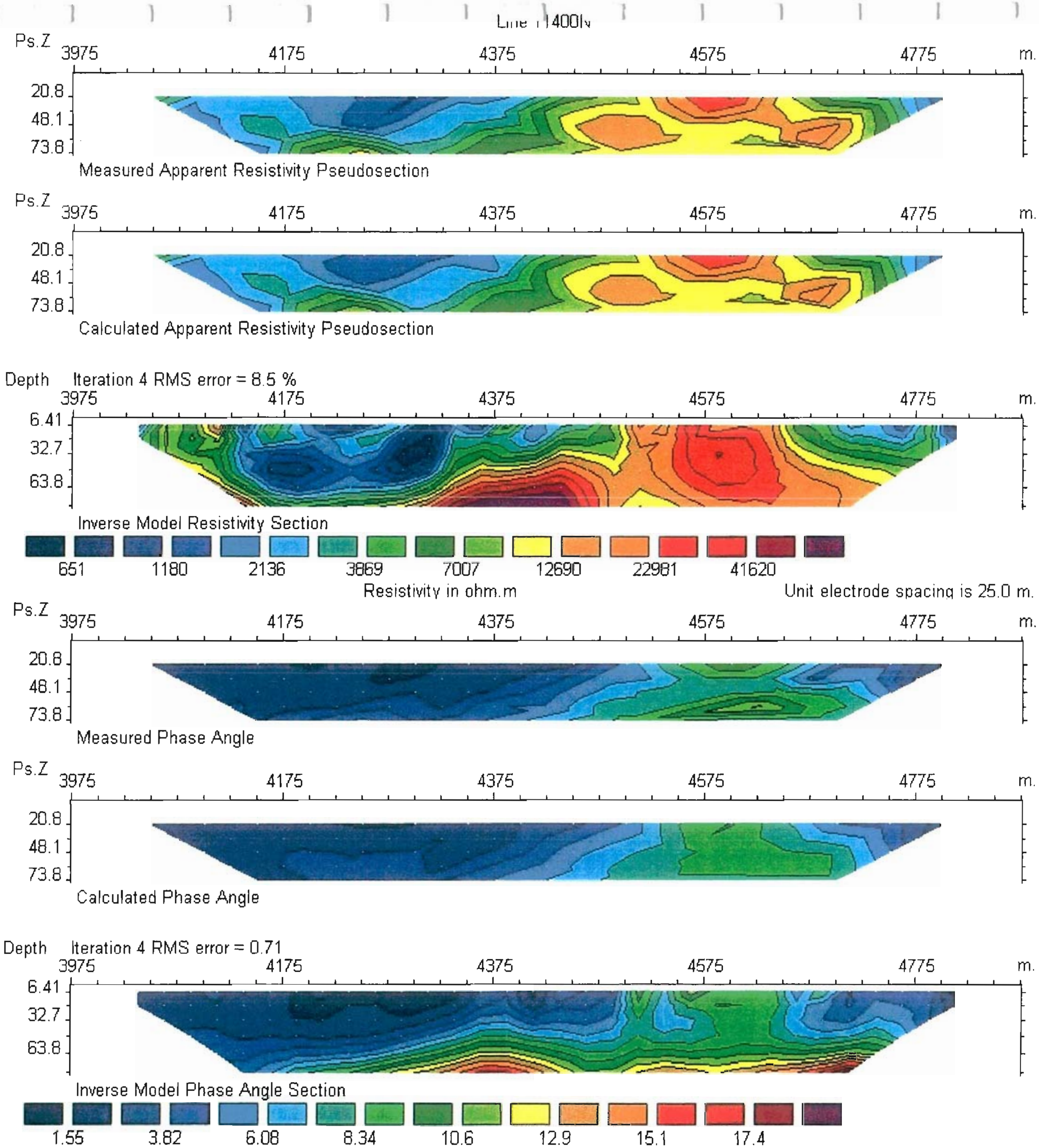
Ps.Z
3975
4175
4375
4575
4775
m.
20.8
48.1
73.8
Measured Apparent Resistivity Pseudosection
Ps.Z
3975
4175
4375
4575
4775
m.
20.8
48.1
73.8
Calculated Apparent Resistivity Pseudosection
Depth
Iteration 4 RMS error = 8.5 %
3975
4175
4375
4575
4775
m.
6.41
32.7
63.8
Inverse Model Resistivity Section
651
1180
2136
3869
7007
12690
22981
41620
Resistivity in ohm.m
Unit electrode spacing is 25.0 m.
Ps.Z
3975
4175
4375
4575
4775
m.
20.8
48.1
73.8
Measured Phase Angle
Ps.Z
3975
4175
4375
4575
4775
m.
20.8
48.1
73.8
Calculated Phase Angle
Depth
Iteration 4 RMS error = 0.71
3975
4175
4375
4575
4775
m.
6.41
32.7
63.8
Inverse Model Phase Angle Section
1.55
3.82
6.08
8.34
10.6
12.9
15.1
17.4

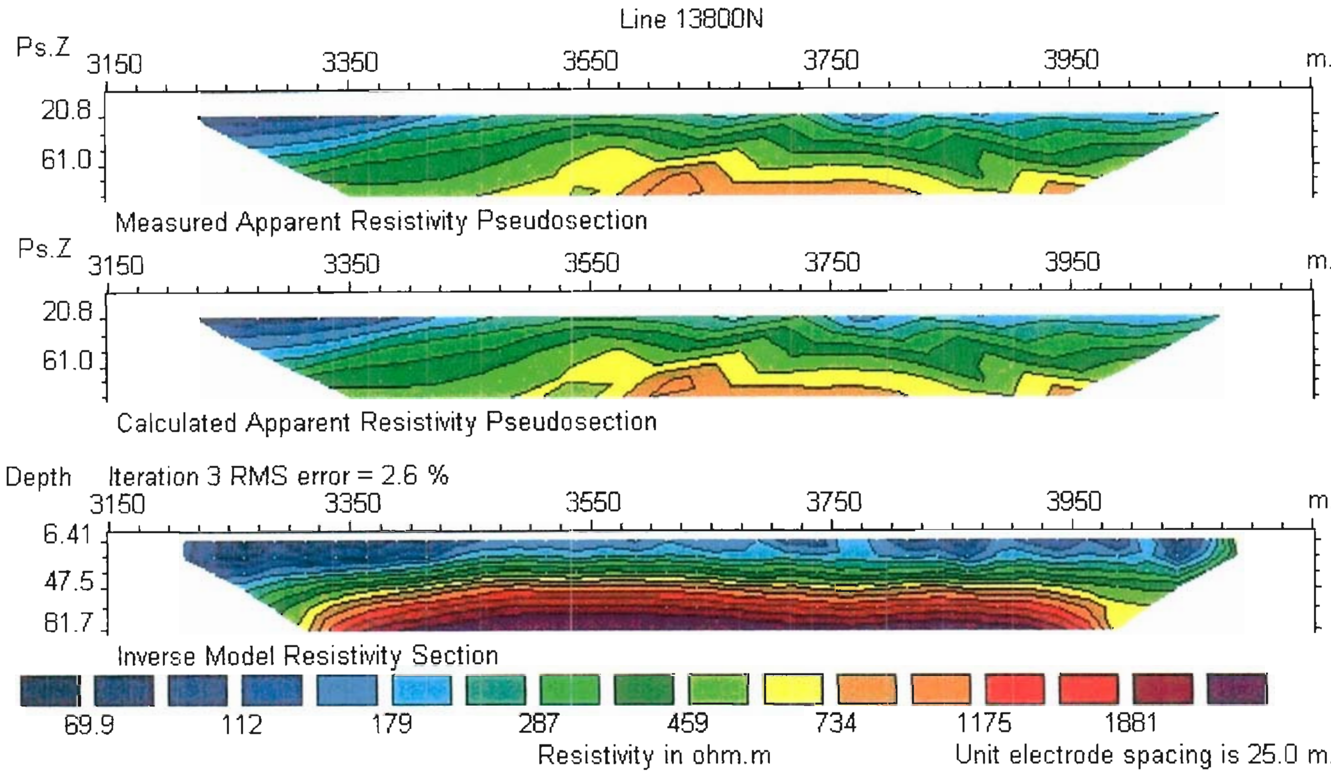

Line 13800N
Ps.Z
3150
3350
3550
3750
3950
m.
20.8
61.0
Measured Apparent Resistivity Pseudosection
Calculated Apparent Resistivity Pseudosection
Depth
Iteration 3 RMS error = 2.6 %
6.41
47.5
81.7
Inverse Model Resistivity Section
69.9
112
179
287
459
734
1175
1881
Resistivity in ohm.m
Unit electrode spacing is 25.0 m.

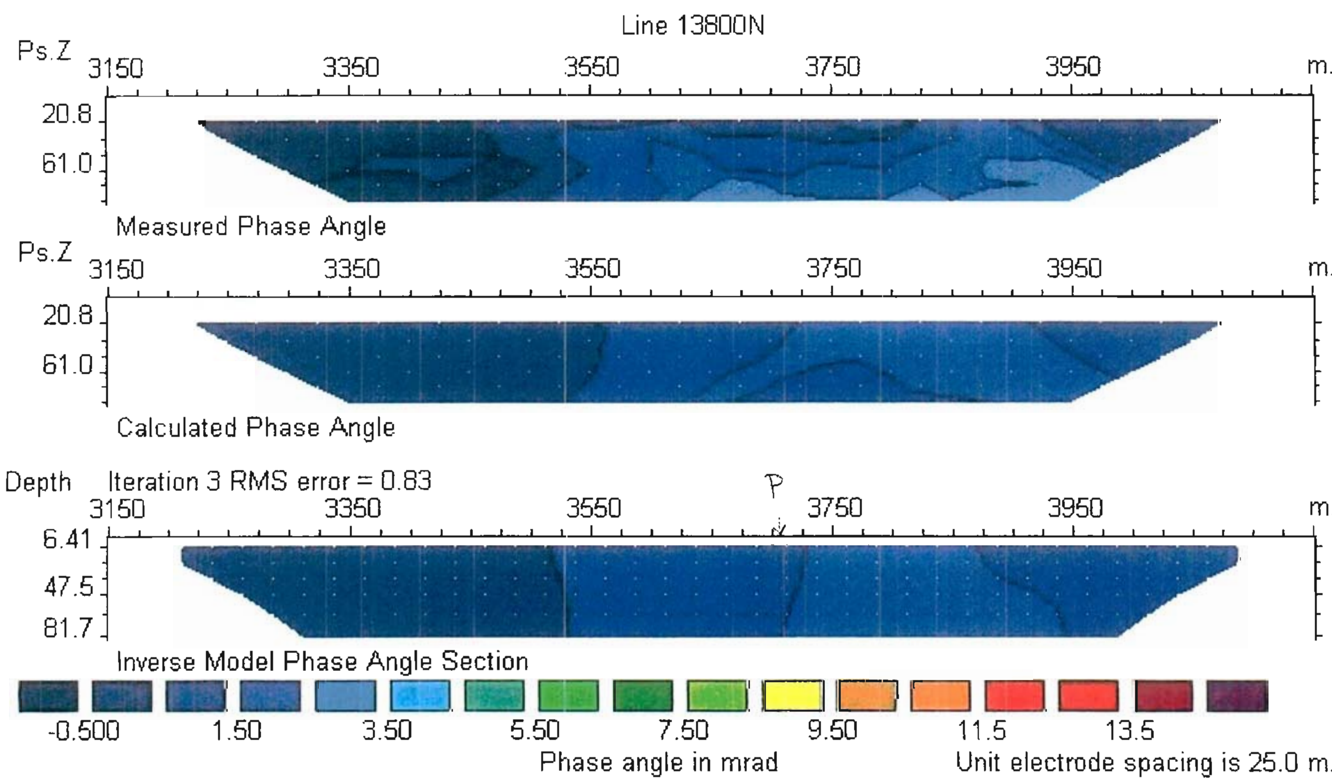

Line 13800N
Ps.Z
3150
3350
3550
3750
3950
m.
20.8
61.0
Measured Phase Angle
Calculated Phase Angle
Depth
Iteration 3 RMS error = 0.83
P
6.41
47.5
81.7
Inverse Model Phase Angle Section
-0.500
1.50
3.50
5.50
7.50
9.50
11.5
13.5
Phase angle in mrad
Unit electrode spacing is 25.0 m.

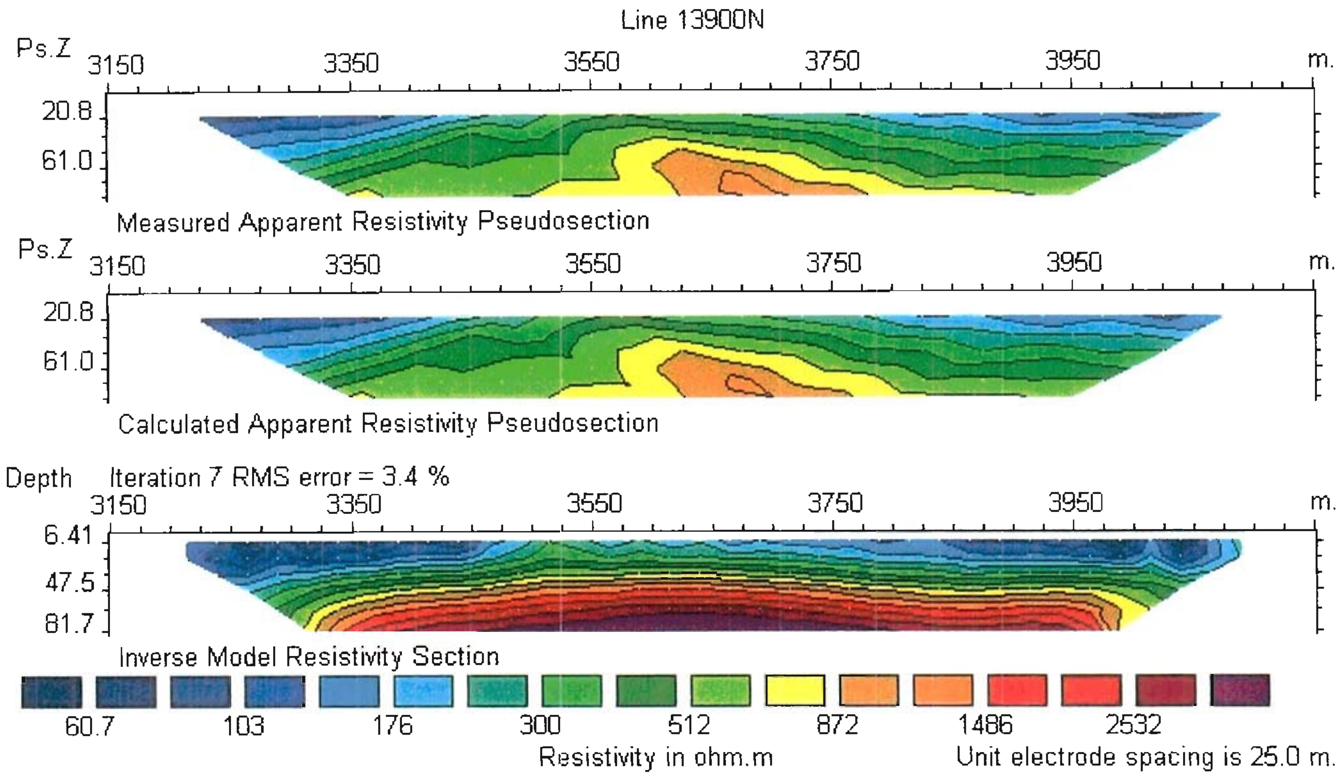
Line 13900N
Ps.Z
3150
3350
3550
3750
3950
m.
20.8
61.0
Measured Apparent Resistivity Pseudosection
Ps.Z
3150
3350
3550
3750
3950
m.
20.8
61.0
Calculated Apparent Resistivity Pseudosection
Depth
Iteration 7 RMS error = 3.4 %
3150
3350
3550
3750
3950
m.
6.41
47.5
81.7
Inverse Model Resistivity Section
60.7
103
176
300
512
872
1486
2532
Resistivity in ohm.m
Unit electrode spacing is 25.0 m.

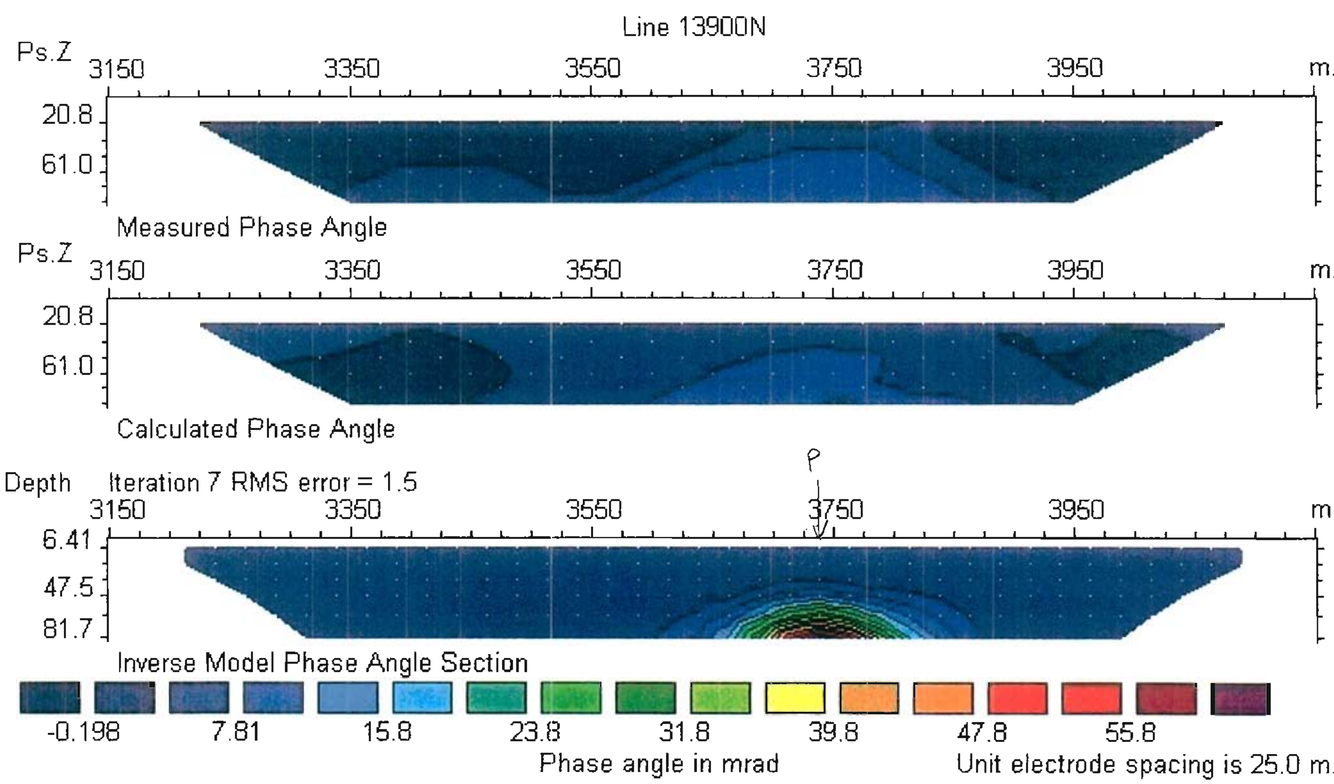
Line 13900N
Ps.Z
3150
3350
3550
3750
3950
m.
20.8
61.0
Measured Phase Angle
Ps.Z
3150
3350
3550
3750
3950
m.
20.8
61.0
Calculated Phase Angle
Depth
Iteration 7 RMS error = 1.5
P
3150
3350
3550
3750
3950
m.
6.41
47.5
81.7
Inverse Model Phase Angle Section
-0.198
7.81
15.8
23.8
31.8
39.8
47.8
55.8
Phase angle in mrad
Unit electrode spacing is 25.0 m.

APPENDIX B

STATEMENTS OF QUALIFICATIONS

Certificate of Qualifications

I, William J. Scott of the City of St. John's, Province of Newfoundland, do hereby certify:

1) That I am a consultant geophysicist and reside at 30 Monkstown Road, St. John's, Newfoundland, A1C 3T3.

2) That I graduated from the University of Toronto in 1962 with the degree of Bachelor of Applied Science in Engineering Physics (Geophysics), with the degree of Master of Arts in geophysics in 1965 and from McGill University in 1971 with the degree of Doctor of Philosophy in Exploration Geophysics.

3) That I am a Fellow of the Geological Association of Canada, a founding member of the Canadian Geophysical Union, a Registered Professional Engineer and a Registered Professional Geoscientist in the Province of Newfoundland.

4) That I have been practising my profession for a period of 43 years.

5) That I have no direct or indirect interest nor do I expect to receive any interest in the property described in this report.

REGISTERED PROFESSIONAL GEOSCIENTIST
WILLIAM J. SCOTT
SIGNATURE
DATE
NEWFOUNDLAND & LABRADOR

William J. Scott, Ph.D., P.Eng., P.Geo., FGAC.

Certificate of Qualifications

I, Krystal O'Neill of the Town of Conception Bay South, Province of Newfoundland, do hereby certify:

1) That I am a geophysicist in training and reside at 34 Woodview Place, C.B.S., Newfoundland, A1X 5C2

2) That I graduated from Memorial University of Newfoundland and Labrador in 2005 with the degree of Bachelor of Science (Honours) in Earth Science (Geophysics).

3) That I am a Registered Geoscientist in Training in the Province of Newfoundland.

4) That I have been practicing my profession for 1 year

5) That I have no direct or indirect interest nor do I expect to receive any interest in the property described in this report.

Krystal O'Neill

Krystal O'Neill B.Sc., GIT